AMERICAN UNIVERSITY OF BEIRUT

CATALYST DESIGN FROM NATURAL ZEOLITES FOR THE PYROLYSIS AND GASIFICATION OF SCRAP RUBBER TIRES

by
SALOMA SALIBA KHEIRALLAH

A thesis
submitted in partial fulfillment of the requirements
for the degree of Master of Science in Chemical Engineering
to The Baha and Walid Bassatne Department of Chemical Engineering
and Advanced Energy
of the Faculty of Engineering and Architecture
at the American University of Beirut

Beirut, Lebanon
December 2019

AMERICAN UNIVERSITY OF BEIRUT

CATALYST DESIGN FROM NATURAL ZEOLITES FOR THE PYROLYSIS AND GASIFICATION OF SCRAP RUBBER TIRES

by

SALOMA SALIBA KHEIRALLAH

Approved by:

[Dr. Joseph Zeaiter, Associate Professor] Advisor
[Bahaa and Walid Bassatne Department of Chemical Engineering and Advanced Energy]

[Dr. Elsa Maalouf, Assistant Professor] Member of Committee
[Bahaa and Walid Bassatne Department of Chemical Engineering and Advanced Energy]

[Dr. Sabla Alnouri, Assistant Professor] Member of Committee
[Bahaa and Walid Bassatne Department of Chemical Engineering and Advanced Energy]

Date of thesis defense: December 4, 2019

AMERICAN UNIVERSITY OF BEIRUT

THESIS, DISSERTATION, PROJECT RELEASE FORM

Student Name: _Kheirallah____ Saloma _____Saliba_____
Last First Middle

■ Master's Thesis ■ Master's Project ■ Doctoral Dissertation

[✓] I authorize the American University of Beirut to: (a) reproduce hard or electronic copies of my thesis, dissertation, or project; (b) include such copies in the archives and digital repositories of the University; and (c) make freely available such copies to third parties for research or educational purposes.

[ ] I authorize the American University of Beirut, to: (a) reproduce hard or electronic copies of it; (b) include such copies in the archives and digital repositories of the University; and (c) make freely available such copies to third parties for research or educational purposes
after : **One ---- year from the date of submission of my thesis, dissertation, or project.**
Two ---- years from the date of submission of my thesis, dissertation, or project.
Three ---- years from the date of submission of my thesis, dissertation, or project.

Saloma 23/1/2020

Signature Date

ACKNOWLEDGEMENTS

I am beyond grateful to my advisor Dr. Joseph Zeaiter an exceptional person, who mentored and trusted me in my work, shared his experience and knowledge and always made sure that I was on the right track. I thank him for believing in me and encouraging me to take risks and explore different parts of the field.

I would like to thank my committee members Dr. Elsa Maalouf and Dr. Sabla Alnouri for providing me with their appreciated experience and feedback helping me to perform my best towards completing my master's degree. I would like to give a special thanks to Mr. Nicolas Aramouni who was the first person that guided me through experimental work and taught me how to use several characterization equipment's used throughout my project. Nicolas was always available to help, answer any technical or theoretical question and do whatever he could to be of support. Mr. Marc Ayoub assisted my experiments during the early stages and was of great help. Not to forget Mr. Mohamad Berjawi, Mrs. Rita Khalil, Ms.Nouhad Al-Rifaii, Mr.Mohamad Hamdan, Ms. Elise Farah and Mr.Emile Atallah. Thank you all for your technical assistance. I am extremely grateful to every single person I encountered while working in the labs especially in the Oxy building. You guys put smiles on my face and made the hard work seem easy.

I would finally like to express my eternal gratitude to my parents for allowing me to be where I am today, without their support I wouldn't have reached this level. My family and friends' everlasting love and support are what pushed me. Thank you Christine El-Khoury and Elena Najjar for being backbones.

AN ABSTRACT OF THE THESIS OF

Saloma Saliba Kheirallah for Master of Science
Major: Chemical Engineering

Title: Catalyst design from natural zeolites for the pyrolysis and gasification of scrap rubber tires

Pyrolysis and gasification are waste to energy thermal techniques that enhance the breakage of chemical bonds into smaller chains at elevated temperatures. Pyrolytic oil is known to be concentrated with heavy compounds that are difficult to remove for the use of oil in further applications.

The objective of this project is to enhance the degradation of scrap tires by designing catalysts from natural zeolites to maximize gas yield at the outlay of the oil yield. In this work, pyrolysis was conducted at a fixed temperature of 580℃ whereas gasification was conducted at three different temperatures of 580, 680 and 780℃ accompanied with ethanol.

Nine catalysts, from natural clays were activated with two different methods to form Kaolinite, KM_4, Brown clay, BC_6, Montmorillonite, M_6, M_4_3, Bentonite and BN_4 with inorganic H_2SO_4 in order to enhance Si/Al ratio and hence catalyst acidity. Acidity of a zeolite enhances its catalytic cracking activity. Catalysts behaviors and activities were analyzed using several characterization techniques; Scanning Electron Microscope (SEM), Energy Dispersive X-ray(EDX), Brunauer-Emmet-Teller (BET) and X-ray Diffraction (XRD).

Thermal pyrolysis results indicated that montmorillonite modified with low acid concentration, M_4_3, yielded the highest pyrolytic gas yield at 30 wt.%. M_4_3 had a Si/Al of 5.61 and a high surface area of 224 m^2/g. The acidity, surface area and pore size of the catalyst triggered higher selectivity and large chain decomposition on its surface. Liquid product yields were analyzed with GC-MS and contained alkanes, alkenes, alkynes, olefins and aromatics of them contained benzene, toluene and styrene. As for gasification, the syngas yield increased to 41.1 wt.% obtained at 780℃ with montmorillonite as a catalyst.

CONTENTS

LIST OF ILLUSTRATIONS

LIST OF TABLES

Table Page

CHAPTER 1

AIM OF PROJECT

Millions of tires are discarded in landfills throughout the world every year. Tires are not easily degradable in the environment and therefore have a long life span. They are usually stockpiled for long periods of time causing many different form of environmental and health hazards such as breeding of insects and unintentional fires (Juan Daniel Martinez, 2013). According to (Freedonia, 2019) it is estimated that about 3 billion tires per year will be sold globally and subsequently that same amount will become of no use. Waste tire management has to follow the well-known waste management hierarchy (European Commission, 1999), to decrease its impact on the environment starting with waste minimization and ending in landfills.

Many energy applications such as power plants, cement kilns and tire manufacturing facilities have used tires as a source of energy in the past (Barlaz MA, 1993) demonstrating theability to extract energy from tires in a safe and environmental form (C. Clark, 1993)**.** Tire derived fuel has been recognized by the US Environmental Protection Agency (EPA) as a sustainable substitute to the use of fossil fuels. It also backs up the use of tires in kilns of Portland cement as long as the tire-derived fuel meets the management and environmental requirements framed by legislation (US Environmental Protection Agency, n.d.). Like any other form of waste, the aim behind waste tire disposal is to minimize its environmental impact. Thermochemical conversion methods such as pyrolysis and gasification have emerged to not only lower the amount of tire stockpiles but also

minimize waste management environmental impact since these methods reduce the amount of NOx and SOx that are emitted during thermal conversion. Tire pyrolysis, amongst different thermochemical techniques has been identified as a favorable technique in comparison to incineration and direct combustion techniques, due to the minimal release of toxic gases and the advantage of recovery of the char, gas and pyrolytic oil and is classified as an economically sustainable process (Labaki, 2016); (Ayanoglu, 2016).

Pyrolysis of scrap tires produces char, that may be used as carbon black or activated carbon gas (C.I. Sainz-Diaz, 2000), (B. Sahouli), (L.K.M. Edward, 2004), which is composed of enough calorific value to provide energy to processes (M.M. Barbooti, 2004) and liquid oil which can be used as a fuel substitute (A.M. Cunliffe) (P.T. Williams, 2003).

Liquid oil derived from tire pyrolysis contains a large amount of aromatic hydrocarbons, which therefore limits its use as an alternative for fuel (A.M. Cunliffe) (P.Williams) (M.F. Laresgoiti, 2004). On the contrary, derived oil contains valuable properties of chemicals like toluene, benzene and xylenes. These products could be extracted from the oil and be used as chemical feedstock in the chemical industry (Shen Boxiong, 2007). For instance, toluene and benzene can be used for the fabrication of surfactants, pesticides and dyestuff, whereas xylenes are used to fabricate all sorts of industrial fibers and plasticizers (Shen Boxiong, 2007) (H.G. Franck).

Pyrolysis of scrap tires is not enough to produce a sufficient amount of these chemicals and therefore catalysts are used (Shen Boxiong, 2007). Product yields from pyrolysis are highly dependable on the operating conditions. It has been seen that the weight percentage of gas yield is lowest amongst solid and liquids (Juan Daniel Martinez, 2013) . Whereas pyrolytic oil is known to be concentrated with heavy compounds that are

difficult to remove and need extensive refining for its use in further applications. Several researchers have used zeolite catalysts with different pore sizes and Si/Al ratios in order to produce more single ring aromatic compounds (P.T. Williams, 2003). Therefore, the objective of this project is to enhance the degradation of scrap tires by designing catalysts from natural zeolites to maximize the gas yield at the outlay of the oil yield. Gasification will also be carried out at different temperatures, then experiments with the raw catalyst that achieved the highest gas yield in pyrolysis will be tested to achieve high gas yields at the outlay of liquid fraction. Eventually, cleaner pyrolytic oils with smaller molecular weight products, simpler hydrocarbons, were detected with activated montmorillonite M_4_3.

Chapter 2 of this thesis contains the literature review section that will describes the waste tire material and its constituents. The pyrolysis process, along with the parameters that affect tire pyrolysis such as temperature, size of scrap tire and the effect of a catalyst will be discussed. Natural zeolites as acidic catalysts for catalytic cracking will be introduced along with the effect of a zeolites acidity on catalytic cracking. Gasification, along with use of ethanol is further elaborated as a reactant and radicals generator.

Chapter 3 introduces the experimental methods adopted in this work. The preparation and activation of natural clays as well as their characterization and analysis methods are discussed. The setup of pyrolysis and gasification experiments are explained with product analysis using appropriate GC-MS methods.

Chapter 4 covers the results and discussion of the pyrolysis experiments with a focus on the gas yield and liquid product analysis. Gasification product yields and gas analysis are also summarized in this chapter.

Chapter 5 concludes the significant results achieved in this project alond with recommendations for future work.

CHAPTER 2

LITERATURE REVIEW

2.1 Waste tires elements

Tires are composed mainly of rubber, carbon black, and various amounts of fillers and accelerators that are added during manufacturing. Fillers are used in order to extend and reinforce the structure and these include calcium carbonate, clay, fumed silicas and hydrocarbon process oils. As for accelerators they are added to prevent the breakdown of rubber and are formed from inorganic compounds such as metal oxides and organic acids.

Tires are classified as thermoset polymers meaning that once they are cured and formed they cannot be permanently reshaped, and therefore are difficult to decompose (Leung DYC, 1998). There are three different types of rubber that are used and blended depending on tire use and they are, natural rubber (NR) derived from the Hevea tree, synthetic rubber (SR) derived from petroleum products (Shulman, 2004), and styrene-butadiene copolymer (Juan Daniel Martinez, 2013). NR, due to its elastic properties, is a principal tire constituent since it provides a better strength and durability(Shulman, 2004).

Carbon black on the other hand is present in tires to strengthen their struccture. Also extender oil, a blend of different paraffinic, aromatic and naphthenic hydrocarbons, is used to enhance the performance of the material. All these materials contribute to the higher calorific value when compared to coal. Therefore, it is useful to consider tires as an alternative energy source while simultaneously reducing their life span as waste material (Juan Daniel Martinez, 2013).

2.2 Waste tires as feedstock for pyrolysis

Pyrolysis of rubber tires permits the separation of solids, carbon black, as well as liquids and gases, which have potential usage in renewable energy applications. Tires are manufactured differently depending if they are made for cars, motorcycles or trucks. The polymeric compounds that come from synthetic and natural rubber are reportedly found in the volatile matter of tires and that of the fixed carbon should be equivalent to the carbon black used in the manufacturing of tires (Juan Daniel Martinez, 2013).

Juan Daniel Martinez (2013) summarized the proximate and elemental analysis performed by many authors and observed that the volatile matter, which should match the amount of the liquid and gas attained from pyrolysis, ranges between 57.5 and 73.74 wt%. The non-volatile matter, fixed carbon residue that remains after pyrolysis, ranges from 19.45 to 32.28 wt% then there is ash content that vary between 2.40 and 20.12 wt%. It is well known that the proximate analysis of tires affects the product yields obtained during pyrolysis (Mastral AM C. M., 1999).

2.3 The pyrolysis process

Tire pyrolysis, amongst all different thermochemical techniques, has been identified as a favorable method (S. Chouaya, 2018) in comparison to incineration and direct combustion techniques, due to the minimal release of toxic gases and the advantage of recovering char, gas and pyrolysis oil. It is classified as an economically viable process (Labaki, 2016); (Ayanoglu, 2016).

Pyrolysis degrades long chain polymers into smaller compounds under intensive heat as illustrated in pressure (figure 1). The process is performed in the absence of oxygen

at high temperatures and at short durations in either vacuum or with an inert gas to prevent the formation of NOx, SOx, CO_2, and CO (Bidhya Kunwar, 2016). Char, oil and gas are the three major products produced from pyrolysis. These products are valuable for many industries. Solid wastes, through this thermal treatment, can be converted into high calorific fuels, chemicals and other valuable materials. The breakage of chemical bonds resulting from thermal treatment produces volatile products that are defined as high-energy-density gases and the non-volatile product carbon black, a carbonaceous solid.

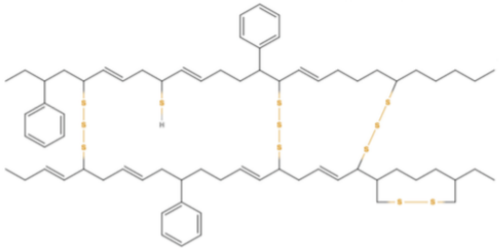

Figure 1 Possible cracking positions of a tire molecule during pyrolysis (Amir Rowhani, 2016)

Pyrolysis is a very flexible process because its parameters are easy to manipulate in order to optimize the quality of the desired product. In fact, the thermal degradation of tires is initiated at around 350℃ and temperatures plays a very important role in the final products. Many researchers have targeted high liquid yields achieved at temperatures ranging between 500−550℃ (Rezaiyan J. C., 2005).

Once temperature is increased, numerous reactions including dehydration, dehydrogenation, cracking, isomerization, aromatization and condensation occur (Rezaiyan J. C., 2005). Low temperatures at about 300-400℃ yield heavy oil fractions, which are not useful for fuel unless further refined. At temperatures as high of 400℃-600℃, gas is produced in higher yields, while the yield of liquid fractions varied depending on other

parameters such as temperature, particle size and carrier gas type and flow rate, as elaborated in the following sections.

The effect of temperature makes pyrolysis an energy intense process. (S. Chouaya, 2018) found after performing pyrolysis on scrap tires at different operating conditions, that the full conversion of the scrap tires occurred at temperatures of 500-550℃. Qu (2006) performed experiments at 430℃ (Wei Qu, 2006). Therefore, there is no definite optimum temperature to perform the pyrolysis of scrap tires, rather just a window of temperatures to perform depending on the desired products.

On an industrial scale the collected gas stream is rich in C_1-C_4 hydrocarbons, which have a high-energy value. The gas stream is could be reused to provide heat for the pyrolysis process, and char is further refined and reused as activated carbon (Wiliams, 2013).

Gasification, an alternative thermochemical method mainly converts material into gas and other by-products such as water, and char at temperatures as high as 800-1000℃ (Amir Rowhani, 2016). Processing biomass at elevated temperatures and in orderly environments ends in converting the biomass into light gas products such as CH_4, C_2H_6, and CO_x (Amir Rowhani, 2016). Raman et al. (1981) examined the effect of temperature on gasification for tire particles (Raman, Walawender, & Fan, 1981). They deduced that by increasing temperature the gas yield increased from 0.21 to 0.76 $N.m^3.kg^{-1}$, however it reduced the gas heating significance from 39.6 to 22.2 $MJ.m^3$ (Amir Rowhani, 2016). Lee (2001) Indicated that when the size of scrap tire particle is less than 0.65mm, the gasification reaction parameters do not impact the products (Lee). Many researchers have

conducted experiments using various agents such as air/CO_2, steam, and air/steam on scrap tires where steam was deduced to produce gas with low heating value (Amir Rowhani, 2016). Concluding from thorough literature review, temperature increases gas yield however other parameters impact the quality and quantity of the gas product obtained (Amir Rowhani, 2016).

2.3.1 Feedstock composition

Each tire brand acquires different rubber ratios as the final composition and these depend on age and type. Ratios of natural rubber and synthetic rubber differ depending on the vehicle category (Scrap tire characteristics, 2012). Table 1 shows different categories of rubber tires with their constituents of natural rubber, synthesized rubber, steel, fabric, carbon black, fillers and accelerator percentages. Reported from Table 1, passenger car tires consist of higher portions of synthetic rubber at 27wt. %, whereas truck tires contain more natural rubber 27wt. % (Scrap tire characteristics, 2012).

Table 1 Chemical composition of tires (Scrap tire characteristics, 2012)

Compound	Passenger car tire (wt%)	Truck tire (wt%)
Natural Rubber	14	27
Synthetic rubber	27	14
Carbon black	28	28
Steel	14-15	14-15

Fabric, fillers, accelerators, antiozonants, etc.	16-17	16-17

The degradation rate is defined as the weight percentage lost per unit time, and matched by the material composition of the rubber tires (Juan Daniel Martinez, 2013). It begins to be significant at 200℃ where an appreciable amount of volatile compounds are highly released, and the degradation behavior is highly dependent on the composition of the feedstock (Groves SA, 1991); (Murillo R, 2006); (Berrueco C, 2005).

The link between feedstock composition and degradation rate was discussed by Kwon (2009) and it was recognized that poly-isoprene rubber reached a rate of 0.21wt. % whereas styrene-butadiene rubber (SBR) met a rate of 0.25wt. % (Kwon E a. C., 2009). The comparison of the tire rubber sample with SBR and poly-isoprene rubber highlighted the important aspect of degradation temperature and degradation rate on the rubber material. SBR and poly-isoprene exhibited a degradation temperature in the range of 320-480℃, whereas tire rubber required a temperature range of 280-500℃ (Kwon E a. C., 2009).

Group passenger car tires (PCT) and truck tire (TT) were compared closely and the differentiation between the product yields and their contents were detected. Ucar (2005) witnessed liquid yields of 47.4% and 55.6% at 550℃ for PCT and TT respectively (Ucar S, 2005). Roy (1997) found that more aromatic compounds are produced by the pyrolysis of pure poly-isoprene rather than the pyrolysis of NR (Roy C, 1997). That is due to the behavior of the aromatic nature of the rubber feedstock with the presence of SBR and the processing oil that is consumed during tire manufacturing. It was

proposed by Kwon (2008) that aromatic radical species are the first reactions that occur during the thermal breakdown of SBR (Kwon E., 2008). Lopez (2009) showed that PCT yielded greater aromatics 43.7 wt. % than TT at 33.4 wt.% at a temperature of 500℃ (Lopez G O. M., 2009). He stressed that TT has been analyzed to have 58 wt.% NR and 0 wt.% for SBR, whereas PCT contained 29.6 wt.% NR and 29.6 wt.% SBR. Thus, the presence of high amounts of aromatic hydrocarbons is linked to SBR cracking.

2.4 Waste tire pyrolysis complex reactions and mechanisms

Polymers are generally structured into carbon atoms that make up single or double bonds. Domenico (1983) mentioned that tires are made of carbon-carbon double bond polymers (Dodds J. Domenico WF, 1983). Through thermal decomposition these carbon-carbon chains produce highly reactive free radicals.

The thermal degradation process as explained Aguado (2006) by fits to a radical chain reaction pathway and comprises of hydrogen transfer steps along with the progressive breakage of the polymer backbone (Aguado J, 2006). Furthermore, many authors have reviewed detailed mechanisms about the rubber pyrolysis reactions. For example, the thermal decomposition of natural rubber was studied by Domenico (1983) using pyrolysis gas chromatography at a set temperature of 500℃ (Dodds J. Domenico WF, 1983). They concluded that the dimer combinations of monomers that form in rubber pyrolysis result from a Diels-Alder mechanism. On the other hand, Mastral et al. (2000) proposed that another reaction pathway for tire conversion may occur through poly-isoprene de-polymerization and additional cyclisation (Mastral AM M. R., 2000).

Pakdel (1991) proposed that an iso-propene intermediate radical forms from a thermal decomposition through a β-scission mechanism. The isoprene intermediate radical is then transformed to isoprene de-propagation; these isoprene molecules in the gas phase combine together to form di-pentene (Pakdel H, 1991).

Waste tire pyrolysis involves intra-molecular free radical reactions altered with pyrolysis conditions. Reactions in tire pyrolysis have been categorized into three main groups by (Li S-Q, 2004). The primary pyrolysis reactions take place at temperatures between 250℃ and 520℃, as for the secondary post-cracking reactions of pyrolytic volatiles which greatly impact the Benzene-toluene-xylene (BTX) yields and pyrolytic carbon black gasifying reaction with $CO_2/H_2O/O_2$ that are found in the gases (Li S-Q, 2004). The impact each stage of the reaction can have on the overall pyrolysis process is related to two parameters: the reaction time and temperature.

Even though pyrolysis follows intricate routes that cannot be summarized by chemical reactions, the pyrolysis reaction scheme can be described based on a mass conservation law, which is represented in an empirical formula (Buekens, 2006)**.**

Table 2 Elemental reaction of a tire pyrolysis process (Buekens, 2006)

Waste tire 100 wt%	**Solid Fraction 40 wt% + Volatile fraction 60 wt%**
Elemental composition C=88.2 wt% H=6.97 wt% O=2.21 wt% N-0.59 wt% S=2.02 wt%	Elemental composition C=94.96 wt% H= 1.12 wt% S=3.41 wt%

It can be seen in Table 2 that waste tires are initially composed of hydrocarbons with main elements of: carbon, hydrogen, oxygen, nitrogen and sulfur. Under thermal treatment and an interval of time these compounds will decompose into fixed solid, carbon black, and volatile products that contain both heavy and light portions. Volatiles can reach a conversion of about 60% (Buekens, 2006).

2.5 Pyrolysis and parameters affecting tire pyrolysis

Pyrolysis is classified into many different categories, depending on operating conditions applied to the process, for example heating rate, volatiles residence time and reaction temperature. Pyrolysis processes are divided into two categories first of which is the general pyrolysis process, which is sub-divided into slow and fast pyrolysis. Juan Daniel Martinez (2013), classified pyrolysis on the basis of the type of environment the process is performed in (Juan Daniel Martinez, 2013). Classification can depend on the heating system as either microwave, plasma pyrolysis, or electrical. In addition, pyrolysis includes hydro-pyrolysis, steam-pyrolysis, oxidative pyrolysis and catalytic pyrolysis.

2.5.1 Slow pyrolysis

Gradual pyrolytic cracking takes place at low temperatures and at longer residence times with low heating rates. Longer residence times yield more thermally stable products, coke, and tar from secondary conversion of primary products. Char production is mainly studied in slow pyrolysis (Buekens, 2006).

2.5.2 Fast pyrolysis

In contrast to slow pyrolysis, quick pyrolytic cracking takes place at higher heating rates. Volatile products that are liberated quickly allow the formation of liquid products since they condense before they can be further broken down into simpler gaseous products at shorter residence times. A small particle sized feedstock is required during fast pyrolysis for quick removal of volatile products. What is then obtained is a liquid fuel having high calorific value. Fast pyrolysis is known to be an effective process for the production of liquid fuels, chemicals and derived products with better yields (Juan Daniel Martinez, 2013). The reaction time occurs in the order of milliseconds to seconds, and Bridgewater (2000) acknowledged that the residence time should be less than 2 seconds (Bridgewater AV, 2000). As for processes with higher residence times, they would behave similar to slow pyrolysis, where a reduction in volatile organic yields would result due to secondary reactions.

2.5.3 Catalytic Pyrolysis

The catalytic cracking of polymeric materials usually involves heating the material to temperatures higher than 450℃ in an inert environment with lower activation energies and better quality products. Reactions are also influenced by the inert gas flow rate, temperature and time. The addition of catalysts in pyrolysis processes can alter the quality of pyrolytic products and yields. For instance, Williams et al. (2002) mentioned that the addition of zeolite catalysts, Y-type and ZSM-5, produced single ring aromatic compounds in the liquid fractions including toluene, benzene and m-, p- and o-xylenes (Williams PT B. A.,

2002). Similarly, improvement of fuel properties and the yields of liquid fractions were found with the use of an expanded perlite as a catalyst (Y., 2011).

Zhang (2008) showed that lower pyrolysis temperatures were favored when NaOH was added (Zhang X, 2008). The productions of liquid fractions were enhanced to a yield of 49.7 wt.% at a temperature of 480℃ along with the increase of H_2 gas portions.

Dung (2009) reported that the use of Ru/MCM-41 catalyst increased the gas yield at the expense of the liquid yield (Dung NA, 2009). A Ni-Mg-Al (1:1:1) catalyst was used with a two-stage pyrolysis gasification process with waste tires at 500-800℃, an increase in H_2 and CO concentrations with a noticeable decrease in CH_4 and C_2-C_4 concentrations were observed (Elbaab IF, 2010). The addition of catalyst during the pyrolysis lowers the refining efforts of the final pyrolysis product.

2.6 Parameters affecting tire pyrolysis

Thermal degradation of waste tires is an endothermic activity that is controlled by temperature, therefore it has a great influence on pyrolysis (Juan Daniel Martinez, 2013). From a thermodynamic perspective, temperature is correlated to equilibrium conversion (X_e), for exothermic reactions; when temperature increases the equilibrium conversion decreases. As for endothermic reactions they are directly proportional conversions, as temperature increases, the equilibrium conversion increases and therefore temperature has a huge impact on both conversion and products formed (Juan Daniel Martinez, 2013).

Additionally, the overall heat transfer mechanism is also influenced by the heating rate, particle size and pyrolysis time. Therefore, gas, liquid and solid distributions and their physiochemical properties are effected (Juan Daniel Martinez, 2013). As mentioned earlier,

the presence of a carrier gas flow is an important parameter to consider since it controls the occurrence of secondary pyrolysis reactions, including re-condensation, thermal cracking re-polymerization and char formation (Juan Daniel Martinez, 2013).

2.6.1 Temperature

Temperature is a vital parameter in waste tire pyrolysis as it is an endothermic reaction which requires thermal energy (Juan Daniel Martinez, 2013). Mastral et al. (2000), Rodriguez (2001), Murillo (2006), Ucar (2005), Berrueco (2005), San Miguel (1998) and Laresgoiti (2000) have determined that the optimal temperature for waste tire pyrolysis is at 500℃ under atmospheric pressure where a total tire conversions could occur (Mastral AM M. R., 2000) (Rodriguez I, 2001) (Murillo R, 2006) (Ucar S, 2005) (Berrueco C, 2005) (San Miguel G, 1998) (Laresgoiti MF, 2000). The main tire compounds that remain in the pyrolytic carbon black processed at lower temperatures are SBR, BR and NR, with a heterogeneous gum like aspect (Rodriguez I, 2001). Although temperature plays a vital role in pyrolysis, the final effect of tire pyrolysis is achieved along with other parameters such as heating rate, pressure, and superficial velocity of the carrier gas. Therefore, if secondary reactions do not occur than the change of temperature is considered useless since it will not change product yields (W. Kaminsky, 1980) (Conesa JA, 1996) (Kaminsky W, 2009) (Lopez G O. M., 2010) (Placeholder1). Table 3 presents different product yields resulted from different experiments by several authors. No significant changes on product yields at various temperature ranges were recorded.

Table 3 No remarkable effect of temperature on pyrolysis product yields from literature (Juan Daniel Martinez, 2013)

Average product yields (wt.%)			Temperature range (℃)	Type of reactor	Experimental conditions
Gas	Liquid	Solid			
17.5	38.3	44.2	From 500 to 700	FBR	A piece of tire of 2-3cm (wide) pyrolyzed under N_2 at 100 cm^3/min and 15℃/min
6	61	33	From 415 to 500	Bench scale reactor	Pyrolysis under vacuum pressure, below 3 kPa
7.6	50.7	41.7	From 550 to 800	FBR	130g of scrap tire pyrolyzed at 7℃/min up to the desired temperature and hold for 1 hr
8	58.4	33.6			
6.8	53.1	40.1	From 500 to 1000	RKR	Particle size, 0.42mm. The sample 200g was heated at 5℃/min up to desired temperature at 500 mL/min of N_2

An increase in gas yield that occurs from the increase in temperature is directly correlated to the presence of secondary reactions. It is important to know that increase in gas yield occurs at the cost of the liquid yield (Y-M., 1996). Different authors recorded different effects of temperature on the product yields in pyrolysis and these are shown in Table 4.

Table 4 Effect of temperature on pyrolysis product yields in literature (Juan Daniel Martinez, 2013)

Average product yields (wt.%)			Temperature range (℃)	Type of reactor	Experimental conditions
Gas	Liquid	Solid			
17.9	41.4	40.6	600	AR	Mixture of tires from trucks, tractors and passenger cars with a particle size

					around 5 m, N_2 flow of 11.4 L_N/h
29.7	31.3	39	700		
31.5	27.5	41	800		
9	47	44	425	FBR	Motorcycle tires of 4 cm^3. The volatiles residence time was around 5 s(8 L/min of N_2)
10	49	41	475		
19	41	40	575		
4.5	58.1	37.4	450	FBR	Passenger car tires as feedstock pyrolyzed at 5°C/min. The maximum residence time in the reactor was around 120s
5.2	56.9	37.8	525		
8.9	53.1	38	600		
6	55.4	38.6	500	FBR	4 g of scrap tires(passenger car tire) were pyrolyzed at 75 cm^3/min
10.8	52.2	37	600		
26.7	36.6	36.7	700		
14	46	38	500	FBR	N_2 as a carrier gas. Similar trend using CO_2
18	43	38	600		
22	38	38	700		
2.4	38.1	49.1	550	RKR	Pilot plant working with a light over-pressure (maximum working pressure of 300mm w.c.): 4.8 kg/h of feeding rate and 1.4 m^3/h of N_2
8.2	33	47.4	600		
10.7	31.8	48.9	680		

The increase in pyrolysis temperatures can also influence the increase of solid fractions. The formation of solid fractions is preferred at high temperatures since it is able to absorb volatile compounds on the surface of pyrolytic char and forms fixed carbon material. The formation of this carbonaceous material is possible in reactors where there is direct gas solid contact by secondary reactions at high heating rates (W. Kaminsky, 1980) (Conesa JA, 1996) (Kaminsky W, 2009) (Lopez G O. M., 2010).

To better understand the relationship between temperature and different parameters, three cases are further looked into. Figure 2 (a) illustrates the first case where the liquid, solid and gas yield show no change with the increase of temperature, therefore no secondary reaction is taking place.

The second case portrays the gas yield increase at the expense of liquid yield which drops in return and solid yield remains constant figure 2 (b). Usual variations of all of the three pyrolytic yields are demonstrated in part (c) of figure 2, which are in the presence of dynamic gas-solid contact. The gas portion increases while the liquid fraction decreases and secondary reactions take place in the solid portion.

2.6.1.1. Temperature effect on liquid yield

It is critical to know that quality of produced pyrolytic oil is heavily affected by temperature. Literature demonstrates that as temperature increases the composition of liquid

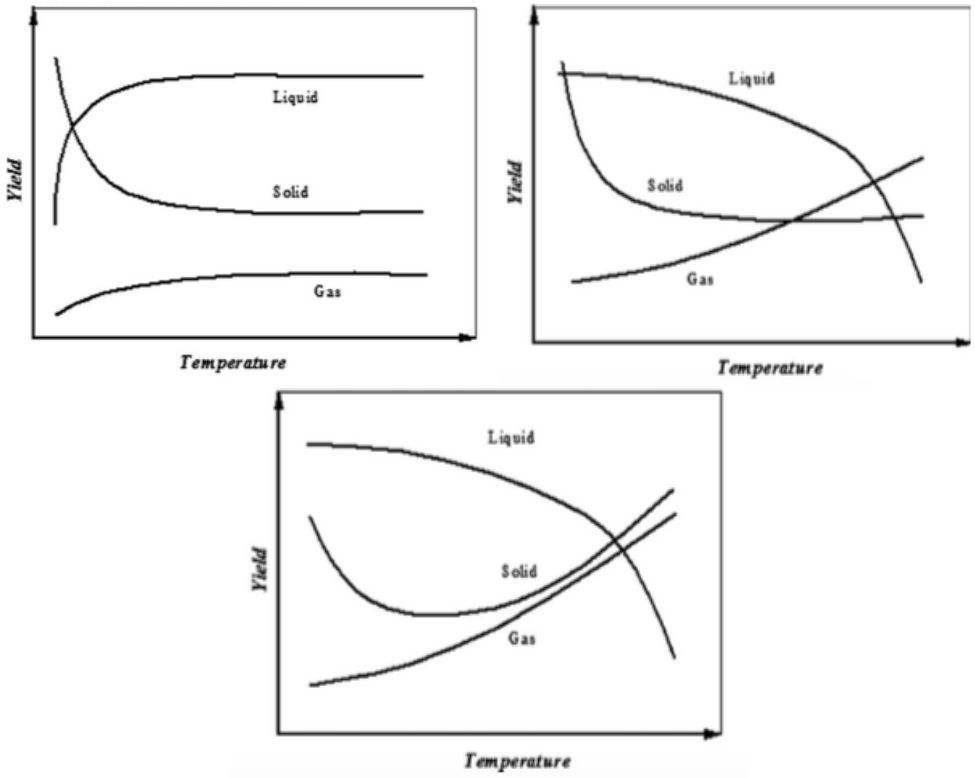

Figure 2 (a) Top Left; Constant solid, liquid and gas yield, (b) Top Right; Constant solid, liquid yield decreases and gas yield increases and (c) Bottom Image; Solid and gas yields increase and liquid decreases (Juan Daniel Martinez, 2013) (Juan Daniel Martinez, 2013) (Juan Daniel Martinez, 2013)

fraction would change from a majority of aliphatic compounds to aromatic compounds at higher temperatures (Williams PT B. S., 1995); (Cunliffe Am, 1998)**.** Cunliffe (1998) illustrated his finding that liquid fractions at 600℃ mostly contain aliphatic compounds (Cunliffe Am, 1998). Meanwhile, at 700℃ aromatic compounds were more dominant. Olefinic acid and di-olefinic hydrocarbons were found at lower temperatures, they are known to be undesirable in gasoline (Juan Daniel Martinez, 2013). Note that the tendency of having aromatic compounds is not strictly governed by temperature, but is associated to the presence of secondary reactions in the liquid phase.

2.6.1.2. Temperature effect on gas fraction

Two important aspects of gas fraction are tested and they are the yield and the composition. This highlights the influence of temperature on the gas fraction. The gas fraction behaves similar to the liquid yield where the difference of each gas yield production and composition is due to the existence of secondary reactions (Juan Daniel Martinez, 2013). Many authors recognized that by changing operating temperatures a change in simpler compounds such as methane and hydrogen gases were detected when compared to other complex hydrocarbons. Therefore, gaseous compositions and calorific values changed.

Some authors stated that simpler hydrocarbons would be found in the gas yield rather than heavier ones. They determined that compounds such as CO_2, C_2H_6, C_3H_6, and C_4H_6, hydrocarbons and their calorific values drop as temperature surges (Diez C. Martinez O, 2004). Additionally, the total yield of a gas fraction would increase as temperature increases, yielding a greater portion of simpler hydrocarbons in the gas yield.

As reported by Diez et al. (2004), as temperature increases from 350℃ to 550℃ the gas yield increases from 20 wt.% to 29 wt.% (Diez C. Martinez O, 2004). Similarly, gas yields increase from 6.3 wt.% to 37.1 wt.% as temperature increases from 600℃ to 800℃ (Conesa JA, 1996). To sum up, temperature complemented with secondary reactions is considered to be a governing parameter that affects both the gas yield quality as well as the composition.

2.6.1.3. Temperature factor on solid fraction

(a) and (b) shown in figure 2 show the solid composition is constant as the temperature increases. That is not always the case as solid fractions are reflected to decrease as temperature increases or in other cases the char yield of pyrolysis might increase as the process temperature increases. The latter (c) shown in figure 2, where the solid yield increases as a result of the secondary reactions and char formation (Ogasawara S, 1987); (Lehmann CMB, 1998).

The governing parameter, temperature, and its effect on physical properties of the solid fraction such as the pore size and surface area is still a debate among researchers. Fernandez et al. (2012)Reported that an increase of temperature is insignificant on the surface area and on pore sizes (Fernandez AM, 2012). Carbon black extracted from pyrolysis was studied and had a constant mesopore aspect (2-50nm) and a constant change in BET surface area, which were 68 m^2/g and 61 m^2/g in a temperature of 550℃ and 900℃ respectively.

2.6.2 Particle size

The influence of scrap tire particle size has not been looked into deeply due to the fact that most studies found on pyrolysis are fast pyrolysis reactions. The particle size if small has an isothermal behavior and particles that are larger have an opposite behavior (Larsen MB, 2006). This could be explained by the effect of particle sizes on heat transfer and temperature gradients (Beaumontt O, 1984). Therefore, coarser particle tires impose heat limitations for their degradation in pyrolysis reactions (Islam MR, 2008). In that way some tire parts cannot be targeted, this is not the case for smaller particles. Consequently,

initiating a reaction with coarser particles would result in lower liquid and gas yields assuming that a similar reaction is performed on smaller particles at a fixed time. Literature made it clear that a reduced size in tire particles would allow for more reaction area, which alternately lowers char and increases secondary reactions and hence gas yields. Therefore, yields and tire particle sizes are inversely proportional. Many pyrolysis reactions are therefore performed with the use of smaller particle sizes in order to attain higher conversions from primary reactions and to minimize mass and energy effects.

2.6.3 Carrier gas flow

Carrier gas flow rates and types impact the quality and quantity of products from pyrolysis reactions. Whether the reaction is slow or fast directly correlates to the occurrence of secondary reactions such as thermal cracking, re-condensation and the formation of char (Williams PT B. S., 1990). The presence of a carrier gas eliminates the presence of oxygen, which may cause oxidation, and the higher the flow rates the lower the occurrence of secondary reactions, due to the shorter residence times of the volatiles in the reactor.

As for the type of carrier gas, non-inert has proven to cause different homogeneous and heterogeneous secondary reactions (Juan Daniel Martinez, 2013). Kaminsky et al. (2009) used steam as a carrier gas and noticed an increase in C_2H_4 and C_3H_6 compounds. On the other hand, Lucchesi and Maschio (1983) used CO_2 and determined that there was a significant desulphurization effect on both the liquid and solid products (Lucchesi A, 1983). Mastral et al. (2000) stated that no noteworthy differences were noticed when N_2 was used as a carrier gas (Mastral Am, 2000).

2.7 Gasification

Gasification is an efficient and flexible practice for handling biomass. Through it 60-90% of energy content can be transformed into syngas such as carbon monoxide and hydrogen as well as other byproducts like tar (T.B. reed, 1988). It has been reported that ethanol has been identified to produce hydrogen through steam reforming (Shuang Jia, 2017). Ethanol is known to be low in toxicity relative to methanol and contains a significant hydrogen source which can be produced from biomass (Shuang Jia, 2017). Through gasification with ethanol at elevated temperatures and with biomass several reactions occur (Shuang Jia, 2017); (P. Parthasarathy, 2014):

Water gas reaction: $C + H_2O \rightarrow H_2 + CO$

Water gas shift reaction: $CO + CO_2 \leftrightarrow H_2 + CO_2$ and

Boudouard reaction: $C + CO_2 \rightarrow CO$

In addition to the reactions illustrated in figure 61.

Increase in hydrogen is mainly due to the water gas reaction and the water shift reaction at elevated temperatures. However, hydrogen decrease can also be observed due to the equilibrium shift in the water gas shift reaction. Boudouard can also cause a hydrogen decrease due to carbon consumption (Shuang Jia, 2017). Reforming reactions of ethanol during bio-char gasification can be divided into two optimum stages and they are the decomposition stage and the reforming stage. During reforming decomposed gases are reformed into the water gas shift reaction and boudouard reaction (Shuang Jia, 2017). Catalyst can be added in the same reactor under gasification as a primary catalyst or in a downstream reactor as a secondary catalyst to get rid of tar or further breakdown volatile products (Matthew E., 2018).

2.7.1 Catalytic cracking under gasification

Nobel metal-based catalysts such as nickel, palladium, and platinum have been proven to be extremely effective for cracking tar (K.Tomishige, 2003); (Y.F. Shen, 2014). These catalysts can be very expensive and highly toxic, which therefore makes them less feasible for gasification technologies that consumes large quantities of biomass or tire waste (A. Orio, 1997). Miccio (2009) suggested that dolomite, magnesite and olivine are cheap natural mineral based substitute catalysts for gas conditioning (F. Miccio, 2009). Dolomite has been used as a tar cracking catalyst for many biomass gasification experiments (F. Miccio, 2009); (P.A.Simell, 1997). (L.Devi K. P., 2005) reviewed the effect of calcined dolomite, sand and untreated olivine in secondary reactors downstream for biomass gasification. The results were studied through GC and it showed that calcined dolomite was able to reduce the total amount of PAHs by 90% (L.Devi K. P., 2005). Delagado (1997) emphasized that calcined dolomite was effective in producing high gas yields (J.Delgado, 1997). Several other authors confirmed the effectiveness of calcined dolomite. Apart from being a good catalyst for gas yields, calcined dolomite went through abrasion and disintegration (F. Miccio, 2009); (S. Rapagna, 2000); (S. Koppatz, 2009). Tingting (2019) performed gasification experiments with zeolite catalysts to crack ethanol at reaction temperatures of 500℃ (Tingting Zhao, 2019). The liquid products obtained from the cracking mechanisms were olefinic compounds. An intramolecular dehydration reaction occurs which converts ethanol to ethene or C_2H_4 or to $CH_3CH_2OCH_2CH_3$ (Tingting Zhao, 2019). An oligomerization reaction that occurs between ethylene and a carbene radical could convert ethanol to C_3H_6. Ethanol through dimerization could be converted to C_4H_8.

C_3H_6 along with C_4H_8 could form aromatics and cycloparaffns through a series of dehydrogenation, cyclization and aromatization reactions (Tingting Zhao, 2019).

2.8 Energy and the Environment

Pyrolysis is an energy intense waste-to-energy process. Therefore it is vital to understand the conversion process in order to perform it keeping the environment and energy requirements a priority.

2.8.1 Energy

Energy required during pyrolysis processes is equivalent to the enthalpy due to the change of temperature from ambient to the operating temperature (Daugaard, 2003). Phase change energies needed for reaction energy of hydrocarbon cracking to occur are taken into account and are termed as reaction enthalpies (Daugaard, 2003). There are many sources of energy adopted during pyrolysis, including: (i) electric heating, (ii) burning of auxiliary fuel, and (iii) burning of pyrolysis gas/ solid fractions.

The pyrolysis process of waste tires is recognized as an overall endothermic process involving a sequence of exothermic and endothermic reactions (Collins L, 1974) (Yang J, 1996)**;** (Aguado R, 2005)**;** (Cheung K-Y, 2011). Exothermic reactions take place prior to endothermic reactions, it is assigned to chemical reactions that take place at early stages of the process, and therefore the endothermic reactions are represented as vaporization of the pyrolysis products (Yang J, 1996). In simpler terms, the primary products, at the beginning of the pyrolysis process, are cracked into smaller fractions under an exothermic reaction. Primary products can be cracked into smaller fractions forming secondary products and vaporizing. The formation of secondary products and vaporization is assisted with

endothermic reactions (Cheung K-Y, 2011)**.** It is important to note that energy demands for pyrolysis are dominantly influenced by endothermic reactions. Yang (1996) quantitatively measured the enthalpy change during atmospheric pyrolysis for natural rubber, SBR and BR tires. The total enthalpy change was 870, 550 and 325 kJ kg^{-1} for natural rubbers, SBR and BR respectively (Yang J, 1996).

An important property that should be pointed out is that in addition to waste tire process being dominated by endothermic reactions, energy efficiency may also include the energy that's linked to feedstock production (Laird DA, 2009). Gomez (2009) stated that endothermic reactions or vaporization is considered to be the most demanding features in a pyrolysis reaction, regardless of other demands (Gomez C, 2009). Based on the heat combustion of tires, the net energy balance for waste tire pyrolysis proposed that the net energy recovery could reach up to 75-82% (Dodds J. Domenico WF, 1983).

2.8.2 Environment

Waste tire pyrolysis is considered to be a cleaner recycling process in comparison to other thermal processes like incineration (Aylon E. C., 2005); (Aylon E. F.-C., 2010) (Galvagno, 2002); (Murillo R. A., 2006a). Hence, pyrolysis has always been a great interest for researchers in terms of the environment. Lower amount of emissions is released into the environment as well as useful solid and liquid products from waste material are easily recovered. Accordingly, these products obtained from pyrolysis can be further used in applications such as new fuel products. As for gases produced from pyrolysis reactions, they are considered to be cleaner in comparison to gases produced from combustion and therefore less gas cleaning systems are required (Sinn, 1976).

Malkow (2004) stated that hazardous traces, found in air emissions, such as dioxins, dibenzofurans and thermal NO_x are greatly minimized during pyrolysis (Malkow, 2004). Bennet (1993) completed this theory and stated that no emissions of that type are found from pyrolysis units (Bennett, 1993). Lloyd (2006) stated that the main reason these toxins are not found is due to the absence of oxygen during reaction processes and therefore prevents partial oxidation of waste tires (Lloyd, 2006). Minor volatile organic compound emissions have been recorded due to leakage of pipe joints and shafts. One of the most important critical points in pyrolysis is CO_2 gas emission. International Energy Agency (2009) indicated that the use of pyrolysis products emitted less CO_2 emissions per unit energy when compared with waste tire combustion (International Energy Agency, 2009). The interaction of solid products during combustion of fossil fuels, produce aromatic compounds which are known as Polycyclic Aromatic Hydrocarbons PAH. PAH's were carefully studied during tire pyrolysis and it became apparent that lower amount of PAHs were recorded during pyrolysis due to the absence of solid material in the volatile fraction.

The removal of hazardous compounds such as sulfur and zinc, are not as much of an issue in pyrolysis in comparison to other techniques. A great amount of sulfur is found in the solid product fraction of waste tires (70 wt.%) and the rest is divided amongst liquid and gas fractions (Rezaiyan J. a., 2005); (Unapumnuk, 2008). Zinc on the other hand, has a boiling point of approximately 901℃; therefore it is not a problem for pyrolysis as reaction temperatures are not as high (Conesa, 2004).

All in all, from an environmental and economical perspective, waste tire pyrolysis is considered to be a feasible waste minimization technology. (Murillo R. A., 2006b) discussed the economic importance of the direct usage of three pyrolysis products, char,

liquid and gas classifies pyrolysis as economically sustainable. Therefore, there is a great opportunity to improve waste tire pyrolysis processes in order to achieve high product quality and enhance the composition of the derived fuel with the application of advanced catalysts.

2.9 Catalysis

Catalytic pyrolysis can be conducted in the presence of many different heterogeneous catalysts to further promote polymer cracking. The non-condensable part of the volatile portion of the tire can be additionally cracked in the presence of a catalyst and therefore results in an increase in the gas yield. There are many different types of catalysts that are applied during pyrolysis with different selectivity and stability towards certain products. Acidic catalysts will be the main focus in this work.

2.9.1 Acidic Catalysts

Zeolites are a class of acidic solid catalysts. Natural Zeolites or crystalline solids are known to be produced from the reaction that takes place between hot lava, which contains molten rock from volcanoes and sea water over the course of many years (De'Gennaro, 2000). They are known to be oxide metals fused with crystalline alumina-silicates within a microporous configuration (Ertl, 1997). A fundamental structure of all zeolites is an alumina-silicate framework with voids and channels where water cations and other molecules may reside. Axel Frederick Cronstedt, a Swedish mineralogist, discovered zeolites in 1756. The usefulness of microporous properties of zeolites in many applications was recognized later in the 19th century. Conversely, a series of zeolites with low Si/Al weight ratios were hydrothermally synthesized in the 1940s, through the imitation of the

geothermal growth of natural zeolites (Ruren Xu, 2007). There are many different forms of zeolites and those that are of interest in different applications are modenite, offertite, erionite, faujasite and chabazite. Zeolites are made up of layered minerals consisting of silica and alumina building units surrounded by oxygen atoms at the edges. The framework consists of SiO_4 tetrahedra and an octahedra containing AlO_4. The tetrahedral and octahedral when combined in different configurations come up with different crystalline structures.

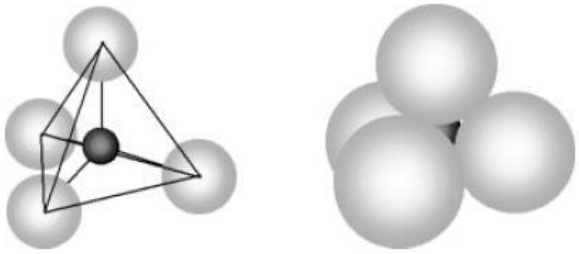

Figure 3 SiO4 tetrahedra building unit (Chorkendorff, 2003)

These silicate units can be structured in different configurations having four, six, eight or twelve membered rings. When these tetrahedra's are inter-connected they form a structure able to allow molecules to enter, and allow for the easy drift of resident molecules into or out of the structure. Positively charged cations that reside in the voids, compensate for the negatively aluminosilicate framework. John Paul Vas (2017) mentioned, that acidic catalysts have better efficiencies compared to catalysts with less acidity, and also the pore size, Si/Al ratio and the catalyst structure all determine the catalysts performance (John Paul Vas, 2017).

Zeolites differ in their structural arrangements; for example the Beta zeolite (BEA) has superimposed porous channels. The pore channels and windows contain surface protons H-$^{+}$, where the entering reactants will react and therefore exit the channels as new species. Zeolite beta is made up of two distinct but relatively close structures which are the polymophs A and B that have complete three dimensional pores with 12-rings. Figure 4 below illustrates the beta zeolite framework.

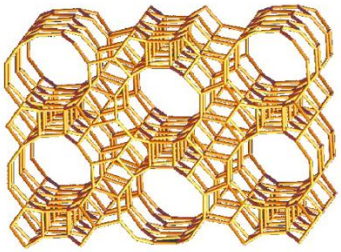

Figure 4 Hbeta zeolite framework (Albayati, 2014)

The type of zeolite catalyst that is of concern to this work is the H-type zeolite catalyst. The H-type zeolite has an acidic surface of either Bronsted or Lewis acid property sites. The Bronsted acid sites are due to protons attached to oxygen atoms and form –OH groups in the tetrahedra. This happens when (Si^{4+}) is replaced by (Al^{3+}) in the tetrahedra structure. In a framework tetrahedra Si has a charge of 4^{+} and is connected with the coordinating oxygen atoms that have a charge of 2^{-}, which leads the unit to have a neutral formal charge ($SiO_{4/2}$). However, the formal charge would change from 0 to -1 once Al replaces Si because it has the charge of +3 ($AlO_{4/2}$) (Cejka J. C., 2010).

Consequently, in order to neutralize the formed charge a cation is added to compensate the net charge. The cation can either be sodium (Na^{+}) or hydrogen (H^{+}). When the hydrogen proton is added the zeolite would be in the form H-X where X defines the

zeolite type that is if it is ZSM or Beta. The location of the hydrogen is known to be a Bronsted acid site with the tendency to donate a hydrogen proton. Figure 5 displays the Bronsted acid site of a zeolite formed on the tetrahedral.

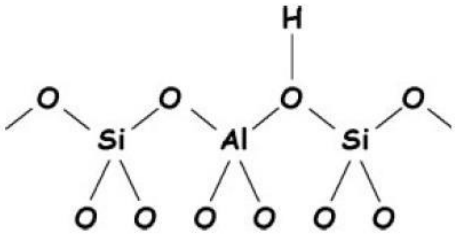

Figure 5 Bronsted Acid site of Zeolite (Chorkendorff, 2003)

The Bronsted acid site that is formed by the hydroxyl proton located on the oxygen bridge connecting the silica and aluminum is weakly bonded and is responsible for the zeolite high catalytic activity (Cejka J. C., 2010). There are some cases where the position of the aluminum atom in the tetrahedra can be replaced by a metal such as iron (Fe). Acidity strength of the bridging hydroxyl proton is greatly affected by the type of substituted metal and bond angle of the bridge. Therefore, the entire composition of the framework has an overall influence on the acidity strength. In short, in order for a zeolite to have a higher acidic strength it should have higher mean electronegativity, therefore, lowering the existence of Al atoms (Cejka J. C., 2010). Komadel (2006) found that the increase of Al atoms will simultaneously increase the hydroxyl protons which represent the acidic sites, however, proton crowding can occur, a phenomena that occurs due to having many Bronsted acid sites, and therefore will weaken the acidic strength (P. Komadel, 2006). Hydroxyl groups can be found in different forms other than bridging, due to the different types of treatment methods.

On another note, Lewis acid sites are produced by tough heat treatment at high temperatures. The high temperature causes dehydroxylation of the Bronsted acid sites and forms the Lewis acid sites. Lewis acid sites can also be formed due to the extra-framework aluminum types such as AlO^+ and Al(OH) as consequence of dealumination. The "true Lewis acid site" is known as the AlO^+ unit, which migrates from the zeolite framework to behave as a cationic extra-framework species (Kuhl G. , 1977); (Kuhl G. H., 1999). The Lewis acid sites that are on the extra-framework of a zeolite are found on a positively charged silicon species that is found near a tri-coordinated aluminum atom. The positively strong silicon species found on the extra-framework has the ability to receive an electron pair and hence act as a strong Lewis acid site (Cejka J. C., 2010). Gonzales (1997) suggested that the extra framework is derived from de-hydroxylation as shown in figure 6 (Gonzales, 1997).

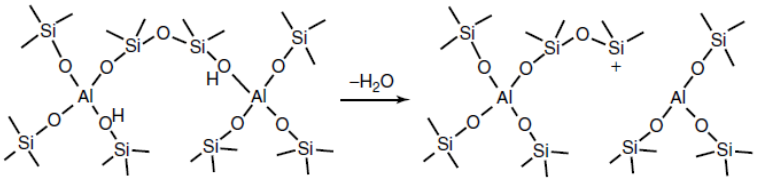

Figure 6 Formation of Lewis Acid extra-framework by dehydroxylation (Cejka J. C., 2010)

The framework Lewis sites act as strong electron withdrawing centers for neighboring bridging OH groups and create Bronsted acid sites with very high strength (Cejka J. C., 2010).

Zeolites in 1959-1970 and were classified according to their Si/Al ratio into three different groups aluminum rich zeolites, intermediate silica zeolites and zeolites that are high in silica (Ribeiro, 1984). Aluminum rich zeolites such as zeolites A and X are

commonly used as adsorbents. These zeolites are made up of a good composition, channel structure and pore volume. his framework is said to have the highest amount of aluminum and therefore has a saturated composition, with a Si and Al ratio Si/Al≈1. Due to the high Al content, these zeolites then have a very high number of cation ion exchange sites, in order to keep the framework in balance, and therefore very high exchange capacities.

Intermediate silica zeolites are formed with tetrahedral aluminum positions of zeolites, which stipulate instability of the structure towards attacks from water or acid sites. Therefore synthetic zeolites that are modified to have better stability properties possess a higher Si/Al ratio of about 3-5. This shows that zeolites with high Si content are needed to improve the thermal and acidic stability of the framework. Type Y zeolite is a commercially used zeolite for catalytic cracking of hydrocarbons, and acquires similar framework as zeolite X which is what made zeolite Y valuable in catalytic applications (Ribeiro, 1984). Mordenite is another important synthetic zeolite, which was able to acquire a Si/Al ratio of ≈5; this increased the thermal and acid stability as well as altered the structure and composition of the zeolite which then classified mordenite to be useful in both adsorption and catalytic applications. Figure 7 is a representation of mordenite, the yellow tetrahedra representing the SiO_4 and AlO_3 is represented as the light blue tetrahedra.

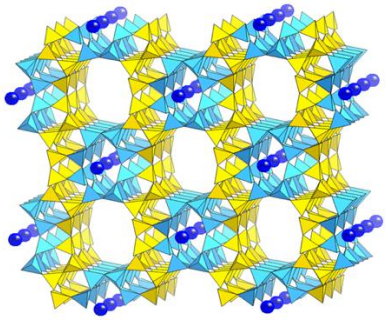

Figure 7 Zeolite mineral Mordenite

High silica zeolite compositions were developed in the early 1970s (Ribeiro, 1984). Zeolite beta and ZSM-5 are considered to be high silica zeolites with Si/Al ratios varying from 10-100 or even higher with changes in surface characteristics. In comparison to the low and intermediate silica zeolites that represent a heterogeneous porous structure, the zeolite with high silica has a surface that is more homogeneous with the characteristic of having more organophilic-hydrophobic selectivity. This means that they weakly interact with water and polar molecules and have a stronger affinity towards organic molecules (Michel Guisnet, 2002). In figure 8 the blue tiles represent channels inside of the structure. Adding on to the surface selectivity, high silica zeolites still contain amounts of aluminum in the framework. The existence of aluminum in the complementary stoichiometric cation exchange locations allow the introduction of acidic OH- groups over zeolites ion exchange reactions which are necessary for the improvement of acid hydrocarbon catalytic properties. However these acid catalytic properties are considered to be very weak.

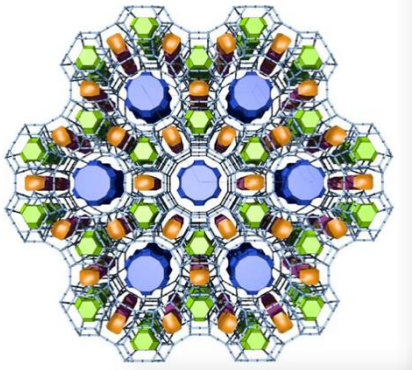

Figure 8 High in Silica Zeolite (Rabo, 2001)

Zeolite catalysis dominated catalytic cracking and hydrocracking as its first industrial applications (Rosinski, 1992); (Rabo, 2001). An important property of a zeolite

as a cracking catalyst is its crystallographic unit-cell size, which is a close measure of the aluminum content in the zeolite framework and therefore is commonly taken as a close measure of its acidity (Cejka J. C., 2010). Therefore, it has a great influence on the yield distributions and product quality. Catalytic reactions take place to convert heavy fractions of crude oil, in FCC, to produce middle distillates (Cejka J. C., 2010). It is vital to understand the reactions that take place in catalytic cracking. These reactions involve the appearance of carbonium and carbenium ion intermediates (Chorkendorff, 2003).

In the initial protonation step, carbonium ions are generated from alkanes,

$$H^+ + C_nH_{2n+2} \rightarrow [C_nH_{2n+3}]^+ \quad [1]$$

The carbonium ion is known to be chemically unstable and therefore it is converted to carbenium ion:

$$[C_nH_{2n+3}]^+ \rightarrow H_2 + [C_nH_{2n+1}]^+ \ [2]$$

Therefore, the cracking step appears as:

$$[C_nH_{2n+3}]^+ \rightarrow C_xH_{2x} + [C_{n-x}H_{2n-2x-1}]^+ \ [3]$$

The adsorbed carbenium ion allows for other hydrocarbons to be included in the reaction:

$$[C_mH_{2m+2}]^+ + [C_nH_{2n+1}]^+_{ads} \rightarrow C_nH_{2n+1} + [C_mH_{2m+1}]^+_{ads} \ [4]$$

Catalysis can be divided into two different roles, those catalysts with acidic supports and those with metal sites. So acid catalysts are altered into bi-functional catalysts with metal doping in order to alter the catalytic reactions occurring from heterogeneous catalyst. The dividing role between acidic sites and metal sites is that, the acidic sites are known to

handle both isomerization and cracking of large hydrocarbons. On the other hand the metallic sites perform dehydrogenation, hydrogenation and to a certain limit aromatization.

2.10 Natural- Synthetic zeolites

Zeolites acquire properties such as high concentration of active sites, high thermal stability, and high size selectivity and therefore are widely used in the petrochemical industry. Though natural zeolites are of great interest, their occurrence in natural form grant them limited use. That is because they most often contain undesired impurities, their chemical structure changes from one deposit to another and also nature has not adjusted their structure for catalytic purposes. Synthetic zeolites are more commonly used commercially due to the purity of their crystalline structure. These zeolites are generally synthesized from cheap silica-alumina, through hydrothermal conditions, similar to clays (Oghenejoboh K M, 2011); (Atta, 2012). The formation of synthetic zeolite from clay material is equivalent to the formation of natural zeolites from natural volcanic deposits or other Si-Al materials (Koukouzas, 2007). This is true because natural clay as well as volcanic ash contain large amounts of alumina-silicate glass. The use of clay to synthesize zeolites replicating “natural zeolites” is a much more cost and time efficient process, since the formation of natural clay can take thousands of years. Kaolin and other types of clays such as smectite, montmorillonite and bentonite are used for the synthesis of zeolites (Emam, 2013). The properties of these clays, which classify them as useful catalysts, are (Rodrigues, 2003); the modification of the original crystalline structure, the unsymmetrical morphology and sizes of the particles and the change of the basal spacing by acid treatment

and modification. Table 5 demonstrates some properties of Kaolin and Smectite clays (Emam, 2013).

Table 5 Different Clay Properties (Emam, 2013)

Kaolin	Smectite
1:1 Layer	2:1 layer
White or near white	Tan, olive green, white
Little substitution	Octahedral and tetrahedral substitution
Minimal layer charge	High layer charge
Low base exchange capacity	High base exchange capacity
Low surface area	Very high surface area
Low viscosity	Very high viscosity

2.10.1 Kaolinite

2.10.1.1 Clay structure

Kaolin is a naturally occurring alumina-silicate with a sheet structure that has SiO_4 tetrahedron and octahedron of $Al(OH)_3$. The arrangement of octahedral and tetrahedral layers creates major differences in both chemical and physical properties of kaolin. Kaolin is a vital industrial clay mineral with a composition of $Al_2Si_2O_5(OH)_4$ (Oghenejoboh K M, 2011)**.** Kaolin has a 1:1 structure meaning one tetrahedral sheet is linked through oxygen

atoms to an octahedral sheet of alumina, (figure 9). This type of structure grants kaolin low surface areas as well as a low surface charge in comparison to smectites. Kaolinite is one of the most commonly used kaolin clays and is considered to be comparatively pure and therefore commercially useable. Kaolinite is known to have many physical and chemical attributes that make it useful in a wide range of applications (Emam, 2013).

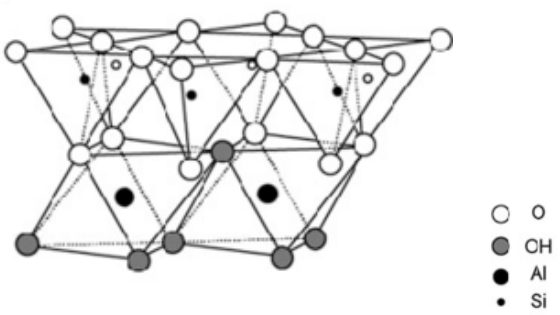

Figure 9 Kaolinite Structure (Shuji Tamamura, 2014)

2.10.1.2 Applications

Many catalysts are used at extreme pressure and temperature conditions and kaolin obtains a character that classifies it suitable for such applications. Hence, kaolin is used in manufacturing many catalysts that are used for different applications. Kaolin is greatly used as a substrate layer in catalysts made for catalytic cracking of petroleum (Murray, 2007) (Rong T-J, 2002). However, kaolin must contain minimal amounts of impurities such as titanium, alkali and alkaline earth metals when used for the catalytic cracking of petroleum. It has been known to be the most important raw material placed in a matrix along with a zeolite for a catalyst in a Fluid Catalytic Cracking (FCC) process (Goncalves. M. L. A.) (Hosseinpour N, 2009); (Tan Q, 2007). The matrix assists with a series of functions such

as: physical strength to the microspheres, resistance to attrition needed to handle stresses as well as protect the zeolite from erosion. Most importantly, the matrix acts as a cracking element for the gas-oil compounds, which are too bulky to pass through the pores of the zeolite (Hayward, 1991). Kaolin, being a part of a matrix, plays a large role in achieving high composition yields as well as reduced coke yield. Other than being introduced as a matrix with zeolites kaolin's have also been used to synthesize zeolites. There are many parameters that affect the formation of zeolites from kaolin such as added water, temperature, and ageing time. Prepared zeolites from kaolin are generally contaminated by trace amounts of calcium, titanium, iron and magnesium, these of which are initially found in kaolin. These contaminants may affect the zeolites physical or chemical properties. Zeolites X-, Y- and ZSM-5 are some of the zeolites that are formed from kaolin.

2.10.2 Smectite: Bentonite and montmorillonite

2.10.2.1 Clay structure

The Smectite mineral is termed as a (2:1) layer mineral. It is constituted of two silica tetrahedral sheets and one octahedral sheet with water molecules and cations inhabiting the space between layers (Emam, 2013) figure 10. The name smectite is given to a unit of silicates with Na, Ca, Fe, Mg and Li-Al (Murray, 2007)**.** Commonly used smectites include Na-montmorillonite and Ca-montmorillonite (Murray, 2007); (Jankovic L, 2010) with the latter being the leading smectite mineral and commonly found in many areas around the world**.** Smectites are classified as dominant components of bentonite clay, which is a clay that is reformed from volcanic ash (Emam, 2013). Bentonite when used in the industry is usually made up of Ca-montmorillonite, Na-montmorillonite with maybe

some saponite and hectorite (Naaman, 2012); (H, 1999)**.**

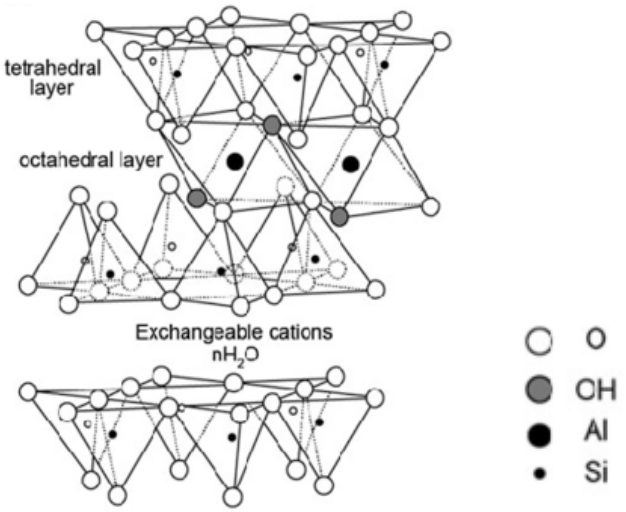

Figure 10 Smectite structure (Shuji Tamamura, 2014)

2.10.2.2 Applications

Acid-modified montmorillonites are broadly used as commercial heterogeneous catalysts for many different applications including petroleum-cracking reactions (T., 2010). Montmorillonite clays are strong acids, not corrosive, are low in cost, have minor reaction conditions and acquire high yield and selectivity (Choudhury T, 2011); (Hart, 2004). Their effectiveness has also been proven in cation exchange to protonate numerous organic species.

2.11 Clay Modified Catalysts

An important setback of using clays as catalysts is when they are exposed to high temperatures their structure collapses and therefore deactivate. Clays may have difficulty to catalyze reactions in polar or non-polar media. A clays structure, composition and texture can be modified to govern the catalytic behavior for a certain reaction. Modifications can

be thermal or acid modifications in order to alter structural properties, enhance acidity, surface area, porosity and thermal stability.

2.11.1 Thermally Modified Clays

Studies have shown that clay catalysts contain both Lewis and Bronsted acid sites (Kaur N, 2012)**.** The Bronsted acid sites are primarily associated with the inner area and the Lewis acid sites are associated with edge sites. Nevertheless, Bronsted acidity is primarily due to the separation of adsorbed water between sheet layers. So, the quantity of water between sheets greatly influences clay acidity (Emam, 2013). Size and charge of cations, Al^{3+} and Fe^{3+}, affect the polarizing power and therefore simultaneously separation. Different acidities can be achieved by thermal treatment of clay and hence different treatment temperatures determine the type and concentration of occurring hydroxyl groups and therefore the acidity (Herrero J, 1990). Temperature needs to be carefully controlled to avoid the collapse of clay structure. For example, heating at a temperature of 200-300℃ would cause the collapse of the interlayer structure of the clay as all the water is driven out and therefore simultaneously decreasing Bronsted acidity (Guggenheim S, 2001). However, at a controlled temperature of 100℃, minimal amount of water remains in the layers and the rest is driven out causing an increase in Bronsted acidity (Guggenheim S, 2001). For the former case, when Bronsted acidity decreases clay acts as a more defined Lewis acid entity, which is caused by the conversion of Bronsted acidity to Lewis acidity.

The effect of calcination of clay depends on the type of silicate layer. Montmorillonite are octahedral-substituted and therefore the vacancies of the octahedral sites would accept transferring protons and hence connect with the lattice oxygen (Emam,

2013). The surface tetrahedral sheet of the structure contains a small diameter and therefore these protons would not be reachable to catalysis. Thus, after calcination these acidic sites would be situated at the edges of the structure. As for clays with tetrahedral substitution, calcination causes protons to connect with the surface oxygen's of the sheet (Emam, 2013). This phenomena results in acidic sites that are comparable to Bronsted acid sites on a Y-zeolite (Kellendonk F J A., 1987).

2.11.1.1. Thermal Modified Montmorillonite

Plee D (1985) pillared montmorillonite and observed that its acidity is much less than that of a Y-zeolite (Plee D, 1985). After characterization of the montmorillonite with 1R spectroscopy, (Plee D, 1985) demonstrated that montmorillonite had low acidity, which therefore mainly corresponds to the Lewis type.

2.11.1.2. Thermal Modified Kaolin

After calcination of kaolinite and dickite, they were tested on catalytic cracking and were studied by (Rong T-J, 2002). They determine that the chemical composition of kaolinite remained unchanged, except for the removal of some impurities. Therefore, Rong T-J (2002) concluded that the action of kaolin-group minerals in catalytic cracking isn't related to their chemical composition and thus to their structure such as their pore size, surface area, and pore volume (Rong T-J, 2002).

2.11.2 Acid Modified Clays

Acid-modified clays can behave as heterogeneous catalysts and are seen as solid acids (Emam, 2013). Acid-modified clays are treated with concentrated acids such as

Hydrochloric acid or Sulfuric acid. The acid alters the surface area, porosity as well as the type and concentration of the ions that are positioned on the exchange site (Choudhury T, 2011). The acid modification removes cations such as Al^{3+} and Mg^{2+} from octahedral positions and migrates them to the interlayer space where they then act as acid centers. This action increases the number of Bronsted and slightly the Lewis acid sites and therefore stimulates catalytic activity. The cations that aren't migrated are dissolved out of the structure creating weak silica sheets (Emam, 2013). This action initiates mesopores, which are able to take in larger molecules for catalysis. Polar organic molecules such as alkyl-ammoniums can also be used to modify surface properties of clay (Moronata A, 2002)**.** Alkyl-ammonium ions keep alumina-silicate sheets always apart and therefore increase the spacing between the sheets where new sorption sites would be visible on the clay (Moronata A, 2002). It has been suggested that when clay is modified with both acid and polar organic molecules both the internal and external surfaces would be involved in the reaction mechanism due to the clays enhanced catalytic activity. That's because when acid is added to the clay, it becomes saturated with hydrogen and therefore creates an environment rich of protons. As for when clay is modified with polar organic molecules, it provides organic cations in the space between the layers allowing easy access and reactivity with organic molecule (Moronata A, 2002).

2.11.2.1 Acid Modified Montmorillonite

Montmorillonite is a widely used solid acid catalyst due to its efficiency and its advantages such as cheapness, non-corrosivity, strong acidity, selectivity and high product yields (Choudhury T, 2011); (Hart, 2004). Montmorillonite catalysts that are modified with

acids are greatly studied in petroleum reactions such as alkylation (V., 2003) isomerization (Hart, 2004), and acylation (V., 2003) reactions.

2.11.2.2 Acid Modified Kaolin

Acid modified kaolin was studied for the reduction of sulfur in gasoline in FCC using a mini-fixed bed reactor by Sun et al. (2005) (SunS-H, 2005). A quicker active pore structure was formed in kaolin microspheres after calcination and acid-activation. This indicated an improved yield distribution as well as higher coke selectivity.

CHAPTER 3

EXPERIMENTAL

A series of steps were performed to achieve the research objectives in an optimal manner. These included careful preparation of the heterogeneous catalysts and optimizing pyrolysis/gasification parameters.

3.1 Catalyst Preparation

Several natural clays were modified and activated with inorganic acid. The clays were modified using a technique that was proven to synthesize Zeolite Y (Mu Mu Htay, 2008). After modification these clays were activated at two different concentrations and at different temperatures and time conditions. This was done to dealuminate the crystalline framework, remove elements such as Magnesium (Mg), Calcium (Ca), Potassium (K) and more importantly, improve the acidity of the framework. This is expected to enhance the surface area and selectivity of the catalyst towards cracking of hydrocarbons. This section will be divided into two main parts, the modification of the catalyst and the activation of the catalyst.

3.1.1 Modification Methods

1. Modification of Kaolinite
    i. Materials

Kaolinite powder $Al_2O_3.2SiO_2.2H_2O$ and a molecular weight 258.16 gram/mole was purchased from Sigma Aldrich. The sodium hydroxide (puriss., meets analytical specification of Ph. Eur., BP, NF, E524, 98-100.5%, pellets) was purchased from Sigma Aldrich. Sodium metasilicate (Linear formula: Na_2SiO_3 and molecular weight: 122.06 gram/mole) was purchased from Sigma Aldrich.

ii. Procedure

Before modification and in order to prepare a zeolite from kaolinite, 5g of kaolinite were fused with 1M aqueous sodium hydroxide and were then calcined at a temperature of 850℃ at a ratio kaolinite/NaOH ratio of 1/1.5 by (wt.) for a duration of 3 hours (Mu Mu Htay, 2008).

After that, in a 250ml glass bottle, 5g of the fused kaolinite was added to 6.35g of sodium metasilicate and were dispersed in 75ml of deionized water. This mixture was continuously stirred for one hour at 600 rpm. The slurry was then carried out to age at 50℃ for 24 hours and was followed by crystallization at 98℃ for 48 hours. The crystals were then separated from the liquor through Buckner filtration with a filter having a media size of 110 mm (ALBET Filtration & Separation Technology) and the crystals were dried at 100℃ for 16 hours.

2. Modification of Brown Clay

i. Materials

Brown clay was extracted from an area in North Lebanon. Sodium metasilicate (Linear formula: Na_2SiO_3 and molecular weight: 122.06 gram/mole) was purchased from

Sigma Aldrich.

ii. Procedure

In a 250ml glass bottle, 5g of Brown clay were added to 6.35g of sodium metasilicate and were dispersed in 75ml of deionized water. This mixture was continuously stirred for one hour at 600rpm. The slurry was then carried out to age at 50℃ for 24 hours and was followed by crystallization at 98℃ for 48 hours. The crystals were then separated from the liquor through Buckner filtration with a filter having a media size of 110mm (ALBET Filtration & Separation Technology) and the crystals were dried at 100℃ for 16 hours.

Similarly, Montmorillonite K-10 powder with (surface area: 220-270 m^2/g) and Bentonite powder were purchased from Sigma Aldrich. They were also modified with same procedure performed on Brown clay.

3.1.2 Activation Methods with inorganic acid H_2SO_4

1. Activation Method 1: 6M H_2SO_4

This activation method was extracted from (Amie Thant, June 2017). With the use of 6M H_2SO_4 at a solid: liquid ratio of 1:30 (g: ml). Both unmodified and modified clays were activated.

i. Materials

Modified kaolinite that was prepared in the previous section will only be activated with inorganic acid. That is because the framework of raw kaolinite will not be able to

withstand the severity of sulfuric acid. Sulfuric acid 95% was purchased from VWR PROLABO CHEMICALS.

ii. Procedure

In a 1000 ml glass bottle 6M of H_2SO_4 were prepared. Calculations of the dilution of H_2SO_4 are in appendix A.1. A solid to liquid ratio of 1 g: 30 ml was used. Therefore, in a weighing boat, 2g of the modified kaolinite were weighed and placed in a 2-neck round bottom flask. A volume of 60 ml 6M H_2SO_4 were measured and poured into the 2-neck round bottom flask along with a magnetic stirrer. The mixture was placed under reflux for 3 hours at a fixed temperature of 100℃ and at a fixed rpm. The solution was then filtered and washed with 500 ml of deionized water. Finally, the filter cake was calcined at 500℃ for 2 hours. This method was extracted from (Amie Thant, June 2017). The rest of the catalyst samples raw and modified were activated with the same procedure applied on modified kaolinite. Some samples have minor differences so Table 6 below shows the samples along with the change in parameters that might have been applied.

Table 6 Materials and procedure alterations for Activation Method 1

Material Used	Change in Procedure
Brown Clay from nature	-5g of Brown clay was weighed -Volume of 150 ml of 6M H_2SO_4
Modified brown clay prepared from the lab	No change, same procedure as the activation of modified kaolinite but with modified brown clay
Montmorillonite K-10 powder from Sigma	-5g of Montmorillonite K-10

Aldrich	-Volume of 150 ml of 6M H_2SO_4
Modified Montmorillonite from the lab	No change, same procedure as the activation of modified kaolinite but with modified brown clay
Bentonite powder from Sigma Aldrich	-5g of Bentonite -Volume of 150 ml of 6M H_2SO_4
Modified Bentonite prepared in the lab	Same procedure as the activation of modified kaolinite but with modified brown clay

2. Activation Method 2: 4M H_2SO_4

This activation method was extracted from (Prakash Kumar, 1995). With the use of 4M H_2SO_4 at a solid: liquid ratio of 1g:5 ml. Both unmodified and modified clays were activated.

3.2 Materials

Modified kaolinite that was prepared in the previous section will be activated with inorganic acid, sulfuric acid 95% was purchased from (VWR PROLABO CHEMICALS).

3.3 Procedure

In a 1000 ml glass bottle 4M of H_2SO_4 were prepared. Calculations of the dilution of H_2SO_4 are in appendix A.1. A solid to liquid ratio of 1 g: 5 ml was used. Therefore, in a weighing boat, 2 g of the modified kaolinite were weighed and then placed in a 2-neck round bottom flask. A volume of 10 ml 4M H_2SO_4 were measured and poured into the 2-neck bottom flask along with a magnetic stirrer. The mixture was placed under reflux for 2

hours at a fixed temperature of 80℃ and at a fixed rpm. The solution was then filtered and washed with 500 ml of hot distilled water. Finally, the filter cake was calcined at 500℃ for 2 hours. This method was extracted from (Prakash Kumar, 1995). Similarly, the rest of the catalyst samples raw and modified were activated with the same procedure applied on modified kaolinite. Some samples have minor differences so Table 7 below shows the samples along with the change in parameters that might have been applied.

Table 7 Materials and procedure alterations for Activation Method 2

Material Used	Change in Procedure
Brown Clay from nature	-5g of Brown clay was weighed -Volume of 25 ml of 4M H_2SO_4
Modified brown clay prepared from the lab	No change, same procedure as the activation of modified kaolinite but with modified brown clay
Montmorillonite K-10 powder from Sigma Aldrich	-5g of Montmorillonite K-10 -Volume of 25 ml of 4M H_2SO_4 -Time 3 hours instead of 2 hours
Modified Montmorillonite from the lab	No change, same procedure as the activation of modified kaolinite but with modified brown clay
Bentonite powder from Sigma Aldrich	-5g of Bentonite - Volume of 25 ml of 4M H_2SO_4
Modified Bentonite prepared in the lab	No change, same procedure as the activation of modified kaolinite but with modified brown clay

3.2 Catalyst Characterization

As described in the previous section, the natural clays were modified and/or activated with H_2SO_4 acid at two different concentrations, using two different methods. The pore volume, surface area, crystal structure and composition of the clays were tested and analyzed.

The most important factor in catalysis is characterizing and understanding the structure of a heterogeneous catalyst. Several technics were considered during the characterization process inlcuding BET isotherm analysis, SEM, EDX, XRD and TGA.

For a heterogeneous catalyst, the catalytic reaction occurs at the solid-gas interface, meaning that a catalyst with a high surface area is expected to have a higher catalytic conversion rate. Catalytic activity in heterogeneous catalysts is thus stimulated through its porous surface. Therefore, the size and variation of the pores impact the composition of the yielded products (Fogler).

3.2.1 BET Isotherm Analysis

BET analysis was performed using the Nova 2200 instrument along with Nitrogen gas as an adsorbate gas for surface area analysis. Before starting with the BET analysis step, the catalyst sample had a weight around 0.02 grams and was placed in the BET quartz cells which was connected to the degassing station for a period of 8 hours in order to remove any volatile contaminant gases that might have been stuck to the surface layer of the catalyst sample. The degassing process was conducted while the cell was jacketed with a heating mantle temperature of 150°C. Afterwards, the sample was removed from the heating mantle

and placed in the BET instrument where the quartz tube was immersed in liquid nitrogen to maintain a low temperature of 75K and testing points of adsorption-desorption were then loaded using installed software. The results of the BET isotherm analysis consist of single and multi-point surface areas including surface area, pore size, and volume of each catalyst. Additionally, the BET analysis provides an adsorption/desorption isotherm related to the portion that's covered with respect to the P/P_0 data during both the pressurizing and vacuuming with nitrogen gas.

3.2.2 SEM Analysis

This characterization technique of Scanning electron microscopy (SEM) is applied on the catalysts in order to observe and test the morphology of the catalyst's surface. SEM is an electron microscope technique that consists of firing a high-energy beam of electrons on a sample in vacuum, and then converting the signal into an image. The electrons fuse with the atoms located on the sample, which therefore produce various signals that quantify information about the composition and surface topography. The electron microscopes can also accommodate other detectors for chemical analysis of the surface. There are two different signals that could be used to acquire the image depending on where the energy is received from, if low energy, the information is from the surface, this shows surface morphology, this signal is called the secondary electron signal. The second signal is the Back-Scattered electron signal, which is composition sensitive and the higher energies may come from inside the sample. As for charging, non-conductive samples would collect static charges from the electron beam which affects the resulting image, so to avoid this, non-conductive samples are coated with a conductive layer (gold, platinum...) by sputtering.

Unfortunately, the microscopic imaging varied with respect to same working distance and voltage intensity because charging occurred on the surface due to the presence of different non-static elements. Hence, suitable working distances, scanning speeds and detectors were used to achieve a high-resolution image of the catalysts morphology.

3.2.3 EDX Analysis

The X-ray detector of the SEM machine allows us to be able to detect the composition of the target region selected off of a catalysts surface. The analysis generates a table of the elements, which corresponds to a selected area. The Si/Al ratio plays an important role not only on the stability of the structure but also on the certain activity the zeolite would have (Smirniotis, 1996). Therefore the Si/Al ratio should be known in order to determine the stability of a zeolite structure for catalytic cracking purposes.

3.2.4 XRD Analysis

X-ray diffraction (XRD) is a technique that is used to analyze the crystal structure of a single crystal sample and its phase composition by scattering X-ray emissions; this is possible by calculating the atomic spacing. The technique for XRD involves shining an X-ray beam on a sample while recording the diffraction pattern. Atom crystals scatter the incident X-ray beams and restriction patterns are recorded at different crystal lattice angles. Different libraries are available in order to analyze the recorded spectrum and identify the different crystal structures or lattice arrangements as well as phase identification present (Kooli, 2009). The diffraction angles provide enough information to have an idea about the crystal geometry those are cubic, orthorhombic and tetragonal.

D8 Advance by Brucker with Avinci design diffractometer; Diffrac.Eva and Diffrac measurement center was the software used recorded the X-ray diffraction arrangements. The x-ray generator functioned over 40 kV and 40 mA. The average increment of the x-ray emission was at 0.02 and the preliminary and end angles ranged between 5 and 50. XRD graphs display the intensity of the peaks with respect to the angle of theta (2θ). XRD peaks that were generated for each catalyst were carefully analyzed and compared with library matches when applicable, constituting of same compounds of the catalyst. The broadness and displacement of the peaks provide further information on how the surface of the catalyst altered.

3.2.5 TGA Analysis

Thermogravimetric analysis (TGA) is an analysis method which measures the thermal stability of a specimen as it is subjected to a constant temperature for a specific period of time. A measured sample is placed inside of a furnace where its mass is monitored for mass increase of decrease. The weight of the sample measured is about 5mg. The experimental environment is purged with inert or reactive gas that flows over the sample, controlling the environment (PerkinElmer, 2015). The TGA can be coupled with a mass spectrometry or an FTIR in order to analyze the degradation of products. Other than mass loss or gain, the TGA can be used to measure carbon buildup on a spent catalyst. A thermal curve is displayed once the experiment is over and indicates the weight loss of the sample from left to right with respect to temperature increase.

Nine different catalysts after analysis were chosen to be used for the pyrolysis experiments and they are:

-Kaolinite and Kaolinite modified and activated with method 2 (KM_4)

-Brown clay and Brown clay only activated with method 1 (BC_6)

-Montmorillonite, Montmorillonite only activated with method 1 (M_6) and Montmorillonite only activated with method 2 for 3 hours (M_4_3)

-Bentonite and Bentonite only activated with method 2 (BN_4)

3.3 Pyrolysis

Thermal catalytic pyrolysis experiments were run using an electrical furnace with two heating zones each having its own temperature controller Figure 11. The temperature controller permits the selection of specific heating rate as well as a steady temperature for a set duration of time.

Figure 11 Electrical Furnaces

Figure 12 shows the experimental setup of the furnace where a large quartz cylinder is placed inside of the circular heating sections.

Figure 12 Large quartz cylinder placed inside circular heating sections

The quartz tube has an inner diameter of 0.70 cm and a length of 129.2 cm and is placed inside of the large quartz cylinder. Scrap rubber tire were grinded with a grinder to obtain pieces of approximately 0.5 mm. Note that the furnace heating zone is 45cm in length.

Thermal pyrolysis runs were conducted on nine raw and activated catalysts that were chosen after analysis at a fixed carrier gas flow of nitrogen, at 80 ml/min and at a fixed temperature of 580℃. Nitrogen was supplied from gas tanks that were connected through small tubes to a flow controller and from the flow meter a small tube extended and connected to the reactor.

Each catalyst was run several times. A catalyst to sample weight ratio of 3:10 was used and sand was mixed in with the catalyst. The scrap rubber tires were placed at the left heating compartment, at the carrier gas flow inlet. Where the catalysts were placed in the right heating compartment so at the outlet side of the gas carrier. The scrap tires and the catalysts were separated at a fixed distance with quartz wool, which surrounded both the scrap rubber and the catalysts keeping them secured in their fixed places.

The outlet part of the quartz tube was connected to a condenser through a connector. The furnace compartments (left and right) were set to an isothermal temperature of 580℃ (inside reactor temperature). The small quartz reactor, after being prepared, was placed inside of the furnace from left to right, keeping the scrap rubber tires out of the reactor for the first 10 minutes in order to activate the catalyst used. Following the activation stage of the catalyst, the rest of the reactor was then fully pushed into the furnace and connected to a condenser. At this stage both the catalyst and the scrap rubber tires were located at the middle of the heating zones. The reactor stayed in the furnace for a duration of 35 minutes.

Volume of heated reactor zone=$\pi r^2 l = \pi * (0.35)^2 * 45 = 17.32\ cm^3$

N_2 Flow rate at 25°C= 80*ml/min* = 80 cm^3/min

N_2 Flowrate at 580°C = 80*(580+273)/(25+273) = 228 cm^3/min

Residence time over heating zone length (τ) $= \frac{17.32}{228} \times 60 sec/min =$ 4.6 $seconds$

Similarly at 780^0C,

Residence time over heating zone length (τ) $= \frac{17.32}{283} \times 60 sec/min =$ 3.7 $seconds$

3.4 Pyrolysis Product Characterization

3.4.1 Gas Yield Calculation

The quartz reactor was weighed before and after the thermal pyrolysis run using an analytical balance to identify the quantity of the non-condensable gases produced. Similarly, the connection to the condenser as well as the condenser was weighed before and after the experiment.

Let *f* be the summation of the connection, condenser and the reactor after pyrolysis and let I be the summation of the connection, condenser and reactor before the pyrolysis experiment.

$$f = m_{\text{reactor after pyrolysis}} + m_{\text{condenser after pyrolysis}} + m_{\text{connection after pyrolysis}} \quad [5]$$

$$I = m_{\text{reactor before pyrolysis}} + m_{\text{condenser before pyrolysis}} + m_{\text{connection before pyrolysis}} \quad [6]$$

Therefore,

$$\Delta m = I - f \quad [7]$$

$$\%\text{Gas Yield} = \frac{\Delta m}{m_{\text{tire scrap added}}} x100 \quad [8]$$

3.4.2 Liquid Product Analysis

To detect the catalytic effect of the catalysts on scrap tires, the oil samples that were collected in the condenser were tested by GC-MS in order to analyse the hydrocarbon compounds. Collected oil samples were diluted with ethanol at a proportion 1:1 and then were filtered using 22μm syringe. Diluted and filtered samples were displaced into glass vilas ready to be placed in the GC auto-sampler. Software used was Trace GC Ultra operated using Xcalibur software. The GC-MS analysis was performed using a capillary column from Thermo Scientific (TG-BOND Q (30m x 0.32mm x 0.10 μm). Column temperature was held at 40℃ for 5 minutes, then ramped up by 10℃/min up to 230℃/minand held for 5 minutes then from 230 to 280℃ at a rate of 5℃/min. Helium was used as the carrier gas with a flow of 0.8 mL/min. The injector and detector temperatures were maintained at 250and 300℃, respectively, and the injection volume was 1μL in split mode with a split ratio of 50:1 and split flow of 50 mL/min.

3.5 Gasification Procedure

Thermal gasification experiments were run using the same setup as the thermal catalytic pyrolysis experiments. The procedure was adopted to conduct pyrolysis-gasification experiments where ethanol was introduced with the nitrogen flow of 80 *ml/min* into the reactor via a heated impinger that contained ethanol set a 40℃. Ethanol is known to have a cracking temperature of about 650℃ (Apichai Therdthianwong, 2001). Gasification was conducted at different temperatures 580, 680 and 780℃ and in the absence of catalysts.

The 780℃ yielded the highest gas yield therefore an experiment was again performed with montmorillonite, a raw catalyst that yielded a high gas yield in the pyrolysis experiments. Nitrogen and ethanol were supplied from gas tanks and the impinger, which were hooked through small tubes to a flow controller and from the flow meter a small tube extension extended to the reactor. For catalytic gasification the catalyst to sample weight ratio was 3:10, similar to the ratio used for pyrolysis. The reactor was kept in the furnace for duration of 35 minutes. Similar to the pyrolysis reaction time. The gas flow was fixed at a constant rate of 80 ml/min. Reactions such as intramolecular dehydration converts ethanol to ethene or C_2H_4 or to $CH_3CH_2OCH_2CH_3$ (Tingting Zhao, 2019) including oligomerization reactions between ethylene and a carbene convert ethanol to C_3H_6. Dimerization reactions could also convert ethanol to C_4H_8. C_3H_6 along with C_4H_8 could form aromatics and cycloparaffins through a series of dehydrogenation, cyclization and aromatization reactions (Tingting Zhao, 2019).

3.6 Gasification Product Characterization

GC-MS analysis was performed using 5975C GC MSD gas chromatograph mass spectrometry from Agilent Technologies along with an Agilent DB-624 capillary column of (30m x 0.32mm x 0.18 μm) dimensions. Column temperature was initially held at 26℃ for 10 minutes, then set to 255℃ at a rate of 25℃/min with a hold time of 4 minutes. The carrier gas used was Helium and with a flow of 1.5 mL/min. The injector and detector temperatures were maintained at 200 and 255℃, respectively, where the injection volume was 5μL in split mode having a split ratio of 45:1 and split flow of 79.1 mL/min with an interface temperature held at 300℃.

CHAPTER 4

RESULTS AND DISCUSSION

Catalysts were characterized with four different characterization techniques SEM, EDX, BET, and XRD to better understand the morphology and catalytic cracking ability of the catalyst. The liquid products from pyrolysis as well as the gas products from gasification experiments were collected and analyzed with GC-MS.

4.1 Catalyst Characterization Results

4.1.1 SEM Analysis

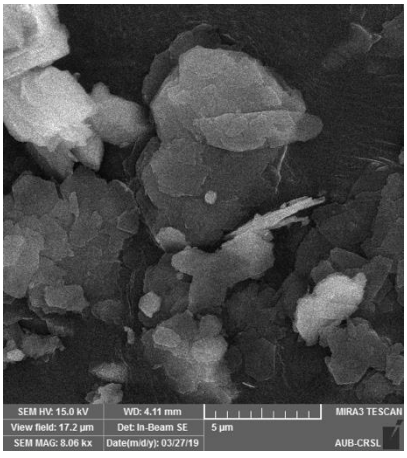

Figure 13 Kaolinite

Figure 13, 14 and 15 show the SEM images of unmodified Kaolinite, along with modified kaolinite, and kaolinite activated with 4M H_2SO_4. The hysteresis loop from BET experiments of Kaolinite determined that it obtains a flat plate like surface shown in figure

15. The modification of kaolinite through calcination and the addition of sodium silicate (KM) (figure 16) changed the framework of the zeolite from having a “house of cards” stack like surface to a more compact and clustered stacked structure (Rouquerol, 1999)**.** As for KM activated with 4M H_2SO_4 (KM_4), resembled KM but with relatively more smoother and flatter surfaces. This can be confirmed from the increase in surface area of KM_4 with respect to KM.

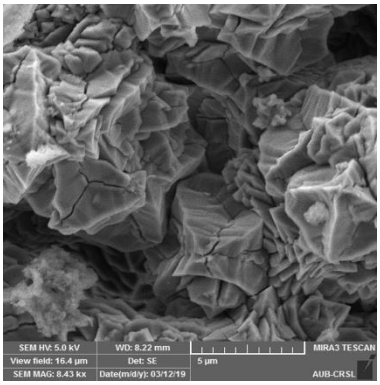

Figure 14 KM SEM Image

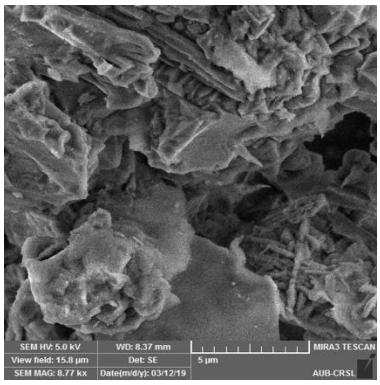

Figure 15 KM_4 SEM Image

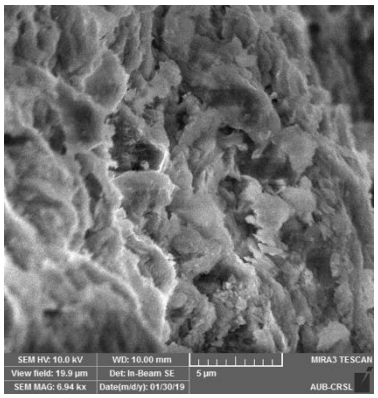

Figure 16 BC SEM Image

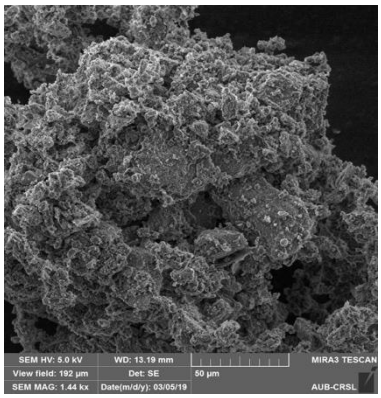

Figure 17 BC_6 SEM Image

Figure 16 and 17 show the SEM images of Brown clay and acid activated brown clay with 6M H_2SO_4 before pyrolysis. Brown clay has an external rough and layered

morphology. Its layers are a mix of amassed flakey and spherical particles (figure 16). Acid activation leached unwanted impurities from the catalyst and therefore increased its surface area and pore volumes. This became more apparent when comparing the surface of brown clay to the acid activated brown clay in figures 16 and 17 respectively. Activated brown clay with 6M H_2SO_4 in comparison to Brown clay has a more distorted rough surface.

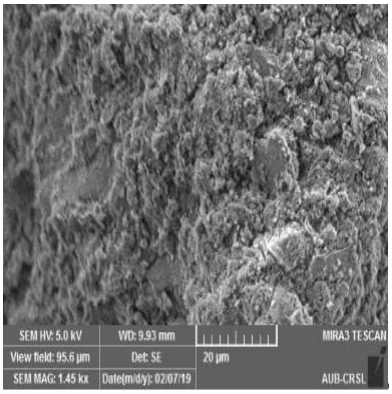

Figure 18 Montmorillonite SEM Image

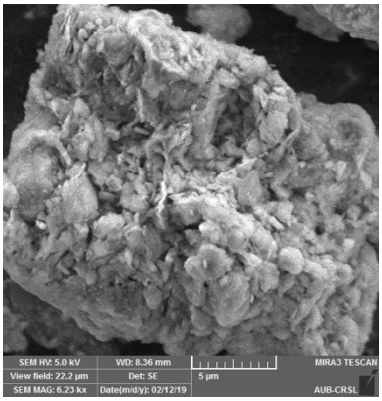

Figure 19 M_6 SEM Image

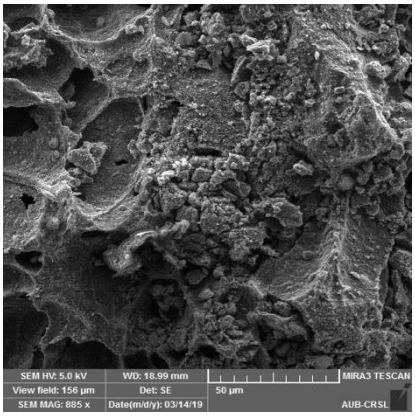

Figure 20 M_4_3 SEM Image

Figures 18, 19 and 20 show the SEM images of Montmorillonite as well as modified Montmorillonite with 6M H_2SO_4 and 4M H_2SO_4 and modified for 3 hours instead of 2 hours. Montmorillonite's physical structure is formed of many layers of sheet like

particles. Montmorillonite obtains a flocculated structure. The external surfaces of M_6 and M_4_3 are very similar to that of montmorillonite in heterogeneity and layered formations.

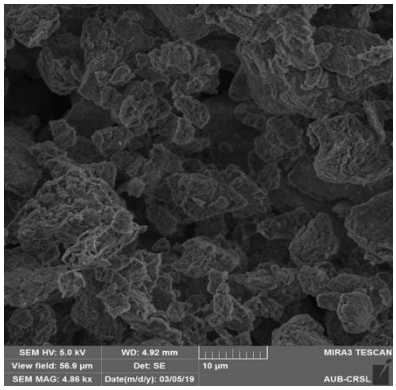

Figure 21 BN **SEM Image**

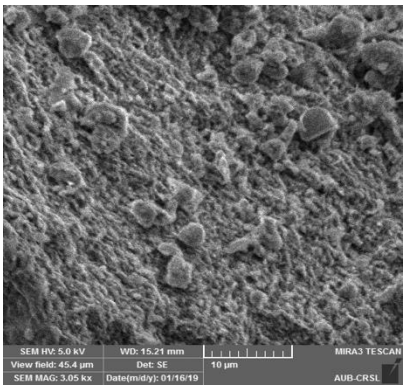

Figure 22 BN_4 **SEM Image**

Figures 21 and 22 display the SEM images of Bentonite and Bentonite activated with 4M H_2SO_4. Bentonite is formed of large plates and is seen as a heterogeneous morphology. It has stacked smooth particles with layer disposition figure 21. Like kaolinite, Brown clay and montmorillonite bentonite's particles do not have definite shaped forms. The effect of acid activation on the external surface of bentonite is shown in figure 22. BN_4 has a more heterogeneous surface with particles not as smooth and more clustered when compared to bentonite.

4.1.2 EDX Analysis

Results from detected elements are shown through peaks from X-rays. Figure 23 displays peaks corresponding to the present elements on the surface of Kaolinite and Table 8 shows the relative weight% and atomic% of these selected elements. Similarly, Figure 24 and Table 9 provide the peak intensity as well as the relative weight% and atomic% of KM_4. The elemental characteristics of these catalysts were studied in order to examine the

Si/Al wt.% present. Kaolinite has a Si/Al ratio of 1.09 wt.%. Kaolinite therefore is considered to be a low silica zeolite meaning they are aluminum saturated. Table 8 shows that the wt.% of aluminum is almost equal to that of Si. Both having tall peaks at 1.5 Kev (figure 23). Additional sodium silicate was added to kaolinite before acid activation to change the Si/Al ratio, this has been also reported by (Chandrasekhar, 1999). The modification of Kaolinite into KM_4, by adding sodium silicate and activating with 4 M H_2SO_4, leached out potassium (K). Potassium is known to be present in the interlayer part of the kaolinite structure and lead to an increase of Si/Al ratio by 6 folds to 6.62 wt.%. Figure 24 portrays a decrease of the Al peak with respect to Si and (Figure 23).

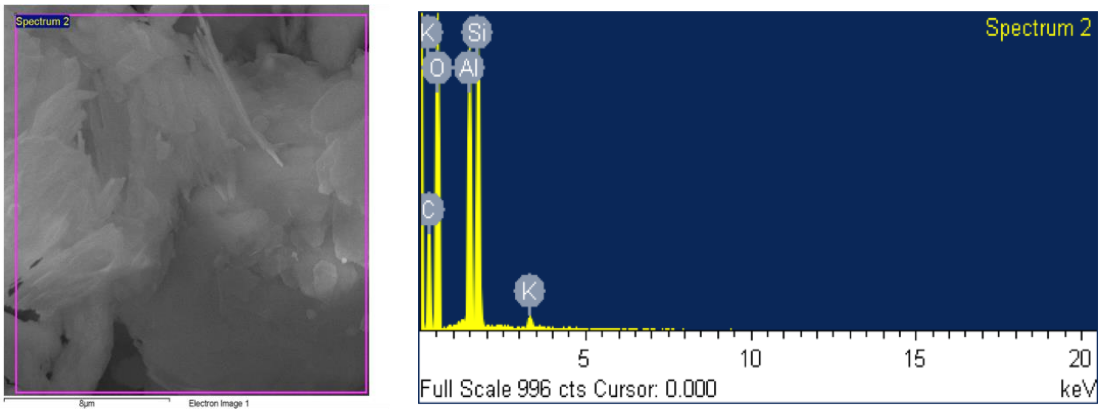

Figure 23 EDX of Kalonite

Table 8 Composition analysis for Kaolinite

Element	Weight %	Atomic %
C K	29.04	38.18
O K	51.27	50.62
Al K	9.08	5.32
Si K	10.08	5.67
K K	0.53	0.22

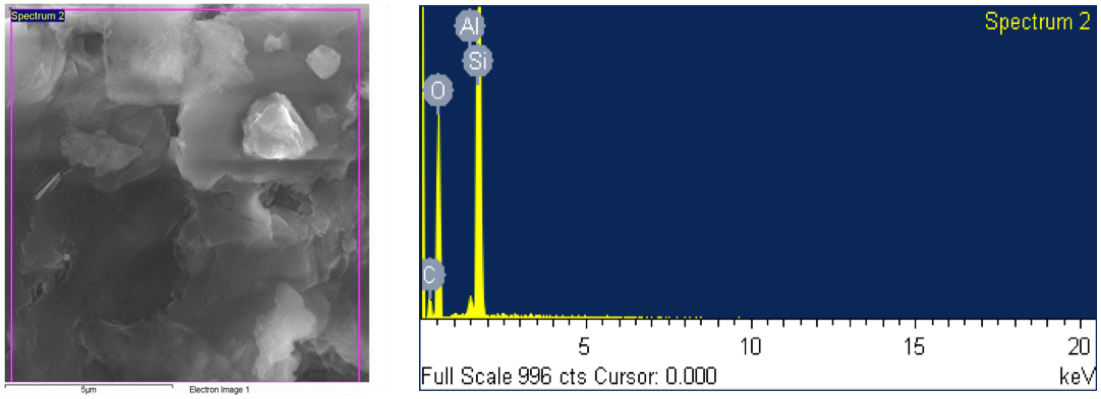

Figure 24 EDX of KM_4

Table 9 Composition analysis for KM_4

Element	Weight %	Atomic %
C K	15.31	23.52
O K	48.22	50.68
Al K	5.3	3.5
Si K	31.17	22.3

Elements that are present on the surface of Brown clay and BC_6 are present in Figures 25 and 26 as peak intensities and in Tables 10 and 11 as weight% and atomic%. Brown clay is considered to be an unknown species so its elemental analysis was necessary to better understand its composition and know whether or not it contained Al and Si. Table 10 displays the elements that were detected at a specific spectrum. Si and Al were present at high peaks at about 1.8 and 1.6 Kev respectively. The Si/Al ratio of brown clay was 2.23, which classifies brown clay as a low silica zeolite (Flanigen, 2010). Comparing Table 10 and Table 11 it becomes evident that the acid leached out Ca, K and Fe totally and lowered the weight% of Al leaving BC_6 with a Si/Al ratio of 13.73 wt.%. The Si and Al peaks are

still at 1.8 and 1.6 Kev respectively however Al has smaller peak intensity in Figure 25 than in (Figure 26).

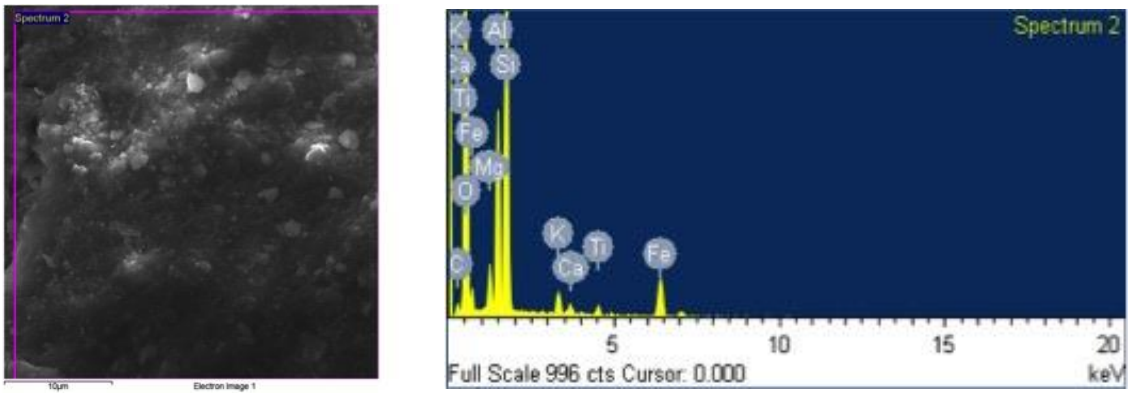

Figure 25 EDX of brown clay

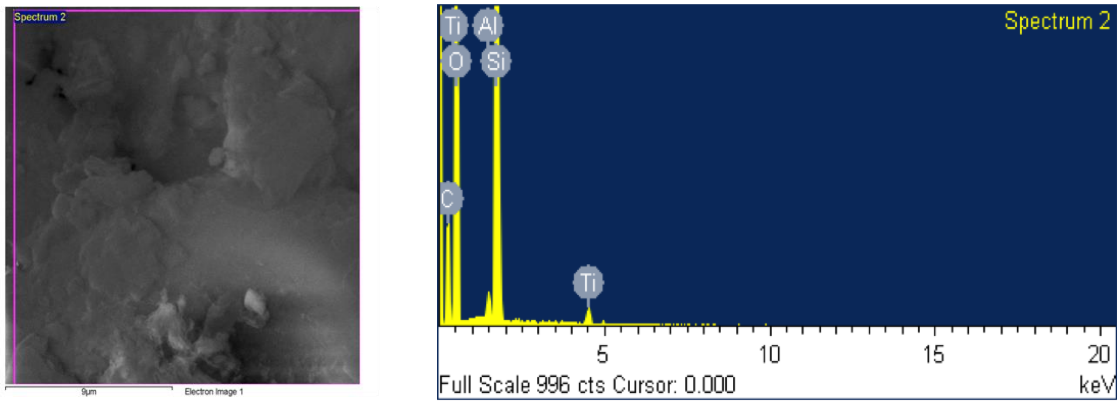

Figure 26 EDX of BC_6

Table 10 Composition Analysis of brown clay

Element	Weight %	Atomic %
C K	4.29	6.87
O K	57.9	69.72
Al K	8.04	5.74
Si K	17.98	12.33
K K	1.45	0.72
Ca K	0.54	0.26
Ti K	0.74	0.3
Fe K	6.97	2.4

Table 11 Composition Analysis of BC_6

Element	Weight %	Atomic %
C K	26.34	35.42
O K	51.66	52.15
Al K	0.55	0.33
Si K	20.47	11.77
Ti K	0.98	0.33

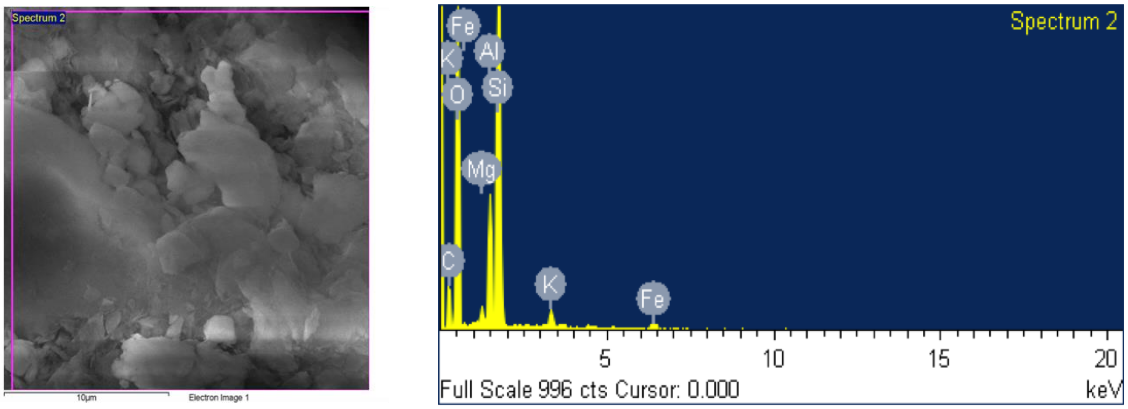

Figure 27 EDX of Montmorillonite

Montmorillonite is a 2:1 clay mineral. It is known that the tetrahedral cations are the most resistant to acid attack whereas the interlayer structure is the most vulnerable. Fe and Mg were completely removed from the octahedral sheets, where they are known to substitute Al. Al leached out remaining at only 1.1 wt.% The Si/Al ratio of M_6 is now 33.3 wt.% which is a tremendous enhancement from 1.33 wt.% for montmorillonite tables 12 and 13. Montmorillonite went from being a low Si zeolite to a high Si zeolite by acid activation of 6M H_2SO_4.

It is important to note that the presence of carbon is from the carbon tape used to fixate the catalyst onto the support used for EDX analysis. For M_4_3 looking at tables 12 and 14 comparing the weight% of Fe and Al, it might be apparent that they have entered the tetrahedral replacing Si and thus caused the slight decrease in surface area. The Si/Al ratio of M_4_3 is 5.61 wt.%.

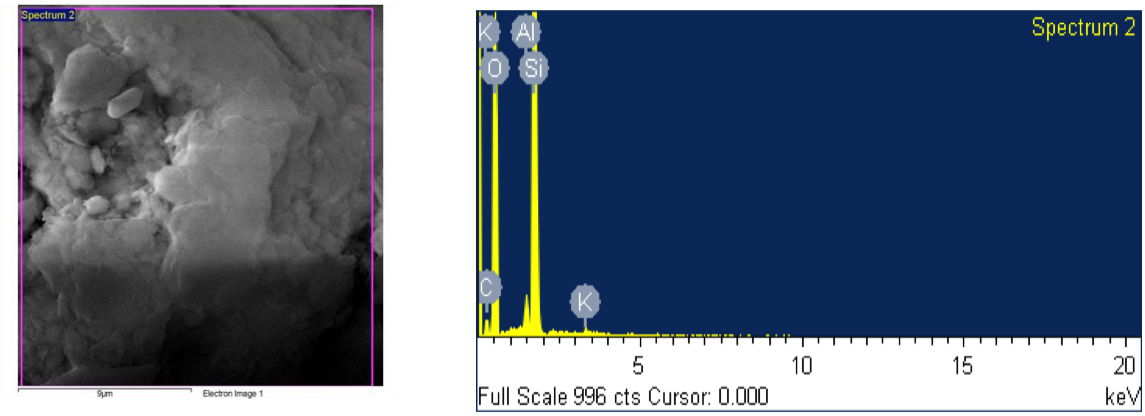

Figure 28 EDX of M_6

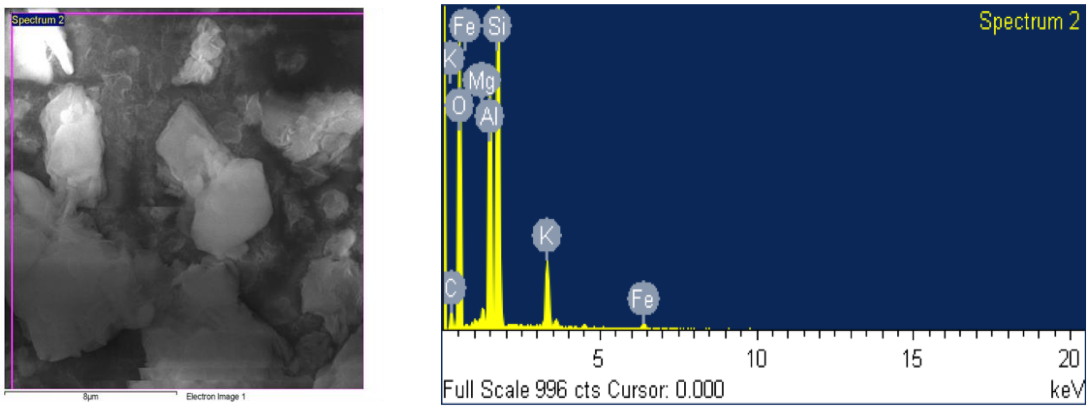

Figure 29 EDX of M_4_3

Table 12 Composition analysis of Montmorillonite

Element	Weight %	Atomic %
C K	16.24	23.45
O K	53.79	58.31

Mg K	0.62	0.44
Al K	4.56	2.93
Si K	22.98	14.19
K K	0.94	0.41
Fe K	0.88	0.27

Table 13 Composition analysis of M_6

Element	Weight %	Atomic %
C K	9.01	13.58
O K	57.25	64.73
Al K	1.1	0.74
Si K	32.3	20.8
K K	0.34	0.16

Table 14 Composition analysis of M_4_3

Element	Weight %	Atomic %
C K	13.66	16.52
O K	52.38	62.37
Mg K	1.69	1.53
Al K	3.86	1.41
Si K	21.69	14.48
K K	4.89	3.34
Fe K	1.83	0.35

The elemental composition of Bentonite and BN_4 from EDX in weight% and atomic% are indicated in tables 15 and 16 as for their peak intensities they are shown in

Figures 30 and 31. Bentonites major components are Si and Al and were detected at 1.8 and 1.6 Kev respectively. The Si/Al ratio of bentonite is 2.63 wt.% meaning it's a low silica zeolite (Flanigen, 2010). BN_4 acquired a Si/Al ratio of 6.11 wt.% almost 3 times the Si/Al ratio of bentonite. Comparing Table 15 and Table 16 it becomes evident that the acid leached out Ca, Mg and Na totally and lowered the weight% of Fe. The Si and Al peaks are still at 1.8 and 1.6 Kev respectively however Al has a much smaller peak intensity in Figure 30 than in (Figure 31).

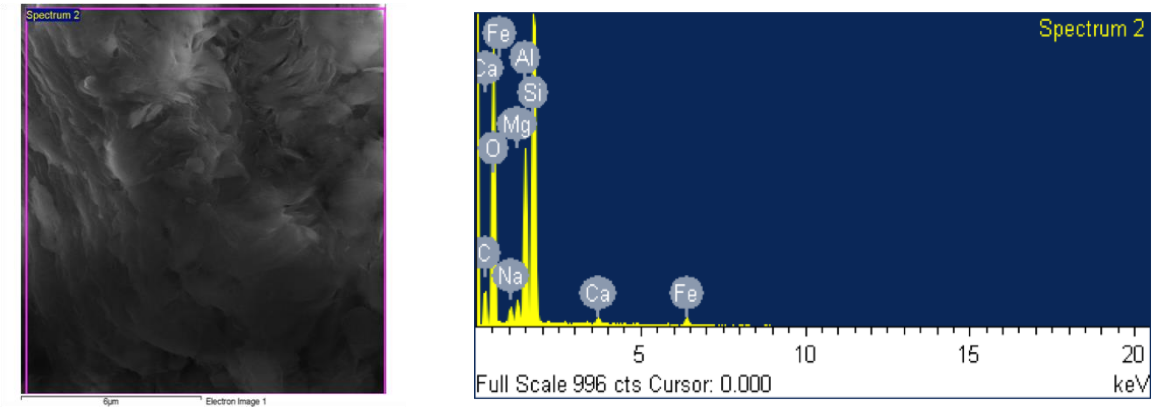

Figure 30 EDX of Bentonite

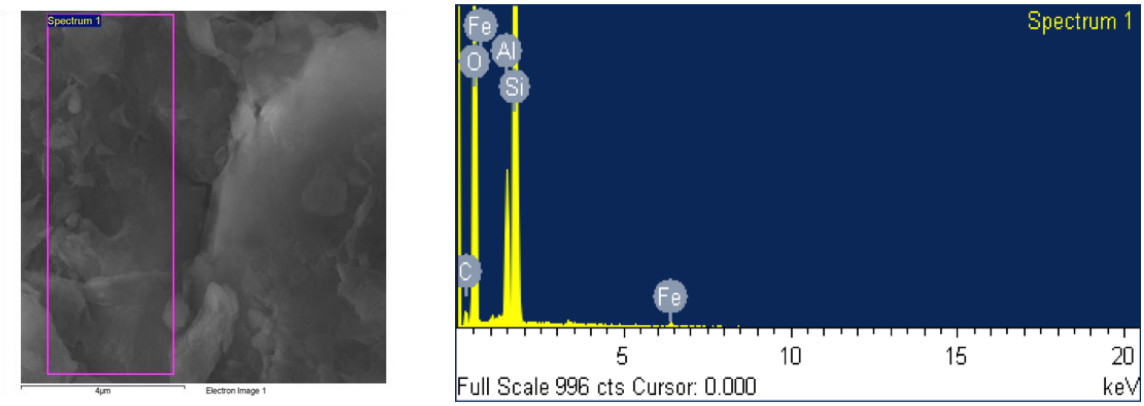

Figure 31 EDX of BN_4

Table 15 Composition analysis of Bentonite

Element	Weight %	Atomic %
C K	19	27.15
O K	50.9	54.6
Na K	1.1	0.82
Mg K	1.08	0.76
Al K	7.58	4.82
Si K	18.21	11.13
Ca K	0.48	0.21
Fe K	1.64	0.5

Table 16 Composition analysis of BN_4

Element	Weight %	Atomic %
C K	7.88	11.96
O K	57.71	65.76
Al K	4.81	3.25
Si K	29.05	18.85
Fe K	0.55	0.18

4.1.3 BET Analysis

Table 16 summarizes the BET results of all catalysts.

Table 17 BET analysis results of catalysts: Surface Area (m^2/g), Pore Volume (cm^3/g) and Pore Size (nm)

Catalyst	**Surface Area (m^2/g)**	**Pore Volume (cm^3/g)**	**Pore Size (nm)**
Kaolinite	7.3814	0.026704	15.0
KM_4	93.0156	0.036732	2.79
Brown Clay	52.8086	0.080828	7.9
BC_6	187.0236	0.185656	4.814

Montmorillonite	249.0511	0.239396	4.23
M_6	154.0144	0.165623	5.0
M_4_3hrs	224.0535	0.223354	4.32
Bentonite	20.5103	0.020473	3.97
BN_4	262.9189	0.33626	4.37

The adsorption/desorption isotherms for each catalyst are also presented in figures 33-41. The most common isotherm is the type IV adsorption/desorption isotherm (figure 32). Also, Table 17 shows that all the catalysts maintain widths of pores of mesoporous shape since the pore sizes ranged from ~2nm-15nm.

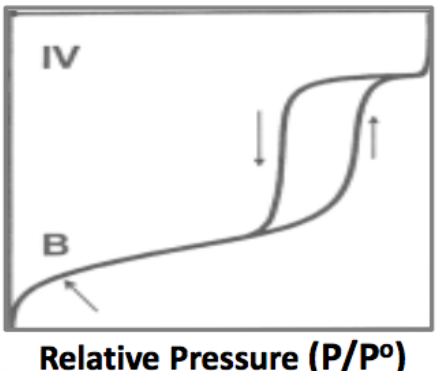

Figure 32 Type IV Adsorption/Desorption Isotherm (Matshitse, 2001)

Figures 33 and 34 show respectively the adsorption/desorption isotherms of Kaolinite and KM_4. Table 17 shows that the initial surface area of kaolinite was 7.3814 m^2/g and was increased to about 93 m^2/g, almost by a factor of 13, this is after modification with Na_2Si and activation with 4M H_2SO_4. An increase in pore volume of kaolinite to KM_4 from 0.026 cm^3/g to 0.036 cm^3/g also occurred. As for the pore size, it decreased from 15 nm for kaolinite to 2.79 nm for KM_4. The catalyst characterization through EDX, showed

that Potassium was present in kaolinite before modification, Potassium has a van der waals size of 270 pm. When comparing the EDX of KM_4 to kaolinite it was noticed that all the potassium was dissolved. Potassium occurs in the interlayer part of kaolinite that is known to be most vulnerable to acid attack. An increase in Si was seen in KM_4. The van der waals size of Si is 210 pm, smaller than that of potassium. So, the introduction of Si through sodium silicate as well as activation with H_2SO_4 drove out the potassium and granted more space for Si to bind to, increasing surface area but however decreasing pore size. With the increase in surface area and pore volume of KM_4, it is bound to have higher selectivity towards more compounds and a higher residence time, which would help with secondary reactions inside of the pores. The decrease in pore size limits the compounds that would be able to actually enter these pores.

Kaolinite behaves as a type II isotherm, a slight inflection point on the adsorption/desorption isotherm indicates full monolayer handling also, knowing the size of the pore at 15 nm kaolinite is considered to be macro porous and is then changed into a mesoporous structure with KM_4 similar to Type II isotherm (Carolina Belver, 2001). Looking into the shapes of the hysteresis loops of kaolinite and KM_4, they exhibited hysteresis loops of types H3 and H4 respectively. Type H3 loop indicates that kaolinite obtains non-rigid aggregates of flat surfaced particles with a channel of partially filled macropores (Matthias Thommes, 2015). As for the H4 loop type of KM_4, are more commonly occurring with aggregated or mesoporous zeolite crystals (Matthias Thommes, 2015).

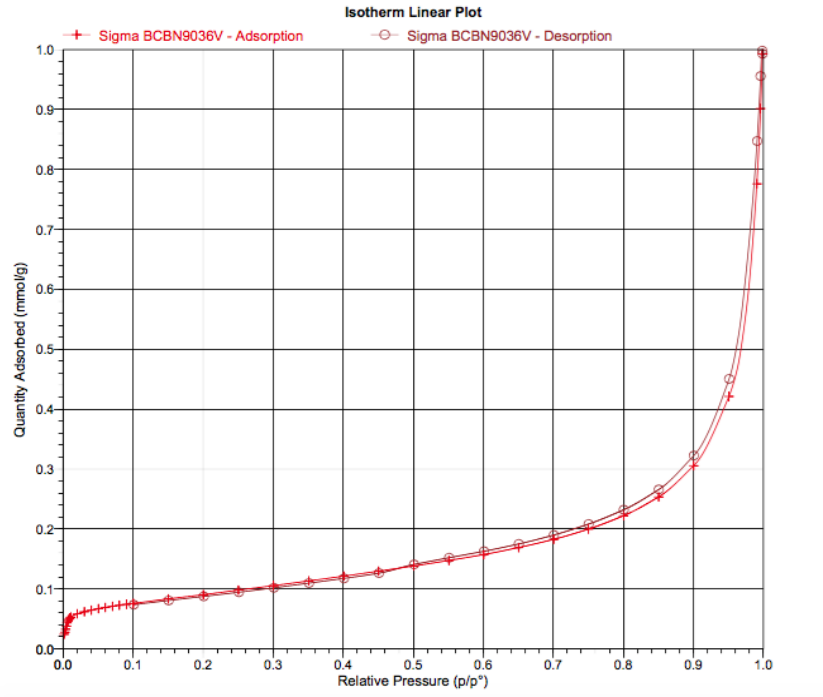

Figure 33 BET adsorption/desorption isotherm of Kaolinite from BET Analysis

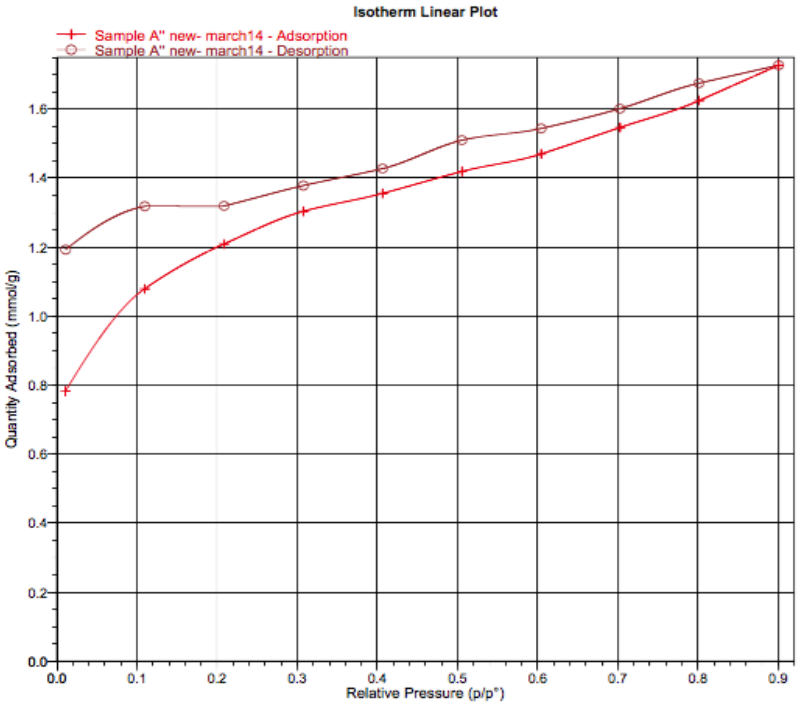

Figure 34 BET adsorption/desorption isotherm of KM_4 from BET Analysis

Brown Clay was extracted from a village in North Lebanon in order to test the behavior of non-processed natural clay. Figures 35 and 36 represent the adsorption/desorption isotherms of Brown clay and activated brown clay with 6M H_2SO_4 respectively. The surface area of Brown clay increased almost 3.5 times with the activation of acid from 53 to 187 m^2/g. Similarly, the pore volume of BC_6, approximately doubled to 0.18 cm^3/g from 0.08 cm^3/g, which justifies the increase in surface area as well. The acid etched into the surface thus increased its area. In reference to tables 10 and 11 for the composition of Brown clay and BC_6, a significant decline of the Al composition and a respective increase in the Si composition was noticed. The respective van der waals sizes of Al and Si are 184 pm and 210 pm. The phenomenon of dealumination and the replacement of Al by Si can be justified by the decrease in pore size from 7.9 nm to 4.8 nm respectively by the activation of Brown clay with 6M H_2SO_4. The great increase in surface area and pore volume of BC_6, qualifies the catalyst to accept more compounds and by also having a longer residence time, which would increase the occurrence of secondary reactions. The decrease in pore size limits the compounds that would be able to actually enter theses pores, making it more selective.

The adsorption/desorption isotherm of Brown clay and BC_6 resembles that of type IV isotherm of Figure 32 where the initial loop classifies a mono and multilayer adsorption phenomenon and where in the mesopores a capillary condensation occurs (Matshitse, 2001). The hysteresis loops give a clearer idea of the multilayer area of the physisorption isotherms. Both Brown clay and BC_6 obtain a hysteresis loop of type H2b (Matthias Thommes, 2015). H2 loops are known to be associated with more complex pore structures. A hysteresis

loop of type H2b links the catalysts to surfaces with blocked pores, also the surface develops a larger distribution of neck width pores (Matthias Thommes, 2015).

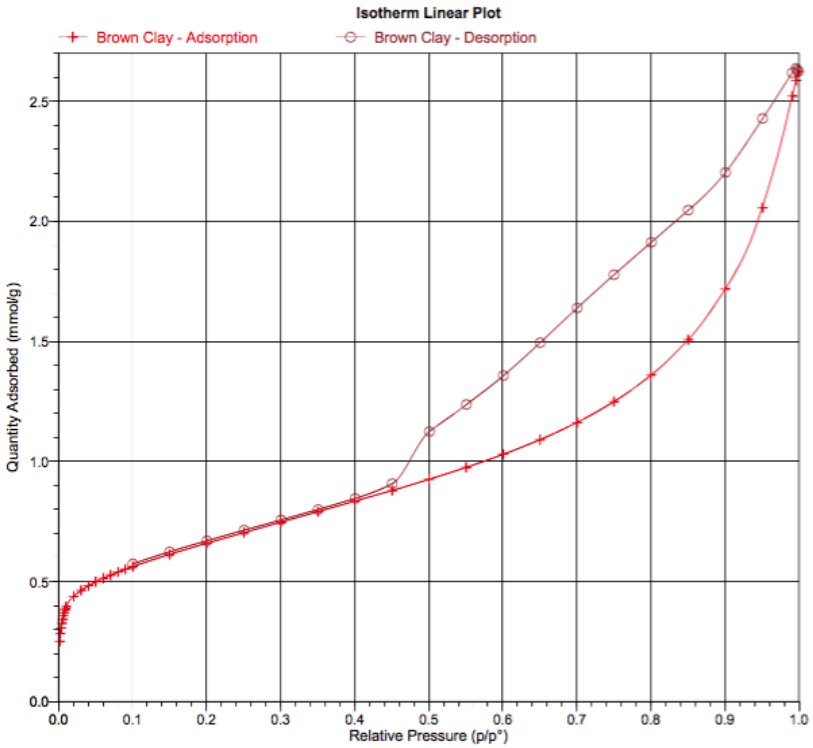

Figure 35 BET adsorption/desorption isotherm of Brown Clay from BET Analysis

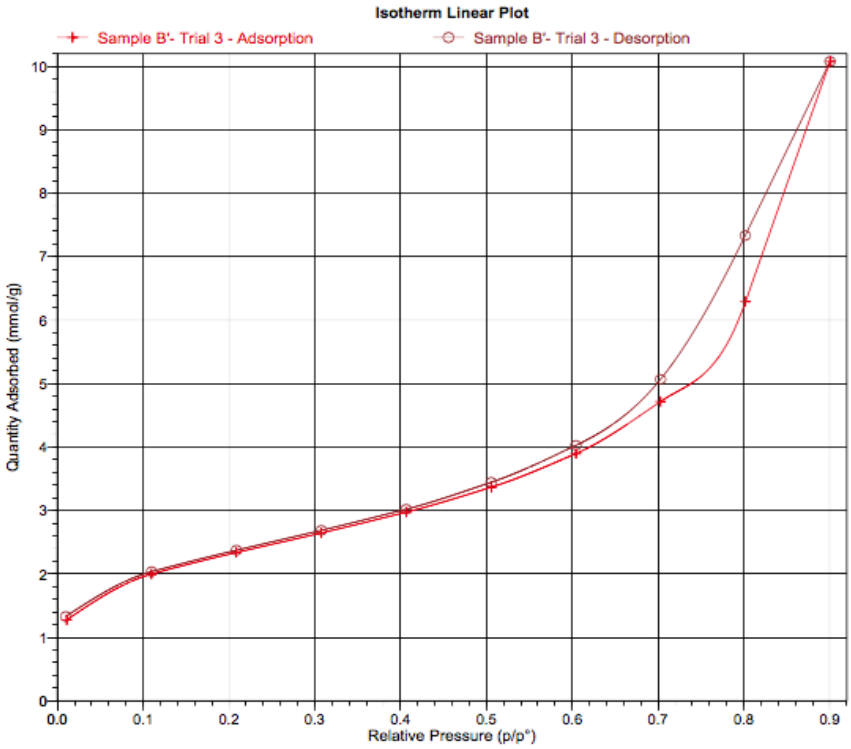

Figure 36 BET adsorption/desorption isotherm of BC_6 from BET Analysis

Figures 37, 38 and 39 show the adsorption/desorption isotherms of Montmorillonite, M_6 and M_4_3hrs respectively. When comparing M_6 with montmorillonite, a decrease in surface area and pore volume was observed from 249 to 154 m^2/g and from 0.239 to 0.165 cm^3/g. On the contrary, M_6 accumulated a larger pore size. Potassium (K), which is known to be a relatively large sized cation and found between the layers of montmorillonite, is completely removed from montmorillonite when activated with 6M H_2SO_4 Table 12 and Table 13. The removal of K, as well as Fe and Mg along with the decrease in surface area and pore volume, indicate the harshness of the strength of the acid causing the collapse of layers.

When comparing montmorillonite and M_4_3hrs there is a very minimal change in surface area, pore volume and pore size. The surface area and pore volume tend to decrease,

indicating pore blockage. This can be explained by the migration of Fe or Al atoms in the tetrahedral replacing Si, this is evident when looking at the change in compositions of Fe, Al and Si in Tables 12 and 14 where Si acquires a larger size compared to Fe and Al. The pore size increased insignificantly from 4.23 nm for montmorillonite to 4.32 nm for M_4_3hrs. The BET results highlighted the impact and severity of high concentration 6M H_2SO_4 on the strength and the effect on the surface of the catalyst when compared to the surface of the catalyst activated with 4M H_2SO_4.

These values relate to what many authors have come across before. Which is the treatment of montmorillonite under severe concentrations generates a decrease in its surface area (Carolina Belver, 2001). The difference in surface areas with respect to 6M and 4M H_2SO_4 are in line with Mendioroz's results (Mendioroz, 1987) who activated montmorillonite under reflux with HCl at 4M and 8M concentrations. He noticed that as he increased the acid concentrations the surface area of the clay decreased. He proposed that silica performs a passive effect on the surface of the clay sheets when exposed to strong conditions. This action prevents the passage of other protons into the clay layers and thus leaves the layers unaltered and decreases the surface area (Mendioroz, 1987). Montmorillonite, M_6, and M_4_3hrs all partake in the Type IV isotherm, where capillary condensation takes part in the mesopores as well as mono and multilayer adsorption. Montmorillonite and M_4_3 take the shape of H2a hysteresis loop. H2a loops might be linked to evaporation induced by cavitation or pore-blockage and this hysteresis loop is common for many different mesoporous silicas. As for M_6 it obtains a hysteresis loop of H2b, which is also attributed to pore blockage with a wide allocation of pore widths.

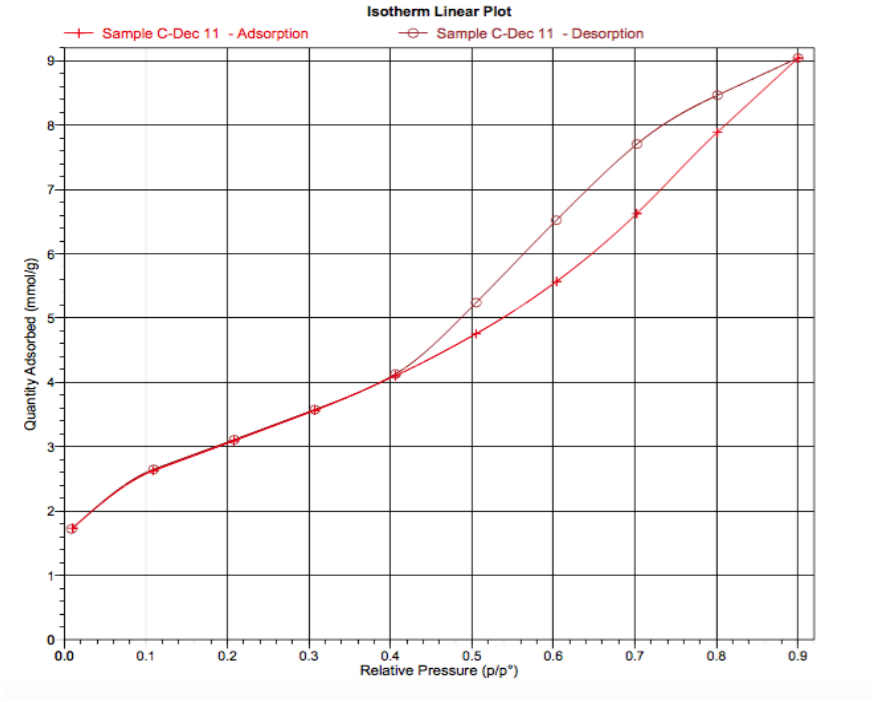

Figure 37 BET adsorption/desorption isotherm of Montmorillonite from BET Analysis

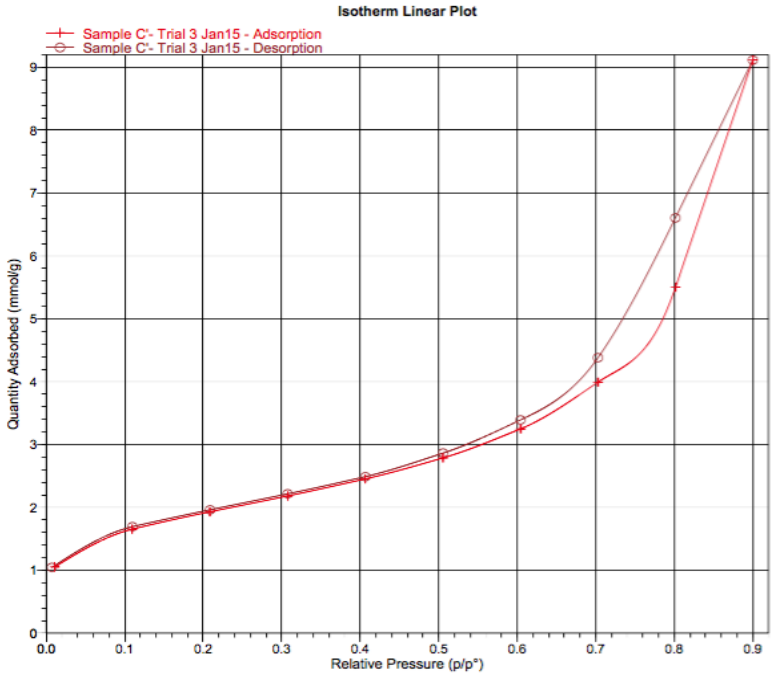

Figure 38 BET adsorption/desorption isotherm of M_6 from BET Analysis

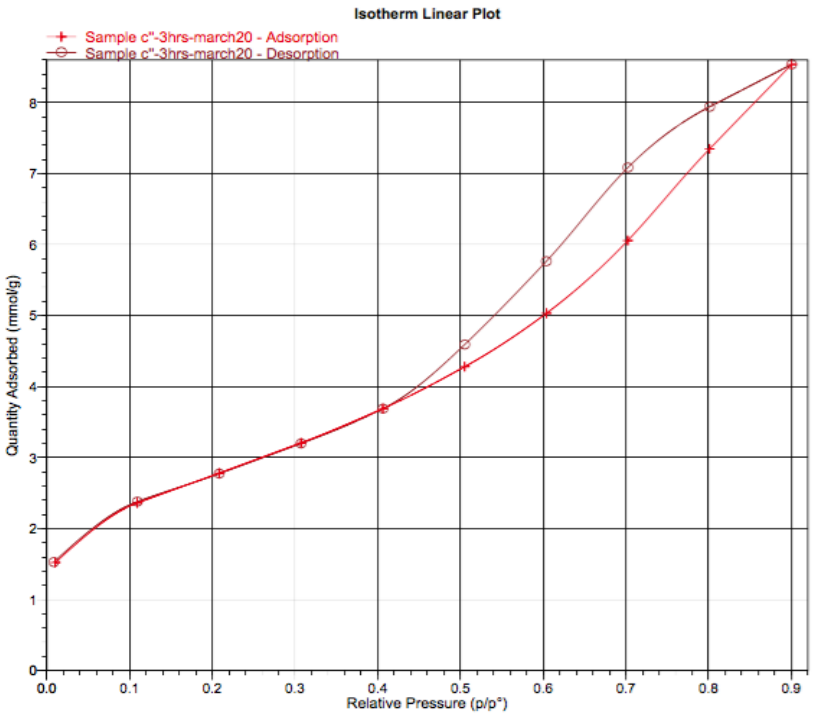

Figure 39 BET adsorption/desorption isotherm of M_4_3 from BET Analysis

The activation of bentonite with 4M H_2SO_4 enhanced the surface area almost 13 times from a surface area of 20 m^2/g to 263 m^2/g, the pore volume also improved almost 17 times more with having had a pore volume of 0.02047 cm^3/g to 0.33626 cm^3/g for bentonite and BN_4 respectively. A similar but not so significant behavior appeared to occur with the change of pore size in BN_4 from bentonite. The increase in surface area and pore volume allows the catalyst to be more receptive to compounds and to partake a longer residence time inside of its structure and thus increase the likely hood of secondary reactions. This can also be said to the increase in pore size, where more compounds with larger molecules would be able to enter the cages of the structure and decompose. Similarly, to brown clay and montmorillonite catalysts, Bentonite and BN_4 acquire a Type IV adsorption/desorption isotherm shown in Figures 40 and 41. Bentonite takes the shape of H3 hysteresis loop

(Matthias Thommes, 2015). This type of loop presents non-rigid combinations of flat-like particles. As for BN_4 takes the shape of H2b loop, which is linked with the blockage of pores and the formation of many different pore neck widths (Matthias Thommes, 2015).

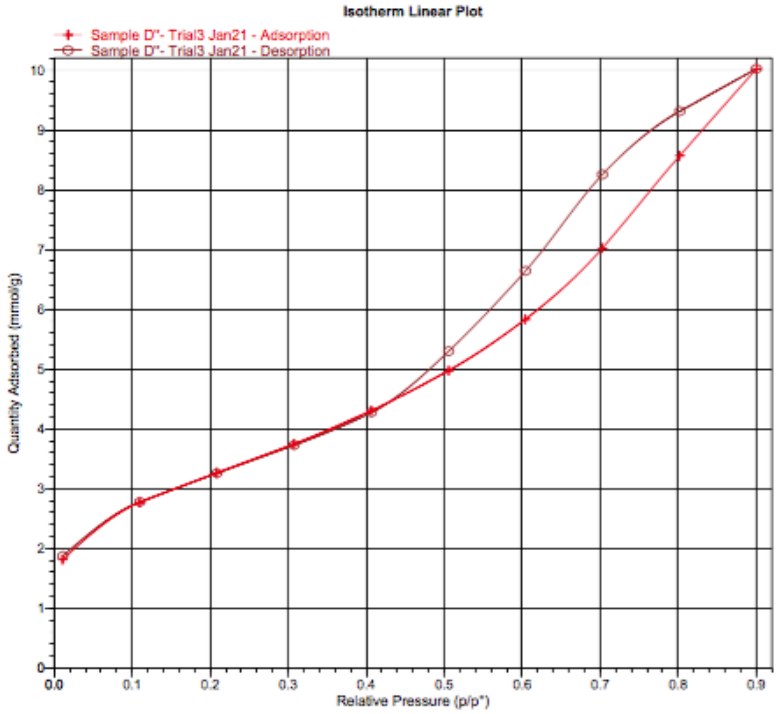

Figure 40 BET adsorption/desorption isotherm of BN_4

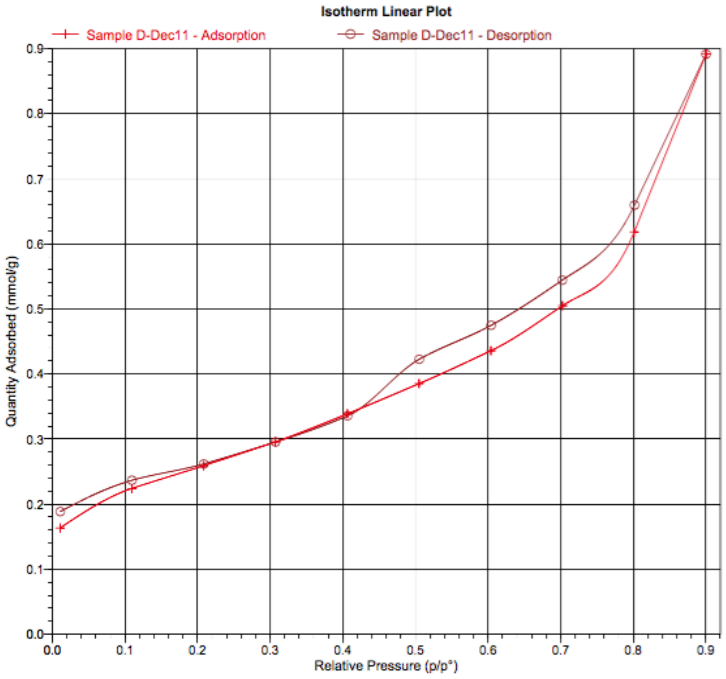

Figure 41 BET adsorption/desorption isotherm of Bentonite

After conducting BET to all the synthesized catalysts it became apparent, that the catalysts modified with sodium silicate didn't have high surface areas, except for Kaolinite. Therefore they were not used for the pyrolysis experiments.

4.1.4 XRD Analysis

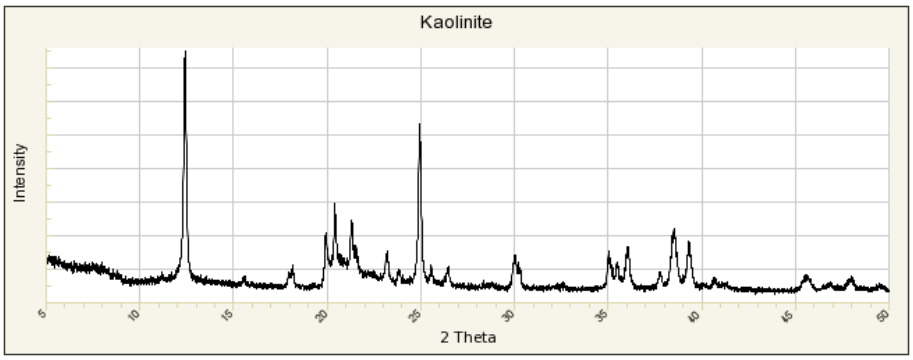

Figure 42 Kaolinite XRD pattern from Database

The XRD pattern of Kaolinite was first analyzed, it fits the same patterns as those in

figure 42 found in data library. Peak intensities were found at around 12° and 25°. With the addition of sodium silicate the peak at 12° broadened and its intensity decreased for KM. This indicates more stacking faults and defects in the crystal structure, which is confirmed from the increase in amorphosity of KM with respect to kaolinite. The XRD pattern of KM_4, showed no peaks at all. The surface area, pore volume and Si/Al were all dramatically enhanced with the acidification of Kaolinite and the amorphosity of KM_4 was slightly higher than that of Kaolinite. These all indicate the strenuous effect of acid and heat on kaolinite. These 3 peaks are better compared in (figure 43).

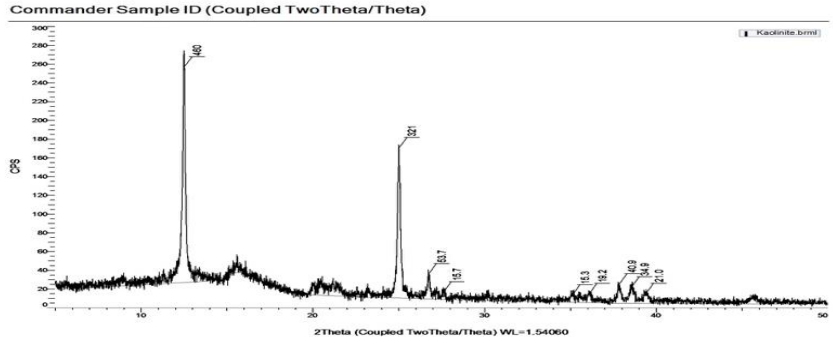

Figure 43 Kaolinite XRD patterns from Xcalibur analysis

XRD peaks of brown clay, being of unknown origin, were compared before and after acidification. Acidification of brown clay, BC_6, showed a broad peak at 15° when compared to that of unmodified clay. Broadness of peak indicates smaller crystal sizes in the structure as well as more stacking or defects in the crystal structure. Defaults were shown in BC_6, where the amorphosity increased by 10% to 62% BC_6 from 52% amorphous for brown clay. The crystal structure also stretched from cubic to tetragonal.

Raw and acid modified montmorillonite XRD patterns are found in figures 44, 45

and 46. According to (J. Temuujin, 2004) the concentration and duration of acidification affects the intensity of the peaks. For a low acidity M_4_3 had higher peak intensities than Montmorillonite and M_6. Nevertheless, XRD patterns showed that M_4_3 has an amorphosity of 36%, which is almost, double that of montmorillonite that was at 16% amorphous. This can be justified by the decrease in Al in M_4_3, which probably disrupted the structure. M_6 had an amorphosity of 53% yet the intensity of the peaks in comparison to montmorillonite was very similar. Therefore it can be concluded that the severe acid concentration of M_6 disordered crystallinity (J. Temuujin, 2004). Similarly, the increase in amorphosity is linearly aligned with the Si/Al ratios increase for M_6 and montmorillonite.

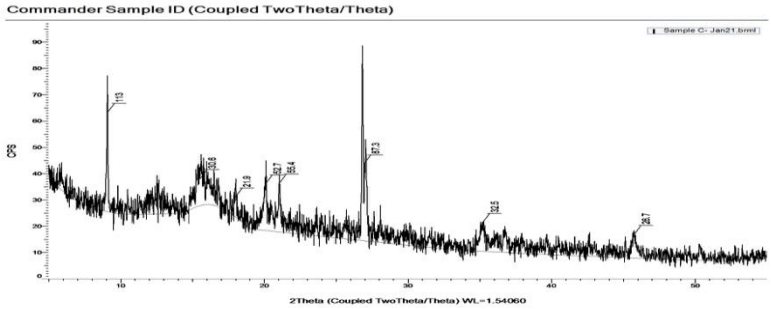

Figure 44 XRD pattern of Montmorillonite

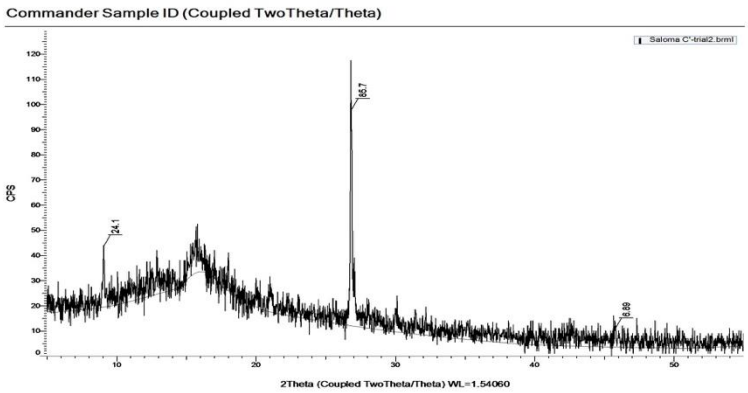

Figure 45 XRD pattern of M_6

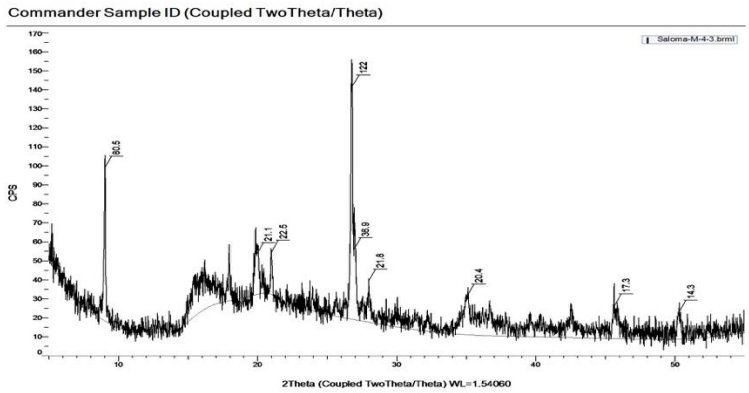

Figure 46 XRD pattern of M_4_3

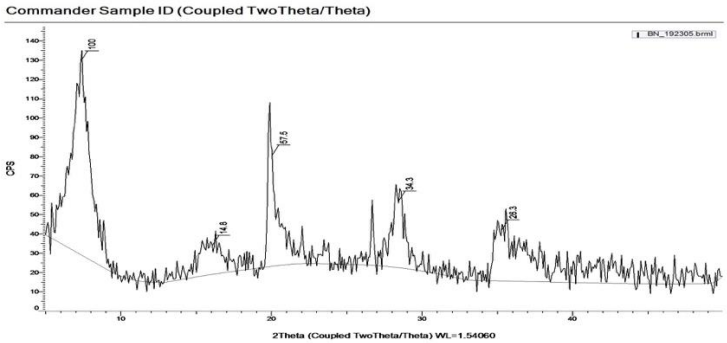

Figure 47 XRD pattern of Bentonite

XRD arrangements of raw bentonite with no modification show that they are similar to those found in Ashaka Bentonite however with mild shifts in basal spacing. This is probably due to differences in unit cell dimensions of the bentonite used and the ashaka bentonite from literature (Abdullah S.L, 2017). Acid modified bentonite, BN_4, was compared with Bentonite (BN) (figure 47). Results indicate that BN was more crystalline than amorphous when compared to BN_4 (figure 48). Cubic bentonite with 24% amorphosity became a tetragonal structure, with almost double amorphosity at 42%. This tetragonal structure is confirmed with the increase in surface area and pore volume measured from BET. The broad basal spacing at 7.2° and intensity 140 for BN, shifted to 9° and a

narrow peak height of 70 for BN_4; the change in the broadness of the peak indicates change in the size of the crystal and change in the homogeneity of the crystal.

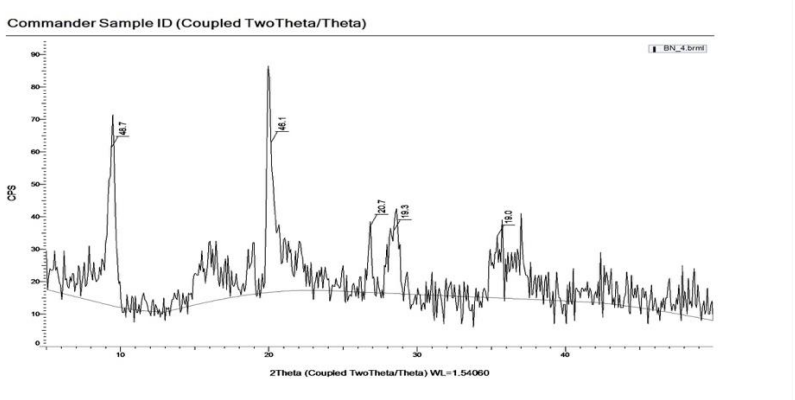

Figure 48 XRD pattern of BN_4

4.1.5 TGA Analysis

Results from thermogravimetric analysis (TGA) of the catalysts are shown through thermal degradation curves. Thermal degradation was performed until a temperature of 980℃. Images are present in appendix B. Kaolinite was weighed at 2.5 mg and lost 10.5 wt.% in total. Mass degradation started at a temperature of 500℃ and from 550℃ to 980℃ there was a loss of 6 wt.%. KM_4 was initially measured at 9 mg and obtained a weight loss of 4.62 wt.% which was much less than that of kaolinite. This indicates that the sodium silicate and acid activation protected the structure from thermal degradation. Brown clay was weighed at 3.4 mg and lost a total of 7.2 wt.% of mass. Mass degradation began at 100℃ and became significant at 580℃. From 580℃ to 980℃ brown clay lost 1.5wt.% of its mass. As for BC_6 was initially weighed at 3.4 mg mass degradation was more significant than Brown clay and had a total mass degradation of 9.7wt.%. This indicates that the acid activation and thermal treatment of the clay weakened the structure. A total weight loss of 5.7 wt.% for montmorillonite was obtained. Weight loss occurred gradually as temperature

increased and unlike kaolinite and bentonite weight loss of the catalyst did not occur suddenly. M_6 was more stable than montmorillonite, it was initially weighed at 1.9 mg and had a total weight loss of 2 wt.%. Even though M_6 was treated with a high concentrated acid it was relatively more stable than montmorillonite, unlike the behavior of brown clay. As for M_4_3 had a total weight loss of 6.1 wt.% Raw bentonite had a total weight loss of 3.7 wt.% and weight loss started at a temperature of 610℃. Similar to the behavior of activated montmorillonite, bentonite treated with 4M H_2SO_4, BN_4, had a smaller weight loss than bentonite in its raw form. BN_4 had a total weight loss of 2.4 wt.%.

4.2 Pyrolysis results

The objective of the pyrolysis experiments was to enhance the degradation of scrap tires in order to maximize the gas yield at the expense of the oil yield. The non-condensable products were determined by weighing the quartz tube before and after experiments. This portion of the product formed from rubber pyrolysis was the gas yield. Results were collected under constant experimental parameters with the use of different catalysts. This study does not contain any experimental errors that may have occurred from catalyst or cotton displacement, or carrier gas instability.

4.2.1 Catalytic Cracking

Zeolite catalysis dominated catalytic cracking (Rosinski, 1992) and hydrocracking (Rabo, 2001)**.** An important property of a zeolite as a cracking catalyst is its crystallographic unit-cell size, which is a close measure of the aluminum content in of the zeolite framework and therefore it is commonly taken as a close measure of its acidity (Cejka J. C., 2010).

It is vital to understand the reactions that take place in catalytic cracking. As rubber begins to crack inside the reactor, the gas has two passages: either it is a part of primary reactions and flows crossing the catalyst or undergoes secondary reactions that take place between the gas and the solid. A primary reaction is when the pyrolytic gas is in direct contact with zeolite catalyst. The efficiency of the interaction between gas and catalyst depends on the surface area, crystallinity, and acidity of the zeolite. If sufficient bonds were obtained between acid sites and the adsorbed hydrocarbon chains then intermediate cations would form. Intermediate cations occur due to formation and cracking of the hydrocarbon chain through beta-scission mechanism. Polymer recombination, condensation and carbonaceous reactions occur due to secondary reactions or between solid and gas.

4.2.2 Catalytic pyrolysis vs. thermal pyrolysis

The nine different catalysts were tested several times and their results along with the experimental variability in percent are listed in Table 18.

Table 18 Product yields from catalytic pyrolysis at 580℃

Materials	Product Yield (wt%)		
	Gas	Liquid	Solid
Tire	11.8 $\pm$**3.0**	48.8 $\pm$**1.5**	39.4 $\pm$**2.5**
Tire/Kaolinite	21.8 $\pm$**1.4**	37.3 $\pm$**2.0**	40.9 $\pm$**0.9**
Tire/KM_4	22.7 $\pm$**2.0**	37.1 $\pm$**2.6**	40.2 $\pm$**0.7**
Tire/Brown Clay	20.1 $\pm$**1.1**	40.8 $\pm$**1.2**	39.1 $\pm$**0.4**
Tire/BC_6	21.4 $\pm$**1.9**	39.4 $\pm$**2.4**	39.2 $\pm$**0.9**
Tire/Montmorillonite	27.4 $\pm$**0.3**	33.9 $\pm$**1.3**	38.7 $\pm$**0.9**
Tire/M_6	30.0 $\pm$**0.5**	30.9 $\pm$**1.7**	39.1 $\pm$**1.8**
Tire/M_4_3	29.8 $\pm$**1.0**	29.9 $\pm$**0.6**	40.2 $\pm$**1.3**
Tire/Bentonite	22.8 $\pm$**1.1**	37.3 $\pm$**0.7**	39.9 $\pm$**0.4**
Tire/BN_4	26.5 $\pm$**0.5**	34.0 $\pm$**0.1**	39.5 $\pm$**1.5**

In order to compare the impact of the catalysts with pyrolysis of waste tires, tires were first pyrolyzed in the absence of catalysts. The supposed catalyst bed was replaced with sand of almost same weight. Results in Table 18 illustrates that elevated liquid yields of 48.8 wt.% and low gas yields of 11.8 wt.% were obtained from tire pyrolysis in the absence of a catalyst. Comparable results were recorded in literature (B.Benallal) (C. Roy) (A. Lucchesi). Formation of coke on the sand bed was neglected in this study. From figure 50, it is clear that the total composition of liquid produced from un-catalyzed pyrolysis of scrap tires was aromatics. (M.Rofiqul Islam, 2008) mentioned that aromatics are present in tire-derived oil due to the natural source of polymeric materials and SBR in tires. These polymeric materials readily contain aromatic rings, and under extreme temperature and pressure conditions, these rings split and lead to the production of cyclization of olefin arrangements over dehydrogenation reactions that take place during pyrolysis process.

A decrease of liquid wt.% and an increase of gas wt.% were seen with the use of catalysts in waste tire pyrolysis figure 49. That is because more materials were broken down into more gaseous products under the effect of the catalyst. Zeolite catalysts have been successfully used by (P.B. Venuto T. H.) and (P.T. Williams, 2003) for catalytic cracking of scrap tires both authors showed an increase in the gaseous products with a simultaneous decrease in the liquid products formed. Figure 49 clearly demonstrates the trend of the increase of gas yield on the expense of liquid yield.

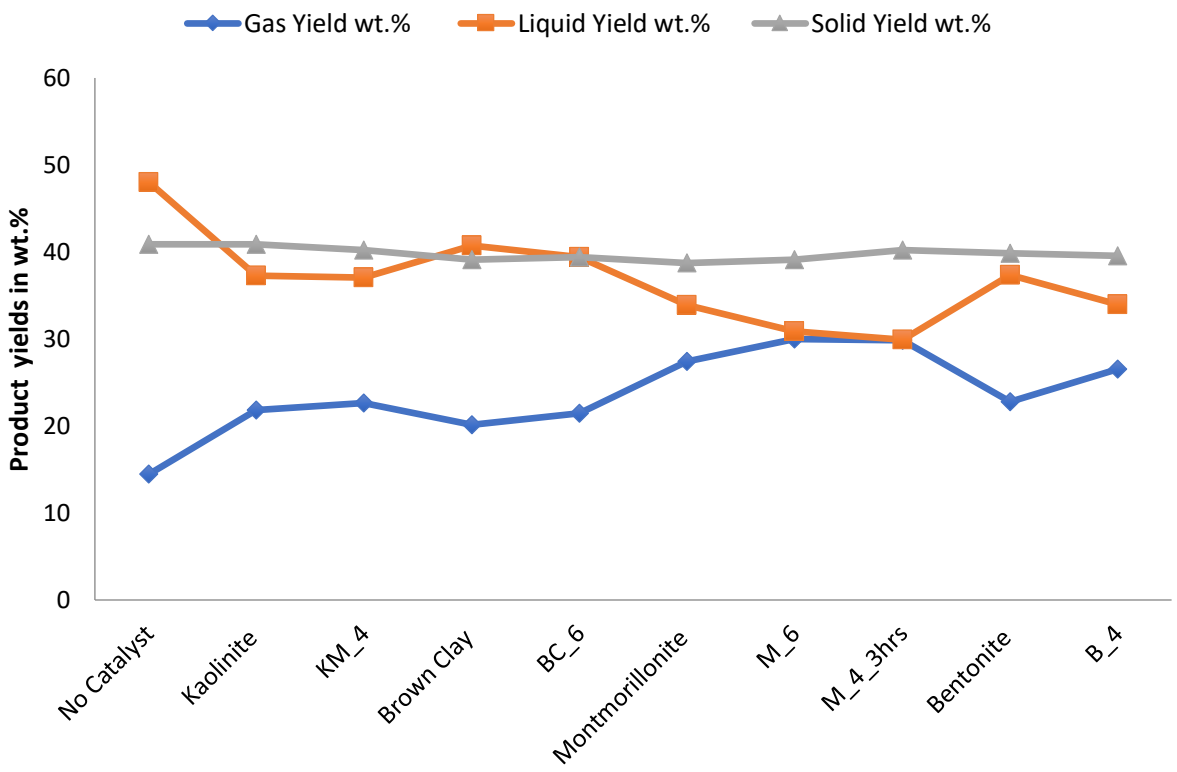

Figure 49 Liquid, Solid and Gas fractions in weight percent for each catalyst

As displayed, the solid yield remained almost constant for experiments that were both catalyzed and un-catalyzed. The catalysts used were all activated "natural clays" and had similar properties and behaviors of synthetic zeolites. What differentiated them from each other were their pore sizes and Si/Al ratios. These two properties play a large role on the selectivity and activity of the catalyst.

4.2.3 Liquid product analysis of no catalyst vs. catalytic pyrolysis of scrap tires

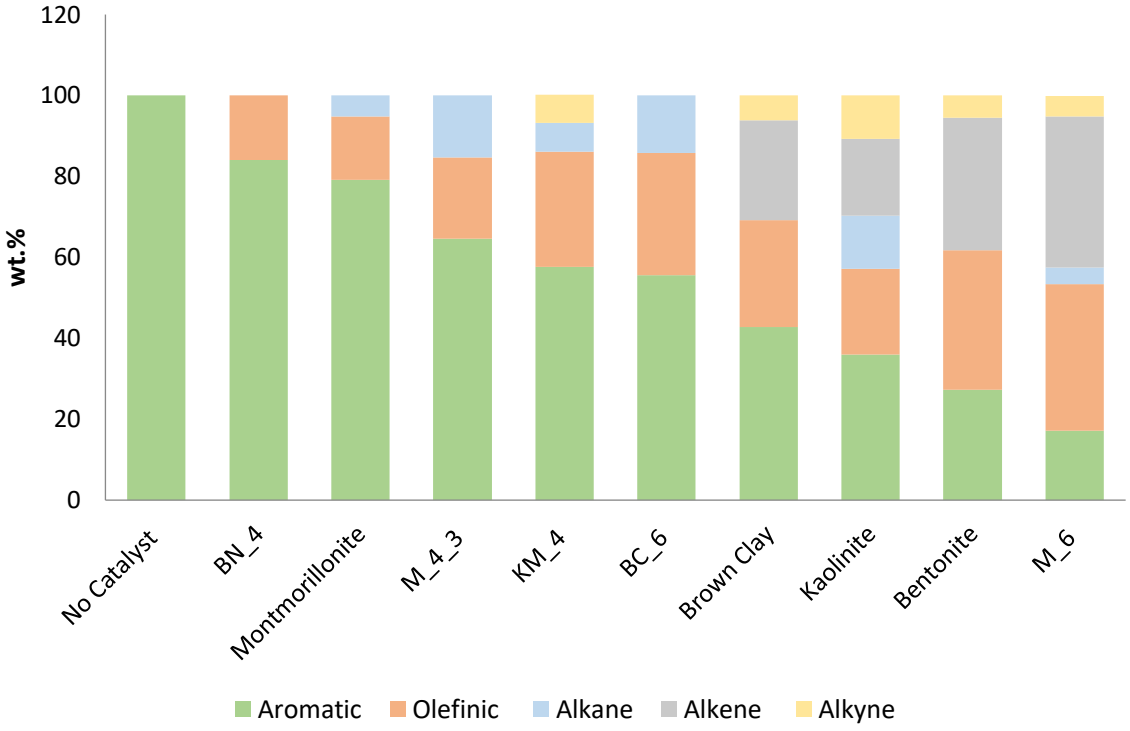

Figure 50 GC results of Scrap tire pyrolysis with all catalysts

Liquid products derived from tire contained mostly large ringed aromatics specifically polycyclic aromatic hydrocarbons (PAHs). Figure 49 shows both kaolinite and KM_4 obtained similar liquid and gas yields of 37 wt.% and 22 wt.% respectively. Although kaolinite and KM_4 had similar liquid fractions, figure 51 shows that the constituents of the liquid products were different. The aromatic and olefinic yields were higher when KM_4 was used rather than kaolinite. It is important to note that KM_4 had a larger surface area and smaller pore size than that of kaolinite. Also, the Si/Al ratio increased to 6.62 for KM_4 from 1.02 for kaolinite. Alkenes, alkynes, alkane, aromatics and olefins, were identified in the oil products. These five groups are shown in figure 51.

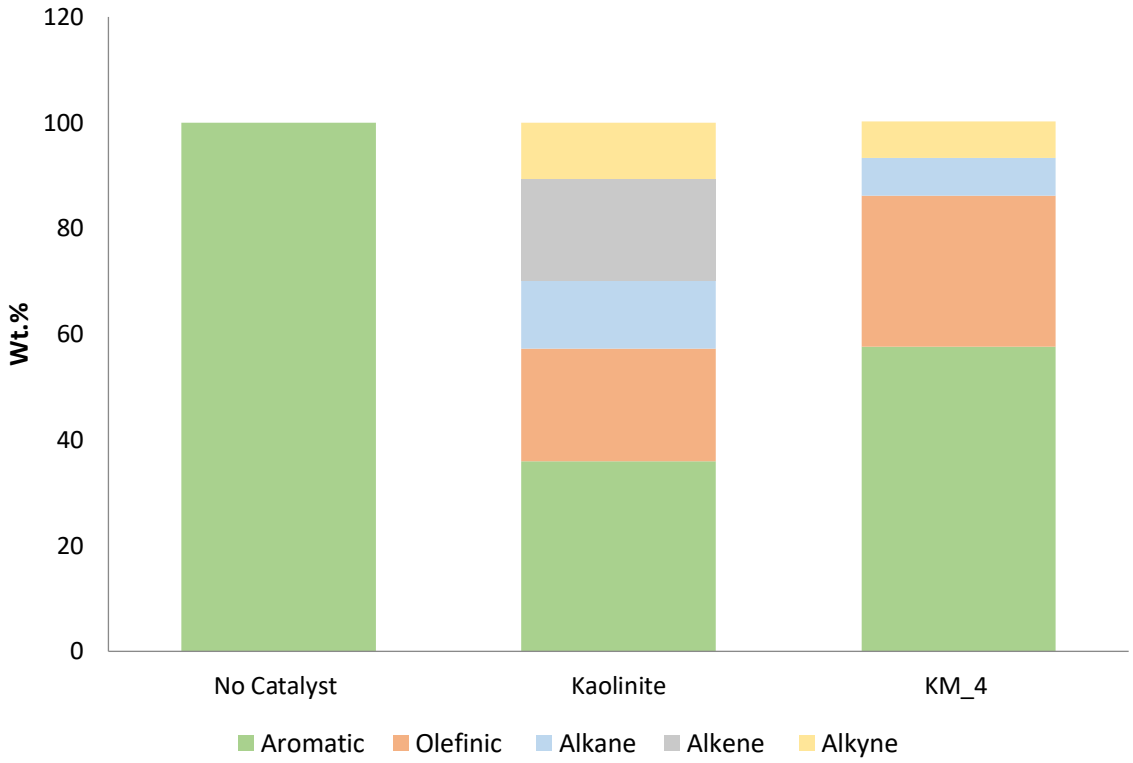

Figure 51 Liquid product comparisons between No Catalyst, Kaolinite and KM_4

KM_4 liquid products illustrate a markedly increase in the concentrations of aromatics to 57 wt.% from 35 wt.% and from 21 wt.% olefin to 28 wt.%. From the aromatics produced with KM_4 was Toluene, which was not found in the products formed with kaolinite. (Shen Boxiong, 2007) mentioned that high cracking activity of zeolite USY changed limonene to aromatic hydrocarbons, eliminating limonene and increasing aromatic hydrocarbons in the processed oil. Those results match that of KM_4. D-limonene percentage in liquid oil went from 19% under catalytic activity of kaolinite to 0% with KM_4, indicating its high activity and agreeing to the increase of aromatic content. Also, the absence of alkenes in the liquid oil from KM_4 signifies that secondary reactions occurred

in its presence, which produced more aromatic hydrocarbons. (D.E. Wolfson) observed the behavior of aromatic hydrocarbon increase on the expense of alkenes under elevated temperatures of scrap tire pyrolysis. The scission of polymer chains could produce double bonds, which could be a step to the production of aromatic hydrocarbons. Following cyclisation, conjugated and non-conjugated double bonds form aromatics and olefinic compounds form from the non-conjugated compounds (Shen Boxiong, 2007) (I.E. Katheklakis) (M.A. Golub).

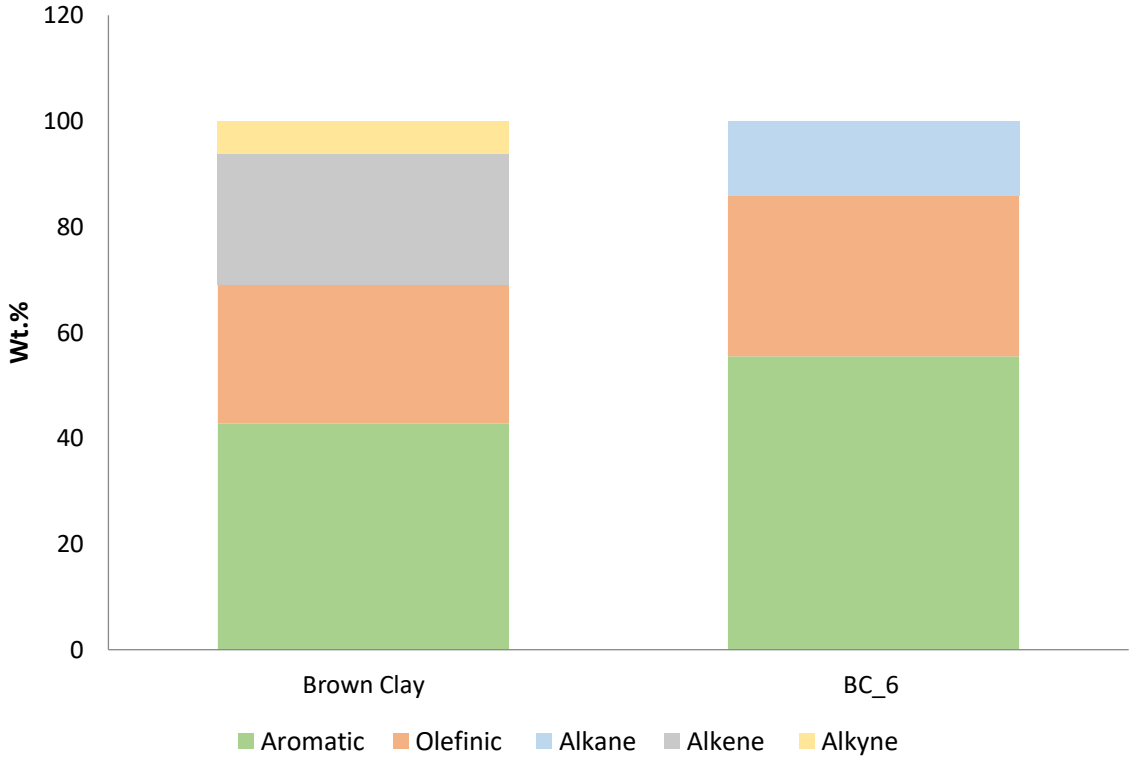

Figure 52 liquid product comparisons between Brown clay and BC_6

The gas and liquid yields of scrap tire under the use of brown clay catalyst were 20 wt.% and 40 wt.% respectively. When BC_6 was used, the gas yield went up by 1 wt.% to

21 wt.% and the liquid yield reached 39 wt.%. The acidification of brown clay was able to increase the gas yield, although slightly, on the expense of liquid yield.

When comparing the results of the liquid yields from catalyzed and un-catalyzed products, there is a difference in the products obtained. Brown clay was able to decompose the large ring aromatics found from un-catalyzed tire pyrolysis into a liquid product composed of aromatics, olefins, alkenes and alkynes (figure 52). The acidification of brown clay into BC_6 resulted in higher yields of both aromatics and olefin and reduced alkenes and alkynes into saturated alkane chains. BC_6 had a surface area almost four times that of brown clay, as well as a higher Si/Al ratio. Pore size of BC_6 was slightly lower than brown clay, which thus affected the selectivity of the products. D-limonene was present in the liquid product obtained from brown clay at 25 wt.%, however with the use of BC_6 as catalyst no D-limonene was formed.

Williams, 2013 stated that limonene under the use of catalysts and high temperatures converts into aromatic hydrocarbons (Wiliams, 2013). This agrees to the activity of BC_6; catalyst since more toluene and benzene were formed and the presence of limonene decreased. The presence of alkenes and alkynes, which are known to be unsaturated hydrocarbons, weren't found in oil produced from BC_6, rather alkanes, or saturated hydrocarbons, probably due to the higher surface area available for reactions to take place as well as the smaller pore sizes which impact the selectivity of smaller chained hydrocarbons. The absence of alkenes at high temperatures with BC_6 highlights the possibility of the formation of secondary reactions where single ringed aromatic hydrocarbons were formed.

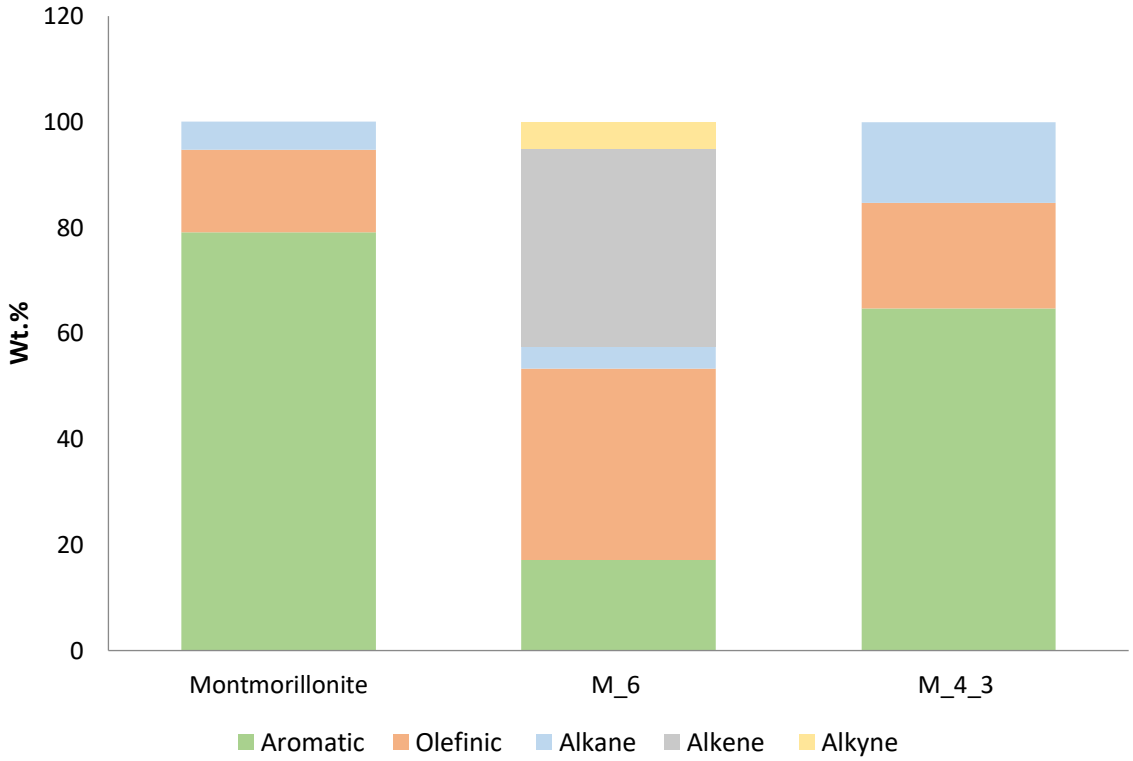

Figure 53 Liquid product comparisons between Montmorillonite, M_6 and M_4_3

Catalytic cracking of scrap tires pyrolysis was done on raw montmorillonite, M_6 and M_4. Montmorillonite on its own yielded 27 wt.% of gas and 33 wt.% of liquid. Liquid constituents consisted of aromatics, olefins and alkanes of them being toluene, benzene and styrene along with PAHs. A surface area decrease of almost 100 m^2 occurred for M_6 than when compared to montmorillonite as well as a decrease in pore volume. Although gas yield increased by 3% on the expenditure of liquid yield, figure 53 shows that the composition of liquid products from M_6 consisted of more un-saturated products than the products formed from raw montmorillonite. Benzene and toluene weren't formed as aromatics however the amount of PAHs decreased. D-limonene and styrene were the major products formed from M_6. The Si/Al ratio of M_6 increased to 33.3, which is considered to be high. In order for a

natural zeolite catalyst to be reactive it should have high acidic strength which comes from lowering the existence of Al atoms in the structure while increasing the hydroxyl protons that represent these desired acidic sites (Cejka J. C., 2010). Literature has stated that a phenomenon such as proton crowding could occur due to the concentrated acid sites and therefore inversely impact and weaken the acidic strength. The presence of alkynes and alkenes indicate that the aromatics decomposed from tires weren't sufficiently bonded to the surface of M_6 for better reactions. However the formation of styrene and D-limonene as products can be useful for many chemical industries.

Catalyst M_4_3 had a surface area and pore volume slightly lower than that of montmorillonite but its Si/Al ratio increased from 1.33 to 5.61. Gas yields from reactions with M_4_3 were 29.8 wt.%, which was higher than the gas yield under montmorillonite as a catalyst. Liquid products extracted from reactions with M_4_3 contained aromatics, olefins and alkanes, these of which were similarly found in the oil products from experiments with montmorillonite, however, at different percentages. Catalytic cracking of waste tires with M_4_3 produced a lower amount of aromatics including benzene , which was not found with M_6 and larger weight fractions of alkanes and olefins than produced with catalytic cracking under montmorillonite.

Comparing the two modified catalysts, M_6 and M_4_3, both have similar gas and liquid yields. However, the compositions of the liquid products obtained were not similar. Catalyst M_6 produced more unsaturated compounds whereas M_4_3 gave aromatics and saturated alkanes. The differences in compositions of the liquid product yields are clearer when studying physical characteristics of the catalyst. M_4_3 had a pointedly larger surface area and pore volume than those of M_6. As previously mentioned, the higher activity of a

zeolite catalyst is due to the presence of strong acid sites within the pores (Shen Boxiong, 2007). The surface acidity of the zeolite is increased with a reasonable surface concentration of aluminum (P.B. Venuto T. H.) (Campbell). (Shen Boxiong, 2007) stated that the zeolite catalyst USY had a higher activity with Si/Al ratio of 5 in comparison to zeolite ZSM-5 with a Si/Al ratio of 38. This is the case of M_6 which has a Si/Al ratio of 33 compared to M_4_3 with a Si/Al ratio of 5.6 (Shen Boxiong, 2007). Nevertheless, both catalysts enhanced scrap tire degradation and aided in the production of useful chemicals such as benzene, toluene, and styrene.

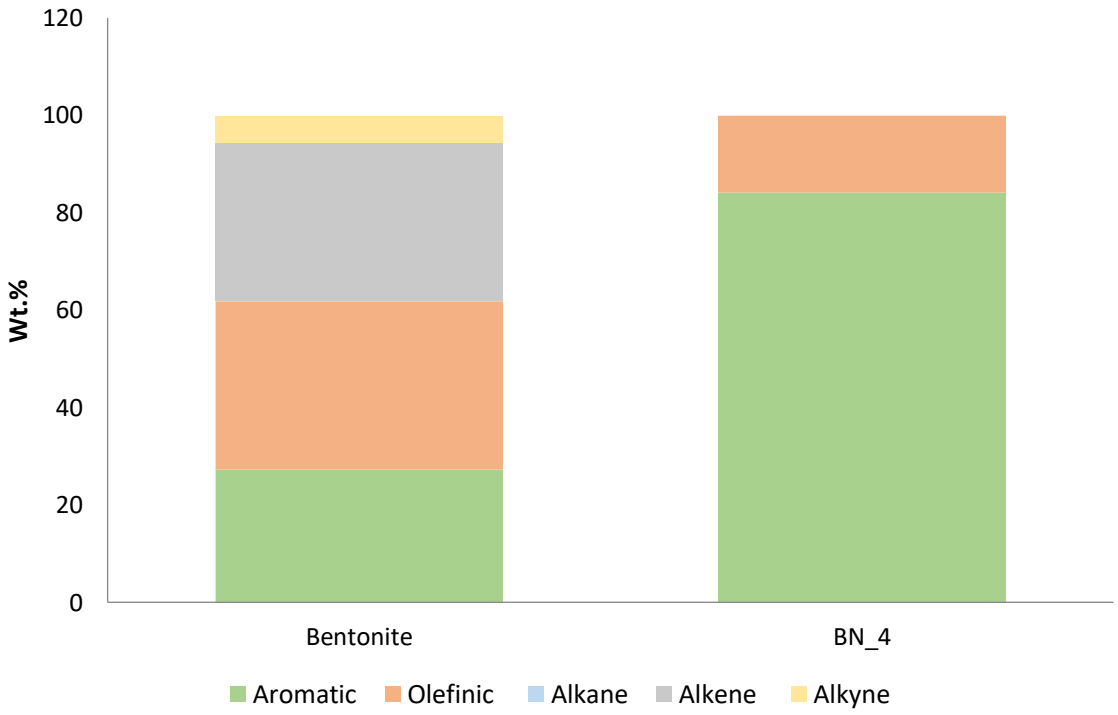

Figure 54 Liquid product comparisons between Bentonite and BN_4

Acid modified bentonite, BN_4, had a surface area, pore volume and pore size significantly larger than that of raw bentonite. This increase had a considerable impact on the gas and liquid yields. Gas yield increased from 23 wt.% to 27 wt.% when bentonite was

activated with acid, and the liquid yield decreased in the same manner from 37 wt.% for bentonite to 33 wt.% for BN_4. This confirms that the modification of raw bentonite with acid and heat enhanced the surface area as well as the gas yield on the expense of liquid yield, keeping the solid yield constant. Figure 54 portrays the difference in the liquid product yields obtained from tire without catalyst as well as tire pyrolyzed with bentonite and BN_4. It is clear that the constituents found in the liquid oil from BN_4 are a result of the secondary reactions that occurred on or inside the surface of the catalyst. Alkenes and Alkynes present in the oil sample of bentonite were not found in the liquid produced under BN_4. Thus the higher surface area as well as higher Si/Al ratio initiated the occurrence of secondary reactions and the conversion of alkenes and alkynes into more single aromatic compounds. D-limonene and 1-propynyl-Benzene were compounds found in liquid samples of bentonite pyrolysis reactions but not found when BN_4 was used. BN_4 produced aromatics such as benzene and toluene which were not produced with bentonite as a catalyst.

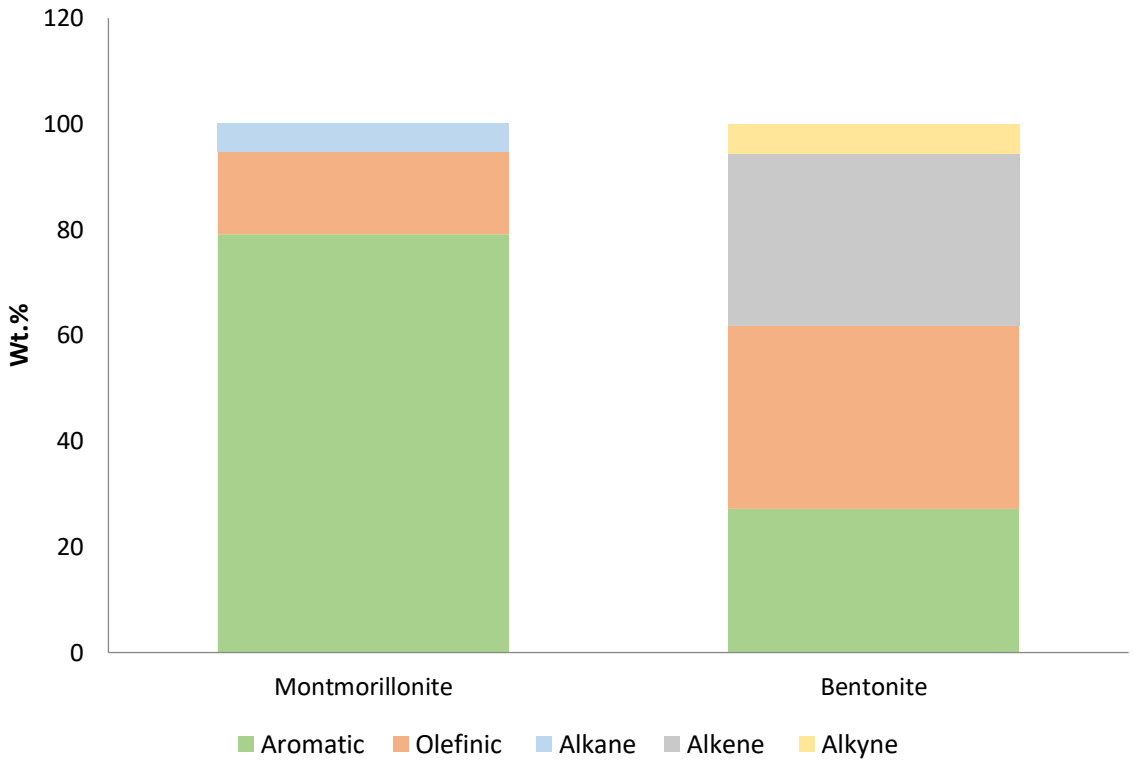

Figure 55 Liquid product comparisons between Montmorillonite and Bentonite

Bentonite is an aluminum phyllosilicate clay rock that is found in nature and contains 80-90 wt.% of montmorillonite (Uddin, 2018). Other smectite properties such as crystalline quartz and feldspar can also be found in bentonite. Montmorillonite that is derived from bentonite may contain sodium or calcium. Different samples of same clay deposits frequently differ in the minerals found in them (A.A, 2017). Catalyst analysis of bentonite and montmorillonite showed that the Si/Al ratio of bentonite was slightly higher than that of montmorillonite as for the BET analysis, montmorillonite had a surface area of 249 m^2/g, which was almost 13 times larger than that of bentonite at 20 m^2/g. Although montmorillonite is derived from bentonite, the differences in surface area and Si/Al ratios of the catalysts were reflected in the products from pyrolysis reactions. Products from reactions with montmorillonite and

bentonite resulted in different liquid compositions (figure 55). Liquid composition from experiments with montmorillonite yielded aromatics such as toluene and benzene which were not found in liquid compositions under bentonite. The presence of alkanes from experiments with montmorillonite can be due to the larger surface area of the catalyst, where more secondary reactions were able to take place. Similarly, the gas yield from scrap tire pyrolysis with montmorillonite was higher than that from experiments performed with bentonite. These results are in agreement with the properties of the catalyst and liquid characteristics.

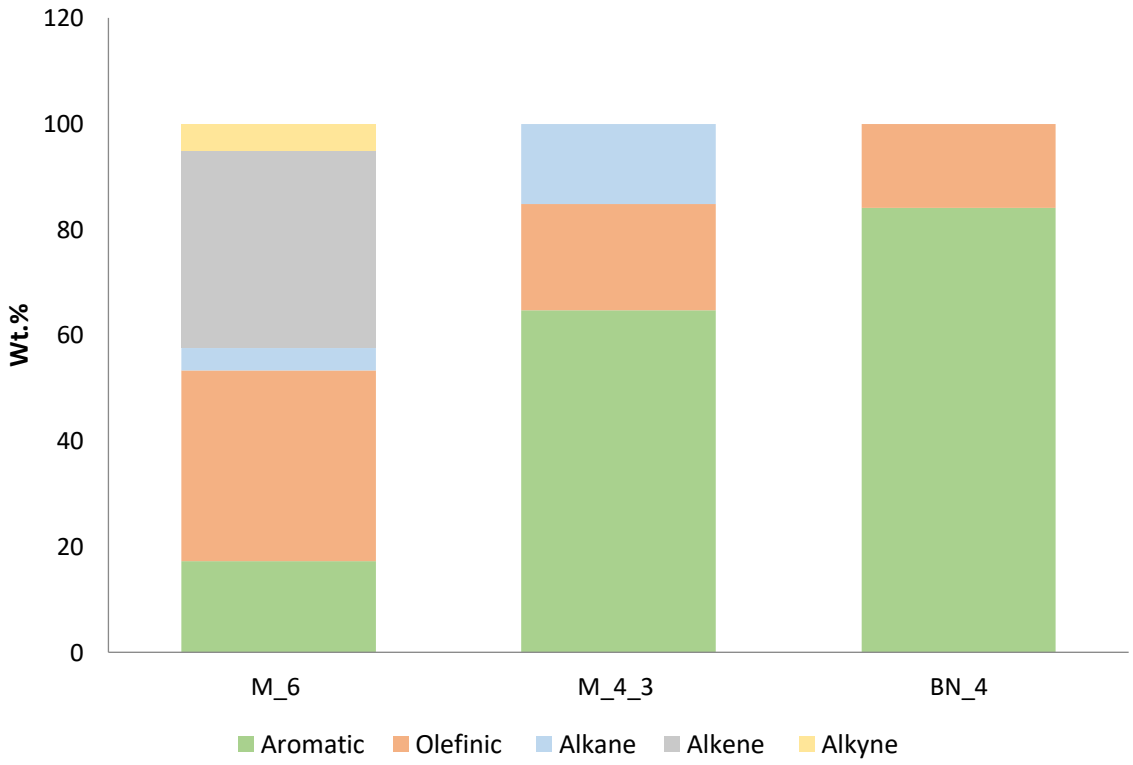

Figure 56 Liquid product comparisons between M_6, M_4_3 and BN_4

The modification of montmorillonite and bentonite with different acid concentrations enhanced the gas yield at the expense of liquid yield. Enhancement was also determined in

the composition of the liquid products. The severity of the 6M H_2SO_4 acid concentrations for M_6 over 4M H_2SO_4 acid concentrations for M_4_3 and BN_4 became clearer when comparing Si/Al ratios. M_6 catalyst had a Si/Al ratio of 33.3 whereas M_4_3 and BN_4 had Si/Al ratios of 5.61 and 6.11 respectively.

Strong acid sites are needed within the pores to obtain high activity (Shen Boxiong, 2007). (Shen Boxiong, 2007) mentions that a high Si/Al ratio such as 33.3 could lead to overcrowding and loss of acidic efficiency inside the pores. The fragility of the acid sites for M_6 was shown through the liquid product composition (figure 56). Even though there is a difference in Si/Al ratios for M_6 and M_4_3 the gas yields obtained for both were at 30 wt.%. On the other hand, M_4_3 and BN_4 were both modified with the same acid concentration, however for different durations. The longer the catalyst was modified the more aluminum was leached out of the pore sites. Despite the different durations, they acquired similar Si/Al ratios as well as BET results. By further inspecting the results in figure 56, their similarities are portrayed by having similar light liquid product compounds. M_4_3 obtained a gas yield 30 wt.% higher than that of BN_4. From the comparisons gathered between M_4_3 and BN_4, it is clear that M_4_3 is more effective than BN_4. Both produced benzene and styrene compounds however at different yields. M_4_3 has a gas yield of 30 wt.%, which was an increase from montmorillonite at the expense of liquid yield. Also, scrap tire pyrolysis with M_4_3 acquired a significant amount of alkanes or saturated hydrocarbons.

4.3 Gasification Results

Even though gasification experiments usually take place at elevated temperatures, initial gasification experiments were performed at 580℃ which was the same temperature used for previous pyrolysis experiments, in order to compare the effect of the added reactant added, ethanol. Ethanol is known to have a cracking temperature of about 650℃ (Apichai Therdthianwong, 2001). Hence, the two other experimental temperatures were above the temperature required for ethanol to undergo cracking. Gas yields were slightly higher than that formed with tire pyrolysis as illustrated in Table 18 and Table 19.

Table 19 Product yields from gasification at different temperatures

Temperature	Product Yield (wt%)		
	Gas	Liquid	Solid
580℃	13.4 $\pm$**1.6**	46.6 $\pm$**5.0**	40.0 $\pm$**4.0**
680℃	21.5 $\pm$**4.3**	40.0 $\pm$**3.3**	38.5 $\pm$**1.1**
780℃	37.7 $\pm$**3.6**	24.1 $\pm$**3.4**	38.2 $\pm$**1.0**
780℃+ Montmorillonite	41.8 $\pm$**2.3**	24.6 $\pm$**2.3**	33.6 $\pm$**0.2**

While keeping all parameters constant, similar experiments were repeated at 680℃ and 780℃. As expected, the gas yields increased with the increase in temperature. The gas yield increased mostly on the expense of the liquid fraction and just slightly on the solids figure 57. At 680℃ the gas yield increased by 60% when compared to experiments at 580℃ which can be related to the cracking of ethanol. A gas yield of 37.7 wt.% was obtained at 780℃. This is a much higher value than that obtained from catalytic cracking during pyrolysis experiments. These results were expected due to high temperatures and reactive ethanol cracking compounds.

Looking further at the liquid compositions obtained from catalytic cracking of scrap tire pyrolysis, out of the four raw catalysts used, montmorillonite achieved higher quality components among all catalysts (figure 49). Ethanol gasification at 780℃ was repeated with the addition of montmorillonite at the same ratios used for the pyrolysis experiments. Table 19 showed that an increase in gas yield occurred, however not as significant as the increase in gas yield that took place from 680 to 780℃. Unlike pyrolysis experiments, figure 57 signifies that an increase in the gas yield with the addition of montmorillonite occurred at the expense of solid yield rather than liquid fraction.

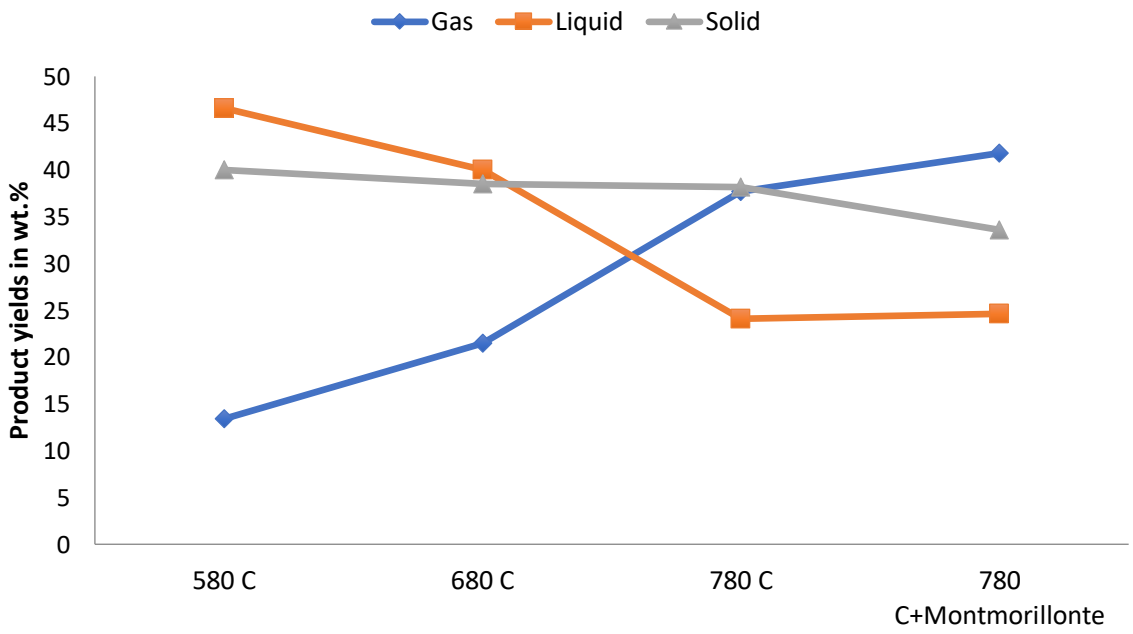

Figure 57 Liquid, Solid and Gas fractions in weight percent at each temperature

GC/MS analysis was performed on a gas sample extracted from the gasification experiment at 780℃ without catalyst (figure 58). The gas composition contained light hydrocarbons (C_2-C_6) chains made up mostly of alkenes and benzene. No CO_x, H_2, and SO_x

were detected in the analysis. However, a large amount of ethene, propene, butene and benzene aromatics were detected. These results indicate that ethanol and rubber materials went through intramolecular dehydration reactions as well as oligomerization and dimerization reactions. These reactions allow the conversion of hydrocarbons and ethanol to convert to C_2H_4, C_3H_6 and C_4H_8. Cyclization reactions are also possible and the presence of benzene agrees to this matter. These results are in agreement with the liquid product analysis performed by Tingting Zhao (2019).

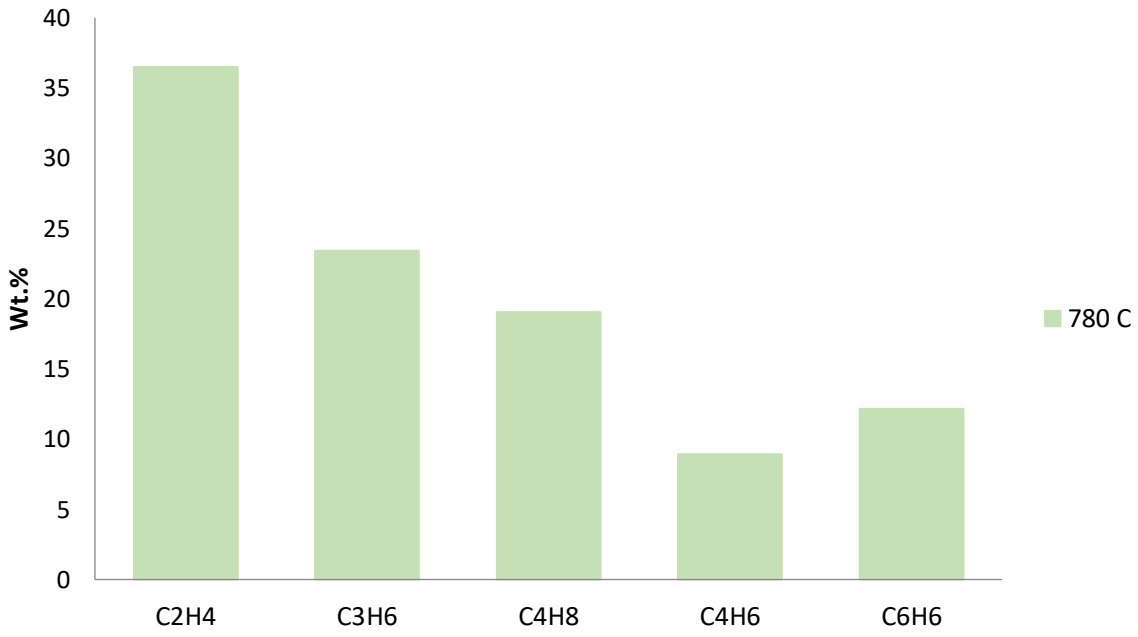

Figure 58 Gasification gas components by weight percent obtained at 780℃

CHAPTER 5

CONCLUSION AND RECOMMENDATIONS

The cracking capabilities of the activated natural clays were investigated by studying pyrolysis product yields and distribution. The highest gas yield was 30 wt.% obtained from both modified montmorillonite catalysts M_6 and M_4_3. The liquid product compositions were investigated using GC-MS and it became evident that the modification method with a lower acid concentration, M_4_3, produced lighter liquid hydrocarbons. In addition, the aromatics formed with M_4_3 catalyst were mostly benzene as for M_6, it produced higher amount of PAHs. The surface area of 224 m^2/g, a pore size of 4.32 Å and a Si/Al ratio of 5.6 for M_4_3 were the main factors for this improved performance over M_6 and other activated natural clays.

Gasification experiments were done at three different temperature of 580, 680 and 780℃ with the aim to further increase the gas yield. As expected the gas yield increased, to 37.7 wt.%, at 780℃. The effect of montmorillonite was tested during gasification producing a high gas yield of 41.8 wt.%. Ethanol/rubber gasification generated lighter products with C_2-C_6 majority compounds. It can be concluded that scrap rubber gasification with ethanol outperformed catalytic pyrolysis; higher gas yields were achieved with the liquid and gas products containing lighter hydrocarbons.

Ethanol gasification of scrap rubber tires should be further studied. Future research should focus on kinetic modeling of the ethanol/scrap rubber gasification process to be able to determine reaction mechanisms. Furthermore, new catalysts should be designed to ensure

the direct reforming and conversion of the gasification products into H_2 and high quality syngas.

APPENDIX

MOLAR CONCENTRATION CALCULATIONS

Specific gravity of H_2SO_4=1.84g/ml

Assume 95% H_2SO_4 in 100ml

Therefore, $[H_2SO_4]= \frac{95ml}{100ml} * \frac{1000ml}{1L} * \frac{1.84g}{ml} = 1748\ g/L$

The Molecular weight of H_2SO_4=98.079 g/mole

Therefore, $Molarity = \frac{1748\ g/L}{98.079\ g/mole} = 17.69\ M$

-For 6M of H_2SO_4 from 17.69 M:

$\frac{6M}{17.69M} * 1000ml = 339.09\ ml\ of$ H_2SO_4. Then 660.91 ml of deionized water are added to the 1000ml glass bottle.

-For 4M of H_2SO_4 from 17.69 M:

$\frac{4M}{17.69M} * 1000ml = 226.11\ ml\ of$ H_2SO_4. Then 773.89 ml of deionized water are added to the 1000ml glass bottle.

TGA IMAGES

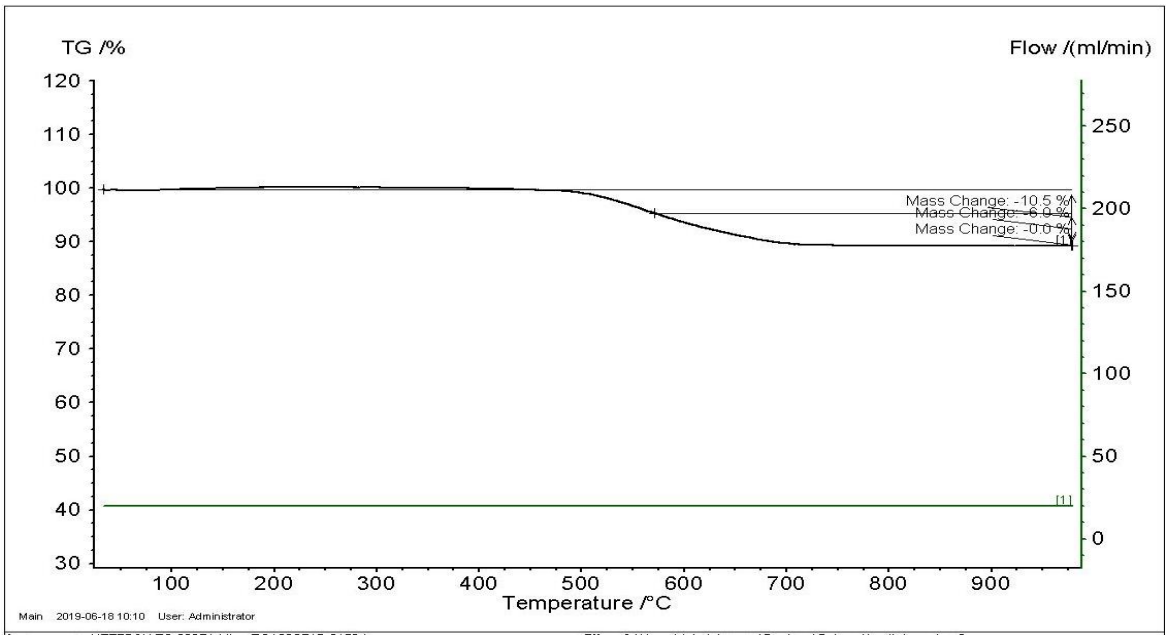

Figure 59 TGA mass degradation curve of Kaolinite

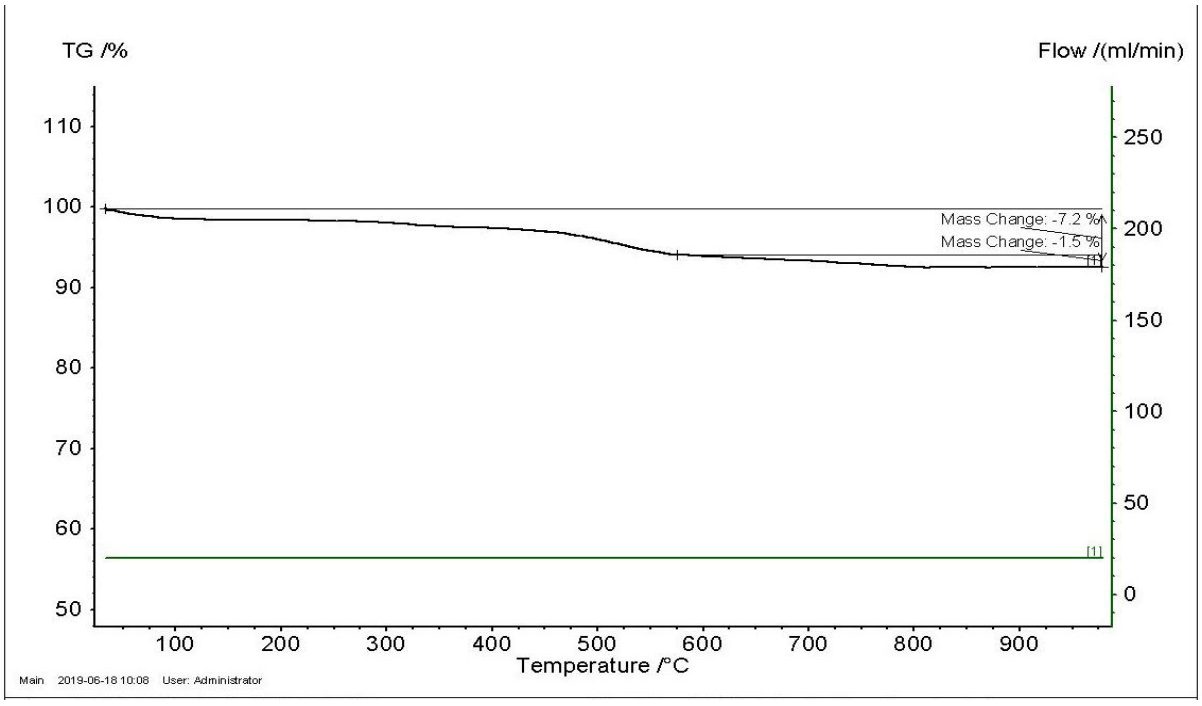

Figure 60 TGA mass degradation curve of Brown Clay

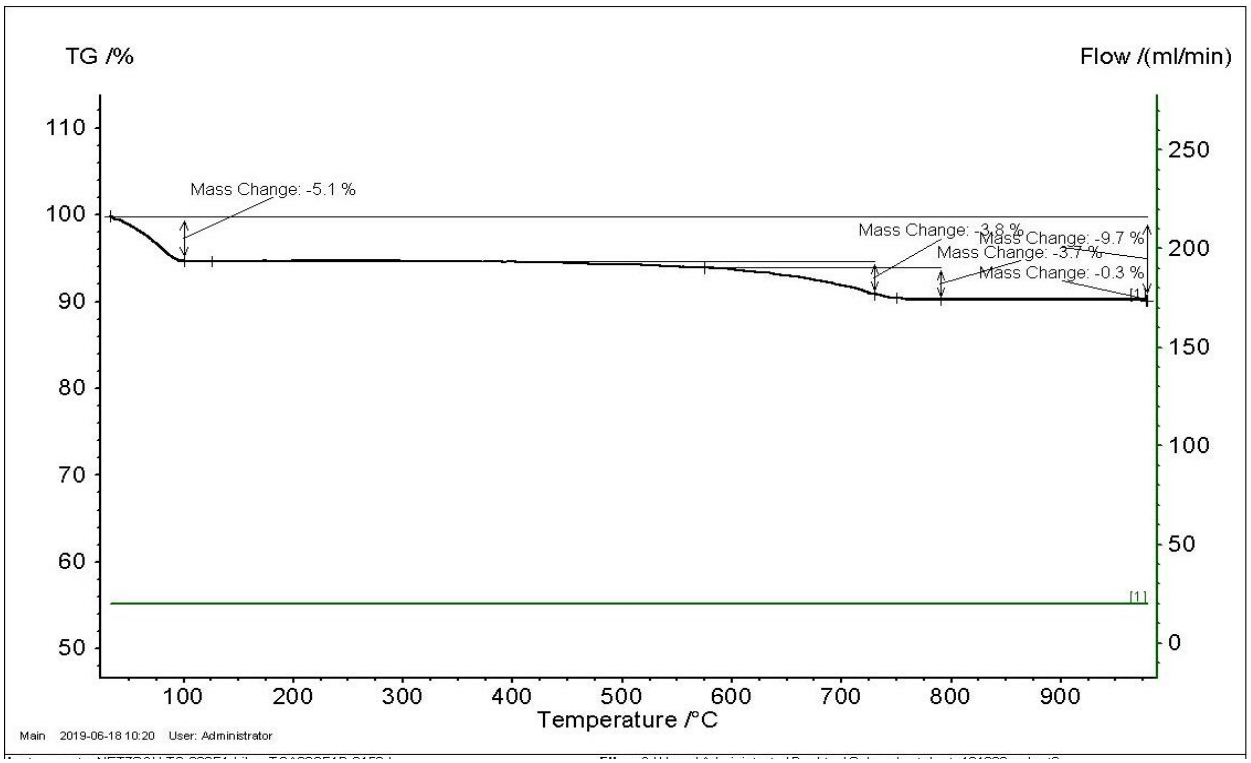

Figure 61 TGA mass degradation curve of BC_6

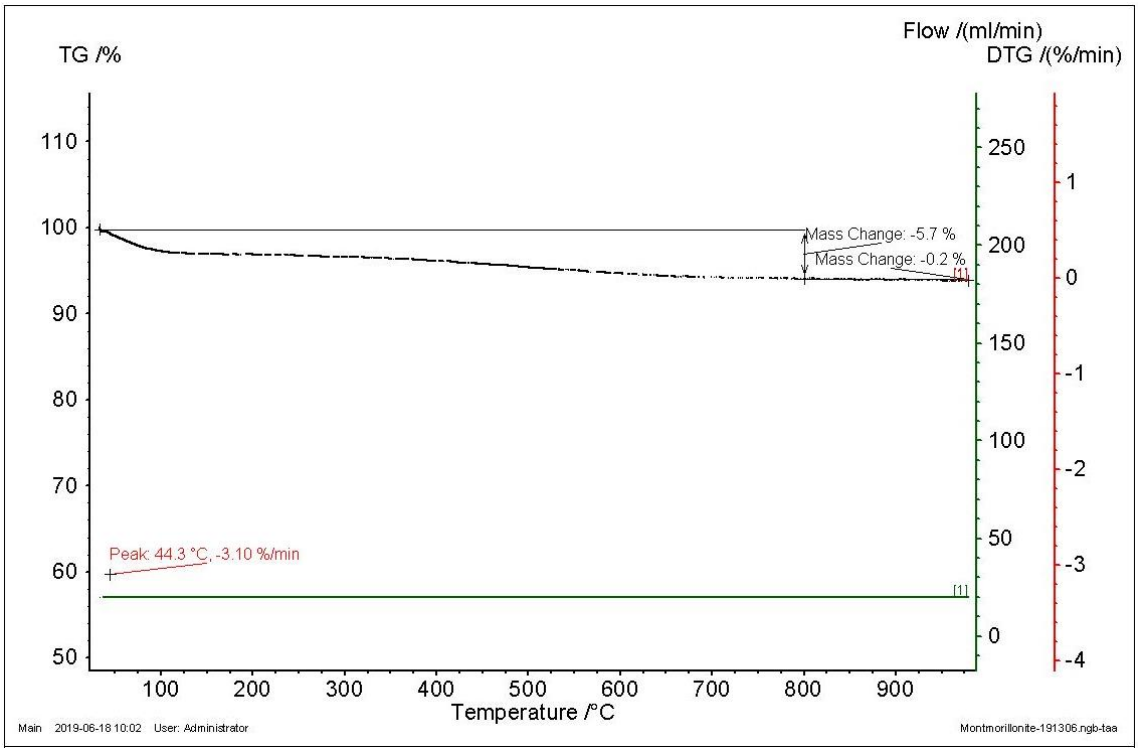

Figure 62 TGA mass degradation curve of Montmorillonite

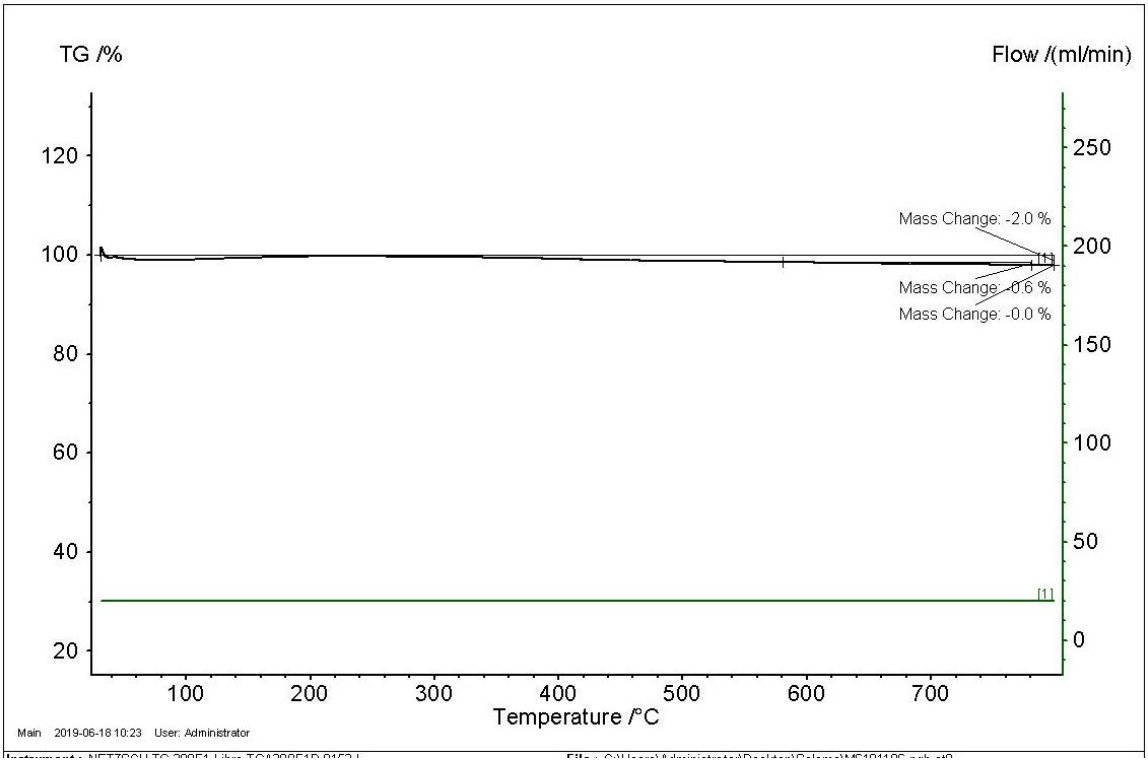

Figure 63 TGA mass degradation curve of M_6

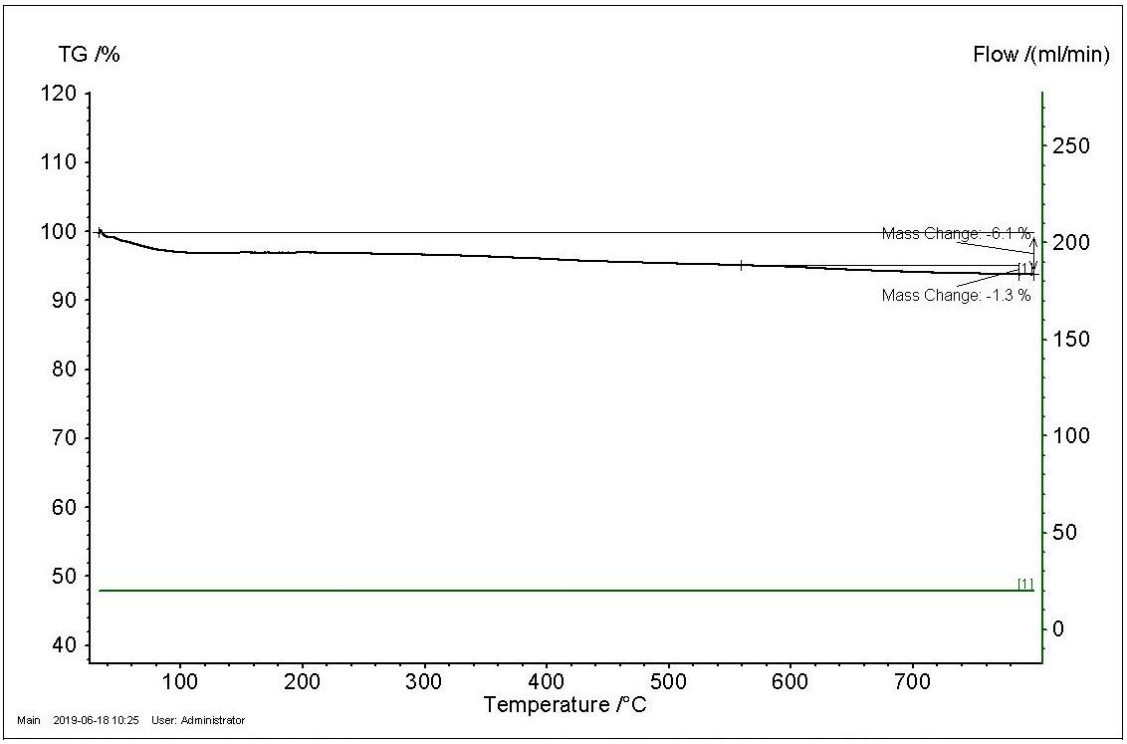

Figure 64 TGA mass degradation curve of M_4_3

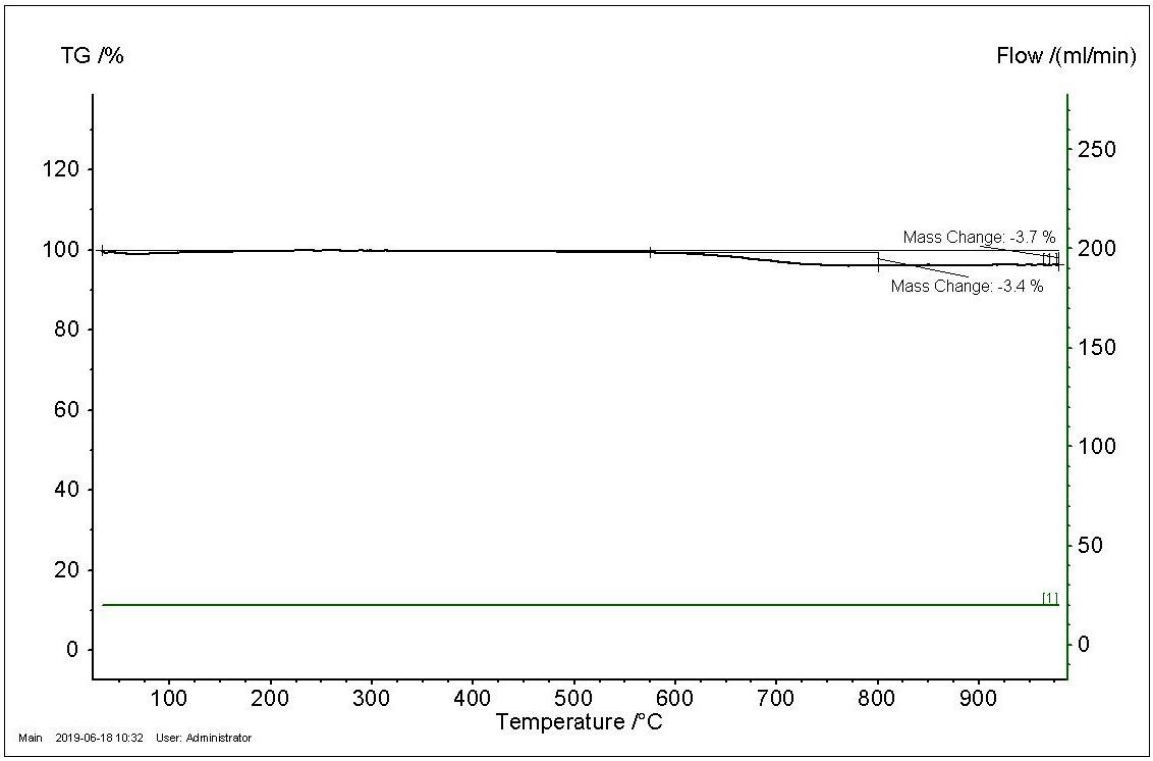

Figure 65 TGA mass degradation curve of Bentonite

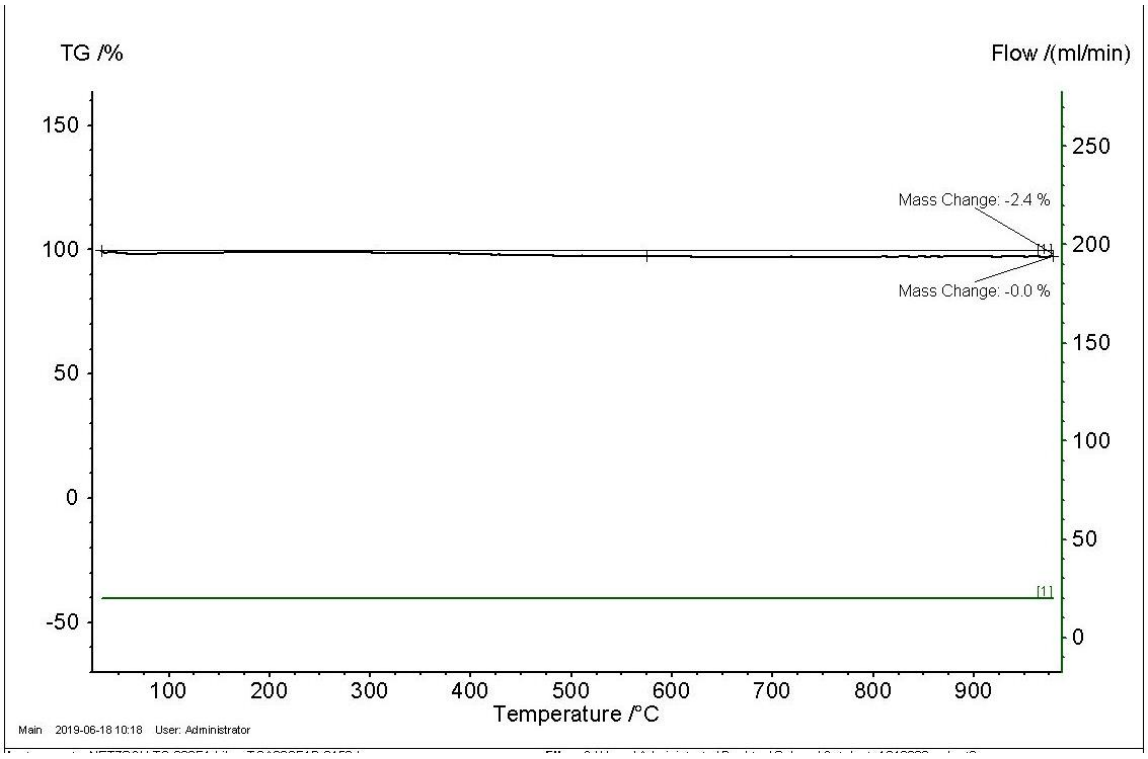

Figure 66 TGA mass degradation curve of BN_4

BIBLIOGRAPHY

A. Lucchesi, G. M. *Conservation and Recycling , 6* (3), 85-90.

A. Orio, J. C. (1997). Performance of different dolomites on hot raw gas cleaning from biomass gasification with air . *Industrial & Engineering Chemistry Research , 36* (9), 3800-3808.

A.A, A. S. (2017). Comparitive Analysis on Chemical Composition of Bentonite Clays Obtained from Ashaka and Tango Deposits in Gombe State, Nigeria . *ChemSearch Journal , 8* (2).

A.M. Cunliffe, P. W. *Analysis of Applied Pyrolysis , 44*, 131-152.

Abdullah S.L, A. A. (2017). Comparative Analysis on Chemical Composition of Bentonite Clays Obtained from Ahaka and Tango Deposits in Gombe State, Nigeria. *ChemSearch , 8* (2), 35-40.

AG., B. (1977). Some observations on the recycling of plastics and rubber. *Conservation and Recycling , 1* ((3-4)), 247-271.

Aguado J, S. D. (2006). Catalytic upgrading of plastic wastes. *Feedstock Recycling and Pyrolysis of Waste Plastics: Converting Waste Plastics into Diesel and Other Fuels* , 73-110.

Aguado R, O. M. (2005). Kinetics of scrap tyre pyrolysis under fast heating conditions . *Journal of Analytical and Applied Pyrolysis , 73*, 290-298.

Aguado, J., Serrano, D. P., Miquel, G. S., Escola, J. M., & Rodriguez, J. M. (2007). Energy Recovery from Municipal Solid Waste by Thermal Conversion Technologies. *Journal of Analytical and Applied Pyrolysis , 78*, 153-161.

Albayati, T. &. (2014). Purification of aniline and nitrosubstituted aniline contaminants from aqueous solution using beta zeolite. . *Chemistry , 23*, 105-114.

Amie Thant, C. S. (June 2017). Optimization of Acid Activation Conditons for Mabisisan Clay and its Application in Pyrolysis of Mixed Plastic Waste. (pp. 18-22).

Bangkok, Thailand: The IIER International Conference.

Amir Rowhani, T. J. (2016, October). Scrap Tyre Management Pathways and Their Use as a Fuel- A Review. (t. E. Amidon, Ed.) *Energies* , 26.

Atta, A. J. (2012). Preparation of analcime from local kaolin and rice husk ash . *Applied Clay Science , 61*, 8-13.

Ayanoglu, A. a. (2016). *Energy , 103*, 456-468.

Aylon, E. C. (2005). Assessment of tire devolatilization kinetics . *Journal of Analytical and Applied Pyrolysis , 74* (1), 259-264.

Aylon, E. F.-C. (2010). Valorisation of waste tyre by pyrolysis in a moving bed reactor . *Waste Management , 30* (7), 1220-1224.

B. Sahouli, S. B. *Fuel , 75* (10), 1244-1250.

B.Benallal, C. R. *Fuel , 74* (11), 1589-1594.

Barlaz MA, E. I. (1993). Potential to use waste tires as supplemental fuel in pulp and paper mill boilers, cement kilns and in road pavement. *Waste Management Research , 11* (6), 463-80.

Beaumontt O, S. Y. (1984). Influence of physical and chemical parameters on wood pyrolysis. *Industrial & Engineering Chemistry Research Desugn and Development , 23*, 637-641.

Bennett, G. (1993). *Scrap Tire Technology and Markets: By US Environmental Protection Agency and C.Clark, K.Meardon and D.Russell of Pacific Environmental Services.* Park Ridge, New Jersey: Noyes Data Corp.,.

Berrueco C, E. E.-B. (2005). Pyrolysis of waste tyres in an atmospheric static-bed batch reactor: analysis of the gases obtained. . *Journal of Analytical and Apploed Pyrolysis , 74*, 245-253.

Betancur M, M. J. (2009). Production of activated carbon waste tire thermochemical degredation with CO2. *Journal of Hazardous Materials , 168*, 882-887.

Bidhya Kunwar, B. R. (2016). Catalytic and thermal depolymerization of low value post-consumer high density polyethylene plastic. *Energy , 111*.

Bridgewater AV, P. G. (2000). Fast Pyrolysis processes for biomass. *renewable & Sustainable Energy Review , 4*, 1-73.

Buekens, A. (2006). Introduction to feedstock recycling of plastics. *Feedstock Recycling and Pyrolysis of Waste Plastics* , 1-41.

Byrappa, K. a. (2001). Hydrothermal Synthesis and Growth of Zeolites. In *Handbook of Hydrothermal Tecchnology* (pp. 315-414).

C. Clark, K. M. (1993). *Scrap tire technology and markets* .

C. Roy, J. U. (n.d.). Pilot plant demonstration of used tyres vacuum pyrolysis. *Pyrolysis and Gasification* .

C.I. Sainz-Diaz, A. G. (2000). *Fuel , 79*, 1863-1871.

Campbell, I. (n.d.). *Catalysis of Surfaces* .

Carolina Belver, M. A. (2001). Chemical Activation of Kaolinite under Acid and Alkaline Conditions. *Chemical Matter , 14*, 2033-2043.

Cejka, J. C. (2010). *Zeolites and catalysis: synthesis, reactions and applications.* John Wiley & Sons,. .

Cejka, J. (2005). *Zeolites and Ordered Mesoporous Materials: Progress and Prospects* (Vol. 157). Czech Republic : Elsevier .

Chandrasekhar, S. P. (1999). Investigation on the synthesis of Zeolite NaX from kerala kaolin. *Journal of Porous Mater , 6* (4), 283-297.

Cheung K-Y, L. K.-L.-L.-Y.-W.-W. (2011). Operation strategy for multi-stage pyrolysis . *Journal of Analytical and Applied Pyrolysis , 91*, 165-182.

Chorkendorff, I. a. (2003). Introduction to Catalysis. *Concepts of Modern Catalysis and Kinetics* , 1-21.

Choudhury T, M. M. (2011). *Material Science , 34* (6), 1273.

Collins L, D. W. (1974). An evolution of discarded tires as source fuel. *Thermochimica Acta , 10* , 153-159.

Conesa JA, F. R. (1996). Gas from the pyrolysis of scrap tires in a fluidized bed reactor . *Energy Fuel , 10*, 134-140.

Conesa, J. A.-G. (2004). Complete study of the pyrolysis and gasification of scrap tires in a pilot plant reactor. *Environ.Sci.Technol., , 38* (11), 3189-3194.

Cunliffe Am, W. P. (1998). Composition of oils derived from the batch pyrolysis of tires . *Journal of Analytical and Applied Pyrolysis , 44*, 131-152.

D.E. Wolfson, J. B. (n.d.). Destructive Distillation of Scrap Tyres.

Daugaard, D. E. (2003). Enthalpy for pyrolysis for several types of biomass . *Energy Fuels , 17* (4), 934-939.

De'Gennaro, M. C. (2000). Genesis of zeolites in the Neopolitan Yellow Tuf: geological, volcanological and mineralogical evidence. . *Mineralogy and Petrology , 139*, 17-35.

Diez C. Martinez O, C. L. (2004). Pyrolysis of tyres. Influence of the final temperature of the process on emissions and the calorific value of the products recovered. *Waste Managemet , 24*, 463-492.

Dodds J. Domenico WF, E. D. (1983). *Scrap tyres: a resource and technology evaluation of tye pyrolysis and other selected alternative technologies.* EGG-2241, US Department of Energy Report .

Dung NA, K. R. (2009). Light olefins and light oil production from catalytic pyrolysis of waste tire. *Journal of Analytical and Applied Pyrolysis , 86*, 281-286.

Elbaab IF, W. C. (2010). Catalytic pyrolysis-gasification of waste tire and tire elastomers for hydrogen production. *Energy Fuel , 24*, 3928-3935.

Emam, E. A. (2013). Clays as Catalysts in Petroleum Refining Industry . *Journal of Science and Technology , 3* (4).

Ertl, G. K. (1997). *Handbook of heterogeneous catalysis.* VCH,. .

European Commission. (1999). Council Directive 1999/31/EC. *Landfill of waste directive.* Brussels: European Commission.

F. Miccio, B. P. (2009). Biomass gasification in a catalytic fluidized reactor with beds of different materials. *Chemical Engineering Journal , 154* (1), 369-374.

Farkaš, A. R.-M. (2005). : Ammonium exchange in leakage waters of waste dumps using natural zeolite from the Krapina region, Croatia. . *Journal of Hazardous Materials B , 117*, 25-33.

Fernandez AM, B. C. (2012). Pyrolysis of a waste from the grinding of scrap tyres . *Journal of Hazardous Materials , 203* (204), 236-243.

Flanigen, E. R. (2010). Zeolites in industrial separation and catalysis. *In: Kulprathipanja, S. (Ed.), Introduction* , 1-26.

Fogler, H. S. *Elements of Chemical Reaction Engineering* (Fourth Edition ed.). Prentice Hall Professional Technical Reference .

Freedonia. (2019). *World Tires* . Retrieved 2019, from The Freedonia Group: https://www.freedoniagroup.com/industry-study/world-tires-3357.htm

Galvagno, S. C. (2002). Pyrolysis process for the treatment of scrap tyres: Preliminary experimental results. *Waste Management , 22* (8), 917-923.

Gokalp, J. K. (2015). Pyrolysis, Combustion, and Steam Gasification of Various Types of Scrap Tires for Energy Recovery. *Energy&Fuel , 29*, 346-354.

Gomez C, V. E. (2009). Influence of secondary reactions on the heat of pyrolysis of biomass. *Industrial Engineering Chemistry Research , 48*, 10222-10233.

Goncalves. M. L. A., B. J. (n.d.). *Journal of thermal analysis and calorimetry* .

Gonzales, N. B. (1997). Density functional theory calculations of the effects of local composition and defect structure on the proton affinity of H-ZSM-5 . *The Journal of Physical Chemistry B , 101* (48), 10058-10064.

Groves SA, L. R. (1991). Natural rubber pyrolysis: Study of temperature-and thickness-dependence indicates dimer formation mechanism. . *Journal of Analytical and Applied Pyrolysis , 19*, 301-309.

Guggenheim S, V. G. (2001). *Clays and Clay Minerals , 49*, 433.

H, M. (1999). *CLay Minerals* .

H.G. Franck, J. S. (n.d.). *Industrial Aromatic Chemistry* .

Hart, M. b. (2004). Surface acidities and catalytic anctivities of acid activated clays. *Journal of molecular catalysis* , 212-315.

Hayward, R. V.-M. (1991). Matrix vs Zeolite Contributions to the Acidity of Fluid Crackin Catalysts. *Catalysis and Adsorption by Zeolites* , 171.

Herrero J, B. C. (1990). *Applications of Organometallic Chemistry , 4*, 147.

Hosseinpour N, M. Y. (2009). *Fuel Process Technology* , 90-179.

I.E. Katheklakis, L. S.-L. (n.d.). *Fuel* , 172.

Ilkilic, H. A. (2012). Optimization of fuel production from waste vehicle tires by pyrolysis and resembling to diesel fuel by various desulfurization methods. *Fuel , 102*, 605-612.

International Energy Agency. (2009).

Islam MR, H. H. (2008). Liquid fuels and chemicals from pyrolysis of motorcycle tire waste: product yields, compositions and rekated properties. *Fuel , 87*, 3112-3122.

Islam, M. N. (2016). Improvement of Waste Tire Pyrolysis Oil and Performance Test with Diesel in CI Engine. *Journal of Renewable Energy* , 1-8.

J. Han, H. K. (2008). The reduction and control technology of tar during biomass gasification/ pyrolysis: an overview. *Renewable and Sustainable Energy Reviews , 12* (2), 397-416.

J. Temuujin, T. J. (2004). Characterisation of acid activated montmorillonite clay from Tuulan (Mongolia). *Ceremics International , 30*, 251-255.

J.Delgado, M. A. (1997). Biomass gasification with stea in fluidized Bed: effectiveness of CaO, MgO, and CaO-MgO for hot raw gas cleaning. *Industrial & Engineering Chemistry Research , 36* (5), 1535-1543.

J.E. Naber, K. d. (1994). Zeolites and Related Microporous Materials: State of the Art. In H. K. J. Weitkamp, *Studies in Surface Science and Catalysis* (Vol. 84, p. 2197). Amsterdam: Elsevier.

Jankovic L, D. K. (2010). *Physical Chemistry Chemical Physics , 12*.
Jha, B. &. (2016). Fly ash zeolites: Innovations, applications, and directions . *Singapore: Springer Science Busines Media Singapore Pte.*

John Paul Vas, R. M. (2017). Production of High Grade Liquid Fuels For CI Engine by Thermo-Catalytic Cracking of Waste Plastic. *Energy and Power , 7* (3), 81-87.

Juan Daniel Martinez, N. P. (2013). Waste tyre pyrolysis- A review . *Renewable and Susyainable Energy Reviews , 23*, 179-213.

K.Tomishige, T. M. (2003). Catalyst performance in reforming of tar derived from biomass over noble metal catalysts. *Green Chemistry , 5* (4), 399-403.

Kaminsky W, M. C. (2009). Feedstock recycling of synthetic and natural rubber by pyrolysis in a fluidized bed. *Journal of Analytical and Applied Pyrolysis , 85*, 334-337.

Kaur N, K. D. (2012). *Journal of Chemical and Pharmaceutical research , 4* (2), 991.

Kellendonk F J A., H. J. (1987). *Clay-activated Isomerization Reactions* . Academi Press Inc .

Kooli, F. Y. (2009). Reaction of acid activated montmorillonite with hexadecyltrimethylammonium bromide solution. *Applied Clay Science , 43*, 357-363.

Koukouzas, N. (2007). Mineralogy and geochemistry of diatomite associated with lignite seams in Komnina Lignite Basin, Ptolemais, Northern Greece. *International Journal of Coal Geology , 71* (2-3), 276-286.

Kuhl, G. H. (1999). Modification of zeolites . *Catalysis and Zeolites* , 81-197.

Kuhl, G. (1977). The Coordination of aluminum and silicon in zeolites as studied by x-ray spectrometry. *Journal of Physics and Chemistry of Solids , 38* (11), 1259-1263.

Kwon E, C. M. (2009). Fundamental understanding of the thermal degradation mechanisms of waste tires and their air pollutant generation in a N2 atmosphere . *Environmental Science & Technology , 43*, 5996-6002.

Kwon E, C. M. (2008). Investigation of mechanisms of polycyclic aromatic hydrocarbons (PAHs) initiated from the thermal degradation of styrene butadiene rubber (SBR) in N2 atmosphere. . *Environmental Science & technology , 42*, 2175-2180.

Kyari M, C. A. (2005). Characterization of oils, gases and char in relation to the pyrolysis of different brands of scrap automotive tires. *Energy Fuel , 19*, 1165-1173.

L.Devi, K. P. (2003). A review of the primary measures for the tar elimination in biomass gasification processes. *Biomass and Bioenergy , 24* (2), 125-140.

L.Devi, K. P. (2005). Catalytic decomposition of biomass tars: use of dolomite and untreated olivine, . *Renewable Energy , 30* (4), 565-587.

L.K.M. Edward, C. D. (2004). *Carbon , 42*, 2789-2805.

Labaki, M. a. (2016). *Environmental Science and Pollution Research* , 1-31.

Laird DA, B. R. (2009). Review of the pyrolysis platform for coproducing bio-oil and biochar . *Biofuels, Bioproducts and Biorefining , 3*, 547-562.

Laresgoiti MF, R. I. (2000). Chromatographic analysis of the gases obtained in tyre pyrolysis . *Journal of Analytical and Applied Pyrolysis , 55*, 43-54.

Larsen MB, S. L.-J.-J. (2006). Devolatilization characteristics of large particles of tyre rubber under combustion conditionns. . *Fuel , 85*, 1335-1245.

Lee, J. S. Gasification kinetics of waste tire-char with CO2 in a thermobalance reactor. *Energy , 21*, 343-352.

Lehmann CMB, R.-A. M. (1998). Reprocessing and reuse of waste tire rubber to solve air-quality related problems. *Energy Fuel , 12*, 1095-1099.

Leung DYC, W. C. (1998). Kinetic study of scrap tyre pyrolysis and combustion. *Journal of Analytical and Applied Pyrolysis , 45*, 154-169.

Li S-Q, Y. Q.-H.-F. (2004). Pilot-scale pyrolysis of scrap tires in a continuous rotary kiln reactor. *Industrial & Engineering Chemistry Research , 43*, 5133-5145.

Libretexts. (2019, June 5). *How an FTIR Spectrometer Operates*. Retrieved from LibreTexts: https://chem.libretexts.org/Bookshelves/Physical_and_Theoretical_Chemistry_Textbook_Maps/Supplemental_Modules_(Physical_and_Theoretical_Chemistry)/Spectroscopy/Vibrational_Spectroscopy/Infrared_Spectroscopy/How_an_FTIR_Spectrometer_Operates.

Lloyd, A. C. (2006). Technology Evaluation and Economic Analysis of Waste Tire Pyrolysis, Gasification, and Liquefacation. *University of California Riverside, Integrated Waste Management Board, 97* .

Lopez G, O. M. (2010). Continuous pyrolysis of waste tyres in a conical spouted bed reactor. *Fuel , 89*, 1946-1952.

Lopez G, O. M. (2009). Influence of tire formulation on the products of continuous pyrolysis in a conical spouted bed reactor. *Energy Fuel , 23*, 5423-5431.

Lopez, a., de Marco, I., Caballero, B., Adrados, a., & Laresgoiti, M. F. (2011). Thermal and catalytic pyrolysis of plastic waste. *Waste Management , 31*, 1852-1858.

Lucchesi A, M. G. (1983). Semi-active carbon and aromatics produced by pyrolysis of scrap tires. *Conservation and recycling , 6* (3), 85-90.

M.A. Golub, M. S. *Journal of Polymer Science , 11*, 129.

M.F. Laresgoiti, B. C. (2004). *Journal analysis of applied pyrolysis , 71*, 917-934.

M.M. Barbooti, T. M. (2004). *Ana.ysis and applied pyrolysis , 72*, 165-170.

M.Rofiqul Islam, H. H. (2008). Liquid fuels and chemicals from pyrolysis of motorcycle tire waste: Product yields, compositions and related properties . *Fuel , 87*, 3112-3122.

Malkow, T. (2004). Novel and innovative pyrolysis and gasification technologies for energy efficient and environmentally sound MSW disposal . *Waste Management , 24* (1), 53-79.

Managing End-of-Life Tires. (n.d.). Retrieved January 20, 2019, from World Business Council for Sustainable Development: http://www.bir.org/assets/Documents/industry/ManagingEndOfLifeTyres.pdf

Mastral AM, C. M. (1999). Combustion of high calorific value waste material: organic atmospheric pollution. *Environmental Science & Technology* (33), 4155-4158.

Mastral Am, M. R. (2000). Influence of process variables on oils from tire pyrlysis and hydropyrolysis in a swept fixed bed reactor. *Energy Fuel , 14*, 739-744.

Mastral AM, M. R. (2000). Influence of process variables on oils from tire pyrolysis and hydropryolysis in a swept fixed bed reactor. *Energy Fuel , 12*, 739-744.

Mastral AM, M. R.-S. (1996). Coal hydrocoprocessing with tires and tire componets. *Energy Fuel , 10*, 941-947.

Matshitse, R. *Braunauer-Emmett-Teller (BET) surface area analysis* . Rhodes University . National Research Foundation .

Matthew E. Boot-Handford, E. V. (2018). Simple pyrolysis experiments for the preliminary assessment of biomass feedstocks and low-cost tar cracking catalysts for downdraft gasification applications. *Biomass and Bioenergy , 108*, 398-414.

Matthias Thommes, K. K.-R. (2015). Physisorption of gases, with special reference to the evaluation of surface area and pore size distribution (IUPAC Technical Report) . *Pure Applied Chemistry* .

Mendioroz, S. P. (1987). Langmuir . *3*, 676.

Michel Guisnet, J.-P. (Ed.). (2002). *Zeolites for Cleaner Technologies* (Vol. 3). London: Imperial College Press.

Moronata A, F. V. (2002). *Applied Catalysis A , 230*, 127 .

Mu Mu Htay, M. M. (2008). Preparation of Zeolite Y Catalyst for Petroleum Cracking. *World Academy of Science, Engineering and Technology , 48*, 114-120.

Murillo R, A. E. (2006). The application of thermal processes to valorise waste tyre. . *Fuel Processing Technology , 87*, 143-147.

Murillo, R. A. (2006b). Process for the separation of gas products from waste tire pyrolysis. *Ind Eng Chem Res , 45* (5), 1734-1738.

Murillo, R. A. (2006a). The application of thermal processes to valorise waste tyre . *Fuel Process Technology , 87* (2), 143-147.

Murray, H. (2007). *Applied Clay Mineralogy* (Vol. 2). Elsevier Science .

Naaman, .. S. (2012). Evaluation and improvement of gasoline and naphtha cut of Tawke crude oil wells, Zakho. *Journal of Petroleum and Gas Exploration , 2* (4), 69-79.

Ogasawara S, K. M. (1987). Preparation of activated carbon by thermal decomposition of used automotive tires. *Industrial & Engineering Chemistry Research , 26*, 2552-2556.

Oghenejoboh K M, O. E. (2011). *European Journal Science Resources , 54* (4), 445.

P.A.Simell, J. H. (1997). Effects of gasification gas components on tar and ammonia decomposition over hot gas cleanup catalysts. *Fuel , 76* (12), 1117-1127.

P.B. Venuto, E. H. (1979). In M. Dekker, *Fluid Catalytic Cracking With Zeolite Catalysts* (p. 156). New York : Basel .

P.B. Venuto, T. H. (n.d.). *Fluid Catalytic Cracking with Zeolite Catalysts* .

P.T. Williams, A. B. (2003). Journal of analysis and applied pyrolysis. *67*, 143-164.

P.Williams, R. B. *Fuel , 74* (5), 736-742.

Pakdel H, P. D. (1991). Production of dl-limonene by vacuum pyrolysis of used tires. *Journal of Analytival and Applied Pyrolysis , 19*, 301-309.

Plee D, S. A. (1985). In catalysis by acids and bases . Amsterdam : Elsevier.

Prakash Kumar, R. V. (1995). Evolution of Porosity and Surface Acidity in Montmorillonite Clay on Acid Activation. *Ind. Eng. Chem. Res. , 34* (4), 1440-1448.

R. von Ballmoos, D. H. (1997). *Handbook of Heterogeneous Catalysis* (Vol. 4). (H. K. G. ertl, Ed.) Weinheim : Wiley-VCH.

Rabo, J. a. (2001). *Applied Catalysis A , 222*, 261.

Raman, K., Walawender, W., & Fan, L. (1981). Gasification of waste tires in a fluid bed reactor. *Resources, Conservation and Recycling* , 79-88.

Rezaiyan, J. a. (2005). Gasification technologies: a primer for engineers and scientists.
Ribeiro, R. (1984). *Zeolites: Science and Technology* (Vol. 80). (F. (Ed.), Ed.) Springer Netherlands .

Rodrigues, M. (2003). Physical and catalytic characterization of smectites from Boa-Vista, Paraiba, Brazil . *Ceramica , 49* (311), 146-150.
Rodriguez I, L. M. (2001). Pyrolysis of scrap tires . *Fuel Processing Technology , 72*, 9-22.

Rong T-J, X. J.-k. (2002). *57*, 297.

Rosinski, E. (1992). The origin and Development of the First Zeolite Catalyst for Petroleum Cracking. Oxford University Press.

Rouquerol, F. R. (1999). Adsorption by powdeers and porous solids. *Principles, methodology and applications* .

Roy C, D. H.-C. (1997). Characterization of naphtha and carbon black obtained by vacuum pyrolysis of polyisoprene rubber. *Fuel Processing Technology , 50*, 87-103.

Ruren Xu, W. P. (2007). *Chemistry of Zeolites and Related Porous Materials: Synthesis and Structure* . Singapore: John Wiley & Sons .

S. Chouaya, .. M. (2018). Scrap Tires Pyrolysis: Products Yields, Properties and Chemical Compositions of Pyrolytic Oil. *Russian Journal of Applied Chemistry , 91* (10), 1603-1611.

S. Koppatz, C. P.-M. (2009). H2 rich product gas by steam gasification of biomass with in situ CO2 absorption in a dual fluidized bed system of 8MW fuel input. *Fuel Processing Technology , 90* (7), 914-921.

S. Rapagna, N. J. (2000). Steam-gasification of biomass in a fluidised-bed of olivine particles. *Biomass Bioenergy , 19* (3), 187-197.

San Miguel G, F. G. (1998). Pyrolysis of tire rubber: porosity and adsorption characteristics of the pyrolytic chars. *Industrial & Engineering Chemistry Research , 37*, 2430-2435.

Schirmer, J., Kim, J. S., & Klemm, E. (2001). Catalytic degradation of polyethylene using thermal gravimetric analysis and a cycled-spheres-reactor. *60* (2), 205-217.

Scrap tire characteristics . (n.d.). Retrieved 03 2019, from Rubber Manufactures Association: Available at / http://www.rma.org/scrap_tires/scrap_tire_markets/scrap_tire_characteristics/#anchor530383S

Serrano, D., Aguado, J., & Rodriguez, J. (2007). Catalytic cracking of polyethylene over nanocrystalline HZSM-5: Catalyst deactivation and regeneration study. *Journal of Analytical and Applied Pyrolysis , 79*, 456-464.

Shen Boxiong, W. C. (2007). Pyrolysis of waste tyres with zeolite USY and ZSM-5 Catalysts. *Applied Catalysis B: Environmental , 73*, 150-157.

Shulman, V. (2004). Tyre recycling. *Rapra review reports , 15* (7).

Sinn, H. K. (1976). Processing of plastic waste and scrap tires into chemical raw materials, especially by pyrolysis. *Angewandte Chemie International Edition in English , 15* (11), 660-672.

Smirniotis, P. G. (1996). Effect of the Si/Al Ratio and of the Zeolite Structure on the Performance of Dealuminated Zeolites for the Reforming of Hydrocarbon Mixtures. *Industrial & Engineering Chemistry Research , 35* (9).

Songrip, A. R., Masuda, T., Kuwahara, H., & Hashimotot, K. (1994). Catalytic degradation of medium density polyethylene over silica-alumina supports. *Energy & Fuels* , 136-140.

SunS-H, M.-T. P.-M.-B.-L. (2005). *Bulletin of catalysis society of India , 4*, 72.
T., M. (2010). Pillard clays and related catalysts. 99.

T.B. reed, A. D. (1988). *Handbook of Biomass Downdraft Gasifier Engine Systems,*. Biomass Energy Foundation .

Tan Q, B. X. (2007). *Journal of Catalysis , 251* (69).

Ucar S, K. S. (2005). Evaluation of two different scrap tires as hydrocarbon source by pyrolysis . *Fuel , 84*, 1884-1892.

Uddin, F. (2018). Montmorillonite: An Introduction to Properties and Utilization .

Unapumnuk, K. K. (2008). Investigation into the removal of sulfur from tire derived fuel by pyrolysis. *Fuel , 87* (6), 951-956.

US Environmental Protection Agency, Wastes- resources conservation- common wastes & materials- scrap tires. (n.d.). Retrieved from /http://www.epa. gov/osw/conserve/materials/tires/tdf.htmS

V., J. R. (2003). *Bulletin of catalysis society of India , 2*, 157.

V.S, S. M. (2016). An overview of advances in biomass gasification. *Energy & Environmental Science , 9* (10), 2939-2977.
W. Kaminsky, H. S. (1980). Pyrolysis plastic waste and scrap tyres in a fluid bed reactor. . *resources, Conservation and Recycling , 5*, 205-216.

Wei Qu, Q. Z.-Z.-W.-H.-W.-Z. (2006). Pyrolysis of waste tire on ZSM-5 zeolite with enhanced catalytic activities . *Polymer Degradation and Stability , 91*, 2389-2395.

Wiliams, P. T. (2013). Pyrolysis of waste tyres- A review. *Waste Management , 33*, 1714-1728.

Williams PT, B. A. (2002). Catalytic pyrolysis of tyres: influence of catalyst temperature. *Fuel , 81*, 2425-2434.

Williams PT, B. S. (1995). Pyrolysis of automotive tyre waste. *Journal of the Institute of Energy , 68*, 11-21.

Williams PT, B. S. (1990). Pyrolysis of scrap automotive tyres: the influence of temperature and heating rate on product composition . *Fuel , 69*, 1472-1482.

Williams PT, B. S. (1995). Pyrolysis-thermogravimetric analysis of tyres and tyre components. *Fuel , 74* (9), 1277-1283.

Williams, P. (2013). *Waste Management , 33* (8), 1714-1728.

Y., K. (2011). Catalytic pyrolysis of car tire waste using expanded perlite . *Waste Management , 31*, 1772-1782.

Y.F. Shen, P. Z. (2014). In-situ catalytic conversion of tar using rice husk char-supported nickle-iron catalysts for biomass pyrolysis/gasification. *Applied Catalysis B:Environmental , 152*, 140-151.

Yang J, R. C. (1996). A new method for DTA measurement of enthalpy change during the pyrolysis of rubbers. *Thermochimica Acta , 288* (155), 168.

Y-M., C. (1996). On pyrolysis of waste tire: degradation rate and product yields. *Resources, COnservation and Recycling , 17*, 125-139.

Zhang X, W. M. (2008). Vacuum pyrolysis of waste tires with basic additives. *Waste Management , 28*, 2301-2310.